ALTERED INTERMUSCULAR FORCE FEEDBACK AFTER SPINAL CORD INJURY IN CAT

A Thesis
Presented to
The Academic Faculty

By

Irrum Fawad Niazi

In Partial Fulfillment
of the Requirements for the Degree
Doctor of Philosophy in the
School of Applied Physiology

Georgia Institute of Technology
August 2015

ALTERED INTERMUSCULAR FORCE FEEDBACK AFTER SPINAL CORD INJURY IN CAT

Approved by:

Dr. T. Richard Nichols, PhD, Advisor
School of Applied Physiology
Georgia Institute of Technology

Dr. Lewis A. Wheaton, PhD.
School of Applied Physiology
Georgia Institute of Technology

Dena R. Howland, PhD
Kentucky Spinal Cord Injury Research Center, Department of Neurological Surgery
University of Louisville

Dr. Boris I. Prilutsky, PhD
School of Applied Physiology
Georgia Institute of Technology

Dr. Shawn Hochman, PhD
Department of Physiology
Emory University School of Medicine

Dr. Young-Hui Chang, PhD
School of Applied Physiology
Georgia Institute of Technology

Date Approved: 07/ 22/ 2015

“In all things of nature there is something of the marvelous”
(Artistotle)

Dedicated to my father and my husband,
who allowed me to spread my wings and test my limits

ACKNOWLEDGEMENTS

They say it takes a village to raise a child. The work presented in this dissertation would not have been possible without the help and support of many individuals.

Foremost, I would like to express my sincerest gratitude to my advisor, Dr. T. Richard Nichols, Ph.D., for his continuous support during my doctoral studies and research. He provided a strong foundation for my graduate school experience by letting me explore beyond the textbooks and clinic. I feel extremely lucky to know him as a scientist and a very humble human being. His patience, motivation, enthusiasm and immense knowledge helped me in the entire period of research and writing of this thesis. His support through the tough times and belief in me gave me the strength to continue through my second round of the roller coaster ride of a graduate career. Thank you and Patricia for welcoming Fawad, our triplet daughters and me into your lives through these years. I cannot imagine having a better advisor, mentor and a loving family away from home during my Ph.D. studies in the USA.

Thanks to my committee members who have given their time and energy to help me transform from a clinician to a scientist. I especially thank Dr. Dena Howland, Ph.D., for her immense support through these years. You are an amazing researcher, dexterous surgeon and a role model. Thank you for bringing all the amazing animals to our laboratory and sharing your wisdom and knowledge with us. Many thanks to Dr. Boris I. Prilutsky, Ph.D., for always being willing to help and provide best suggestions; Dr. Lewis Wheaton, Ph.D., for inspiration and support to encourage new researchers with an open mind and a generous smile; Dr. Young-Hui Chang, Ph.D., for enthusiasm for science and

innovation to inspire new scientists to think outside the box; Dr. Shawn Hochman, Ph.D., for input regarding many possible ways to make the project successful. Your knowledge, professionalism, wit and passion for science have always inspired me.

To the many current and past members of the Nichols laboratory who have been friends, colleagues and a family through the years. Thank you for your support and guidance. Special thanks to Dr. Mark Lyle, Ph.D., for continued response to my technical emergencies; Gareth Guvanasen for making me laugh while keeping me focused during long experiments; Elma Kajtaz for always providing comic relief and being my family at Georgia Tech; Bill Goosby for honoring my technical support requests; Dr. Victoria Stahl, Ph.D., Dr. Ramaldo Martin, Ph.D., and Chris Tuthill for help and support; and to the faculty, Applied Physiology Department, Georgia Institute of Technology for shaping my carrier as a scientist.

I would like to thank my Mom and Dad for believing in me throughout my carrier. I love you dad and will continue my quest to understand the complexities of brain, in remembrance of your untiring battle with brain tumor and quadriplegia. I would like to thank my triplet daughters Zaina, Sibel and Alishba. Your fight against prematurity and your beautiful smiles have given me a new strength in life. Without doubt, having them after 15 years of struggle will stay as the best memory of my graduate school for years to come. I would especially like to thank and honor my angel daughter, Sibel, for inspiring me to keep my faith in life.

Finally, I would like to thank my dear husband Dr. Fawad Niazi, Ph.D. You have always supported and loved me as my best friend. Your unfailing belief that I can achieve anything made me a strong woman through our years of married life. You made me laugh in the toughest of personal and professional times. Your patience and understanding make me feel truly blessed for being married to you for the last 18 years. I truly consider you to be the best gift. I love you always and forever!

TABLE OF CONTENTS

LIST OF TABLES

LIST OF FIGURES

LIST OF SYMBOLS AND ABBREVIATIONS

DSH	Dorsal Spinal Hemisection
FDB	Flexor Digitorum Brevis Muscle
FDL	Flexor Digitorum Longus Muscle
FHL	Flexor Hallucis Longus Muscle
GA	Gastrocnemius Muscle
GTO	Golgi Tendon Organs
LSH	Lateral Spinal Hemisection
MLR	Mesencephalic Locomotor Region
ms	Millisecond
MTC	Muscle-tendon Complex
N	Newton
PLT	Plantaris Muscle)
SCI	Spinal Cord Injury
SOL	Soleus
t	Time
XER	Crossed- extension Reflex
%	Percentage
+	Excitation
-	Inhibition

SUMMARY

Bipeds and quadrupeds are inherently unstable and their bodies sway during quiet stance and require complex patterns of muscle activation to produce direction-specific forces to control the body's center of mass. The relative strength of length and force feedback within and across muscles collectively regulates the mechanical properties of the limb as a whole during standing and locomotion (Bonasera and Nichols 1994; Ross and Nichols 2009). Loss of posture control following spinal cord injury (SCI) is a major clinical challenge. While much is known about intermuscular force feedback during crossed extension reflex (XER) and locomotion in decerebrate cats, these have not been well characterized in animals with spinal cord injury.

In this study, we mapped the distribution of heterogenic force feedback in hindlimb ankle extensor muscles using muscle stretch (natural stimulation) in intercollicular, non-locomoting, decerebrate cats with chronic lateral spinal hemisection (LSH). We also, determined the time of onset of redistribution of heterogenic force feedback following LSH by collecting force feedback data from cats with acute sci. In addition we revisited heterogenic force feedback between ankle extensors in decerebrate non-locomoting cats during mid-stance to ascertain whether these cats with intact spinal cord depict a certain pattern of force feedback. The goal was to ascertain whether the patterns and strength of feedback was different between the two states (cats with intact spinal cord and cats with SCI). We found that heterogenic feedback pathways remained inhibitory in non-locomoting decerebrate cats in two states. The latencies of inhibition also corresponded to those observed for force feedback from Golgi tendon organs. We

observed variable patterns of force feedback between ankle extensors in decerebrate/control cats. On the other hand we observed consistent results in cats with chronic LSH exhibiting very strong distal to proximal pattern of inhibition from 2 weeks to 20 weeks following chronic LSH. The same results were obtained in acute LSH cats suggest that the change in neuromuscular system appears immediately after SCI and persists even after the animal start walking following SCI. The observed altered pattern of force feedback after spinal cord injury suggests either presence of a pattern intrinsic to the spinal cord or a unique pattern exhibited by the damaged spinal cord. The results are important clinically because even with vigorous rehabilitation attempts patients do not regain posture control after SCI even though they regain ability to walk. Therefore, to effectively administer treatment and therapy for patients with compromised posture control, a complete understanding of the circuitry is required.

CHAPTER 1

Introduction

Balance is vital to normal everyday life activities such as standing, sitting, getting out of a chair, walking, bending over to put your shoes on, washing your hair, driving a car or going grocery shopping. Ability to maintain balance is a complex process that depends on neuromuscular complex integrating systems. This ability is highly impaired after neurological diseases and injury to central nervous system thus affecting the quality of life in millions of people across the globe.

Sensory motor interactions such as spinal reflexes occur within the spinal cord. They can be modified following spinal cord injury (SCI), due to the loss of excitatory inputs from supraspinal structures and changes within the spinal cord (Frigon and Rossignol 2006; Rossignol and Frigon 2011). Despite extensive research work to date on spinal reflex changes after SCI, understanding of the role played by various sensory inputs interacting with intrinsic spinal circuits and their role in the recovery of motor functions especially balance control after SCI is still limited.

It is well known that animals as well as humans can step on a treadmill after SCI although they are lacking good lateral balance control (Barbeau and Rossignol 1987; Carter and Smith 1986; Grillner 1975; Rossignol et al. 1996). Some weight-bearing capacity may remain following SCI and improve with rehabilitation in both humans and animals (De Leon et al. 1998; Edgerton et al. 2001; Nooijen et al. 2009), however the ability to maintain postural equilibrium and balance does not completely recover

(Barbeau and Rossignol 1987; Lyalka et al. 2009), suggesting that these behaviors are mediated by distinct neural mechanisms requiring integration at many levels of neuromuscular integrated control system.

Loss of postural equilibrium on the other hand starts with spinal cord injury and stays there even after partial or complete locomotor recovery. Therefore, there is a debate about the capacity of spinal cord circuitry for balance control as coordinated postural responses may require supraspinal input considering they are not recovered even after rehabilitation efforts. One group of neuroscientists strongly believes that brain stem input to spinal cord is more important than cortical input to maintain balance control. We know that brainstem neurons are active during balance control (Schepens et al. 2008; Stapley and Drew 2009) and disrupting the connectivity between the brainstem and spinal cord impairs balance control and responses to perturbations (Deliagina et al. 2008; Honeycutt et al. 2009). However, it remains unclear whether these responses reflect an attenuated postural response using the appropriate muscular coordination patterns for balance, or are due to fundamentally different neural mechanisms. In humans despite of locomotive recovery SCI patients are often challenged by an environment that requires alterations in basic movement patterns (Amatachaya et al. 2010) and increased potential for falls (Musselman and Yang 2007; Musselman et al. 2011).

Most of the existing data about postural and motor control is from studies which were conducted using training, drugs (Cote et al. 2003; Cote and Gassard 2004; Ichiyama et al. 2011; Lyalka et al. 2008) and electrical stimulation (Musienko et al. 2010). They have demonstrated improvement of reflex activity and locomotion behavior. However,

there is still little information about load responses using natural/physiological stimuli that can provide comparable data to in vivo behavior of neuromuscular system. Therefore, in order to understand the physiological changes in spinal circuits following SCI by using muscle stretch (natural stimulus) in spinal hemisection animal model in our study should answer some of these questions. The main objective of this study is to understand the role of spinal cord in posture maintenance by understanding the altered intermuscular interactions following SCI. We propose that a detailed understanding of the distribution and functional utility of proprioceptive networks, and how they are modulated by spinal injury both immediately and in long term is necessary to exploit the full potential of sensorimotor training and effectively manage SCI in clinical set up.

1.1 Properties of The Muscular System

Posture control is dependent on coordination between muscular and nervous system. The first response of the body to any outside perturbation comes from the intrinsic musculoskeletal properties. These properties are due to the viscoelasticty of the soft connective tissue component of skeletal muscle tissue that changes in response to change in environment and the mechanical properties of actively contracting motor units (Nichols and Hock 1976). As a result of this change in viscoelasticity of skeletal muscles force is applied on the skeleton to which they are attached. The reflextive properties are due to the presence of specialized sensory components of muscle tissue consisted of muscle spindles, Golgi tendon organs, and cutaneous receptors. These organs sense perturbations and relay that information to spinal cord. The spinal cord in turn is connected by a feedback loop through motor neurons activate muscles throughout the body, further contributing to the response of the body to perturbations.

Muscle spindles are located within skeletal muscle in parallel with muscle fibers. Projections from muscle spindles are mainly excitatory, with some pathways distributed primarily to muscles of similar actions (Eccles et al. 1957; Nichols 1999) and regulate muscular stiffness (Nichols and Houk 1976), even across varying background tension (Hoffer and Andreassen 1981). Muscle spindles provide information related to the length and contraction velocity of muscle fibers (Crowe and Matthews 1964; Edin and Vallbo 1990; Prochazka 1981; Prochazka and Gorassini 1998b). It has been shown that direct negative feedback of spindle afferents enhances the stiffness of muscle and as such helps to stabilize posture and movement (Hogan 1985; Nichols and Houk 1976). Furthermore, several theories of motor control propose that muscle spindle information is used by the CNS to generate muscle activation patterns in a predictive manner (Wolpert et al. 1995; Wolpert et al. 1998).

The most direct and quick spinal reflex pathway is the monosynaptic stretch reflex (Eccles and Lundberg 1958; Liddell and Sherrington 1924) where group Ia afferents from muscle spindle make monosynaptic connections in the spinal cord with alpha motoneurons of the same muscle. 1a afferents respond to the rate of change in muscle length, as well to change in velocity of stretch. They fire when the muscle is stretching, as soon as the muscle stops changing length, the firing rate slows and adapts to the new length. The group II afferents also make mono-synaptic connections to the alpha motoneurons (Kirkwood and Sears 1975). They provide position sense of a static muscle, fire when muscle is static (Michael-Titus and Adina 2007). In addition to the stretch reflex, sensory receptors from a given muscle provide excitatory feedback to synergistic muscles, those of similar action, and inhibitory feedback to antagonist

muscles, those of opposing action (Liddell and Sherrington 1924; Lloyd 1946a; Lloyd 1946b) through interneurons in spinal cord.

Golgi tendon organs (GTO's) are located in muscle tendon in series with muscle fibers and senses changes in muscle tension/ loading. It has been shown that influence the dynamic reaction of a muscle to external perturbations (Houk 1979; Kistemaker and Rozendaal 2011; van Soest and Bobbert 1993). Due to its elastic structure the tendon greatly enhances the mechanical efficiency of movements by storing and releasing energy (Alexander 1984; Alexander and Bennet-Clark 1977). Also, without tendons, the maximal shortening speed of the muscle tendon complex (MTC) would be limited by the maximal shortening velocity of the muscle fibers. With tendons, the maximal shortening velocity of the MTC can well exceed that of the muscle fibers and as such allow mechanical work even at high velocities as in throwing a ball (Joris et al. 1985). Tendons also play a role in very fast muscle stretches (Alexander 2002; Cook and McDonagh 1996; Hof 1998) that occur, for example parajumping.

When the muscle generates force by activation or by stretch it stimulates Ib afferent axon from GTO's caries this information to the spinal cord generating spinal reflexes and supraspinal responses which control muscle contraction. The autogenic inhibition reflex assists in regulating muscle contraction force. GTO's have been classified as providing inhibitory feedback to extensor (antigravity) muscles, particularly across joints and axes of rotation, with very few connections to the muscle of origin (Eccles et al. 1957; Nichols 1989). Their distribution across a limb and joints (Bonasera and Nichols 1994; Eccles et al. 1957; Jankowska 1992; Nichols 1989) maintains whole

limb stiffness and interjoint coordination (Nichols et al. 1999). Therefore they play an important role in maintaining the right amount of muscle contraction across joints required for maintenance of balance. Both length and force feedback can be non-uniform, favoring force generation by one muscle of a pair or at one joint over another (Bonasera and Nichols 1994; Eccles and Lundberg 1958; Nichols et al. 1999; Pratt 1995). Therefore, study of these reflexes in SCI can give us an insight into the underlying physiological changes within these pathways that might be responsible for disturbed balance control.

1.2 Hind Limb Ankle Extensors

The cat hind limb muscles exert torques about different joints and axes of rotation. We have used ankle extensors in this study because they are extensively linked by force feedback and they have been previously studied in our laboratory using decerebrate cats. We have used three multiiarticular muscles including the flexor hallucis longus muscle (FHL), the Gastrocnemius muscle (GA) and the Plantaris muscle (PLT), and the uniarticular Soleus muscle (SOL).

FHL is a strong ankle extensor. It also contributes to, ankle planterflexion, adduction, toe flexion and claw protrusion (Goslow et al. 1972). Its moment arm is one third that of SOL (Young et al. 1992) still its large surface area makes it a major extensor of ankle. This muscle produces more force than SOL and TA (Sacks and Roy 1982) and up to two thirds of the torque of SOL (Lawrence and Nichols 1999). It originates from upper part of fibular shaft and inserts into Flexor digitorum longus (FDL) tendon in foot through a long tendon that passes behind the medial malleolus.

GA originates via two heads from medial and lateral sesamoid bones lateral to medial and lateral epicondyles of femur, respectively, and insert via the Achilles tendon into calcaneus. It therefore spans the knee and ankle joints and therefore provides mechanical coupling between these two joints. It is a large muscle with 55 muscle spindles (Chin et al. 1965) and similar numbers of GTO's (Eldred et al.1962) that is more than any other muscle used in our study. Therefore, its role in producing force to maintain balance and interactions with other muscles in hind limb is vital for understanding the changes in neuromuscular interactions after SCI. SOL originates from Fibula and inserts in calcaneus through a long tendon. It is composed of all slow twitch fibers. It is the only uniarticular muscle used in this study.

PLT originates from lateral part of patella and forms a long tendon that passes between GA and SOL finally inserted into tendon of flexor digitorum brevis (Crouch 1969). Interestingly its size is much bigger in cats in comparison to humans probably due to the fact that cats are toe walkers and need this muscle more frequently. Its big size could also be related to more hopping and jumping in quadrupeds. PLT is a toe flexor as well as ankle extensor, plantarflexor and abductor. This muscle yet contributes very little to the off-sagittal movement of the ankle (Lawrence and Nichols 1999).

1.3 Brain, Brain Stem and Reticular Formation Role in Balance Control and Intermuscular Force Feedback Gradient

Our distal joints such as our fingers can perform more skillful movements than our shoulder. On the other hand it's equally true that our hand and finger muscles are much smaller and less strong in terms of force production than shoulder muscles

(Hamilton et al.2004; Tan et al. 1994). These biomechanical differences between limb segments are not only task related but also have the distinct neuromuscular control of proximal versus distal joints (Kandel et al. 2000; Kurata and Tanji 1986). The corticospinal system has stronger influence over distal than that over proximal muscles (Brouwer and Ashby 1990; Lemon and Griffiths 2005; McKiernan et al. 1998; Palmer and Ashby 1992; Turton and Lemon 1999). This could explain distal joints and muscle control loss after stroke and upper motor neurons insult patients like in SCI (Turton and Lemon 1999; Colebatch and Gandevia 1989). Reticular formation and brain stem affects proximal muscles more potently than distal muscles (Davidson and Buford 2006; Riddle et al. 2009; De Domenico and McCloskey 1987; Tan et al. 1994; Hall and Mc-Closkey 1983; Refshauge et al. 1995). These could also be related to the reported gradient in muscle spindle density (Banks 2006; Buxton and Peck 1990). Reticulospinal tract is important in control of posture (Deliagina et al. 2008; Schepens et al. 2008) in cat.

Physiologically, muscles are also classified into proximal and distal categories on the basis of their relative anatomical origin and insertion (Delay et al. 2007). Grossly, muscles acting at more proximal joints (hip and knee) in hindlimb are referred to as proximal muscles while those acting at comparatively distal joints (ankle, tarsometatarso-phalangeal joints) are classified as distal muscles. Therefore, Quadriceps muscle group acting at hip and knee joints is a proximal group of muscle, while Triceps surae acting at ankle is a distal group of muscle. The same principle can be applied to the muscles acting at the same joint, for example; GA is a proximal muscle in comparison to FHL at ankle joint. GA originates from medial and lateral sesamoid bones lateral to medial and lateral epicondyles of femur bone, respectively, and inserts into calcaneus. FHL originates from

upper part of fibular shaft and inserts via long tendon into sole of foot at FDL tendon. This proximodistal gradient was observed in the control of avian running (Daley et al. 2007), in reflex responses of squirrel monkey (Lenz et al. 1983), and in human motor performance and perception (DE Domenico and McCloskey 1987; Gandevia and Kilbreath 1990; Hall and McCloskey 1983; Tan et al. 1994). Daley proposed a proximo-distal gradient in joint control that is vital for maintaining whole limb mechanics for postural control. Long fibered proximal muscles modulate limb and body work, whereas short-fibered distal muscles with long tendons favor more economical force generation and elastic energy savings (Biewener and Roberts 2000). Since the distal joints are the most directly affected by interaction with the ground, regulation of compliance of distal muscles is critical to determining how the limb will react to the ensuing disturbance.

Since we have postulated that inhibitory force feedback contributes to the regulation of joint and limb compliance, it has been of interest to investigate the strength and distribution of these proprioceptive pathways. Previous published data from our laboratory suggested bidirectional inhibition among ankle extensors. In some decerebrate animals a proximal to distal pattern/directionality of inhibition is seen between ankle extensors whereas in others distal to proximal inhibition is noticed (Wilmink and Nichols 2003; Bonasera and Nichols 1994). However, previous studies did not quantitatively analyze the data to see which directionality of inhibition or pattern of intermuscular interaction is statistically more significant than the other. This idea of proximal to distil gradient is consistently noticed in locomotor animals (Ross and Nichols 2009). Our current study presented in chapter 2, however showed proximal to distal, distal to proximal and bi-directional intermuscular inhibitory force feedback between ankle

extensors in control animals. However, the most common pattern of inhibitory force feedback in decerebrate animals is a balanced bidirectional pattern between ankle extensors as explained in detail in chapter 2.

1.4 Spinal Cord Role in Maintenance of Posture

Human as well as cat interneurons in the spinal cord are involved in mediating both simple reflex responses and complex movements. This function is crucial for maintenance of balance and weight support because it is task dependent. These neurons integrate information from the musculoskeletal system and from the brain (Rossignol and Dubuc1994; Grillner 1975; Dimitrijevic et al. 1998). Therefore, they are not a simple connecting system but powerful processing units like computers. When an animal or human starts to develop the ability to walk independently, the added demands of postural control alter the muscle activation. Infants exhibit a stepping response at birth (Peiper 1961), and even in utero (De Vries et al. 1984). This stepping behavior appears to be controlled largely by the spinal and brainstem circuitry, since anencephalic infants exhibit similar responses (Peiper 1961). However, infants can not maintain balance or weight support suggesting that posture control involves input from higher centers.

1.5 Spinal Cord Injury

Traumatic SCI accounts for an estimated annual incidence of approximately 40 cases per million populations (Bernhard et al. 2005). This number excludes those who died at the scene of an accident. Currently, 183,000-230,000 patients with SCI are alive in the United States. The male-to-female ratio in the United States is 4:1 (NSCISC 2014) and the average age is 31.7 years (Burke et.al 2001). Total direct costs for patients with

SCI in the United States exceed $7 billion per year (Sekhon et al. 2003). The cost to society, in terms of health care costs, disability payments, and lost income, is disproportionately high compared to other medical conditions. Therefore, SCI is a major health issue that needs immediate attention since its affecting our young work force. The most common cause of SCI is traumatic injury (car accident, gunshot, falls, sports injuries, etc.). The spinal cord does not have to be severed in order for a loss of function to occur sometimes damage to its blood supply or compression from surrounding structures can also result in injury. Spinal cord injuries are described as either incomplete", which can vary from having no effect on the patient to a "complete" injury which means a total loss of function (Fulk et al. 2007).

In roadside accidents the initial mechanical trauma is secondary to traction and compression forces. Direct compression of neural elements by surrounding anatomical structures (bone fragments, disc material, and ligaments) damages both the central and peripheral nervous system (Tator 1995). Blood vessel damage also leads to ischemia, rupture of axons and neural cell membranes. Micro hemorrhages occur within minutes in the central gray matter and progress over the next few hours. Massive cord swelling happens within minutes that lead to further secondary ischemia. Loss of auto regulation and spinal shock cause (Ditunno et.al 2004) systemic hypotension and exacerbate ischemia. Ischemia, toxic metabolic compounds, and electrolyte changes cause a secondary injury cascade. Hypo perfusion of gray matter extends to the surrounding white matter and alters the propagation of action potentials along the axons, contributing to spinal shock. Glutamate is a key element in the excitotoxicity. Massive release of glutamate leads to overstimulation of neighbor neurons and production of free radicals,

which kill healthy neurons. Excitotoxic mechanisms kill neurons and oligodendrocytes, leading to demyelination. AMPA (alpha-amino-3-hydroxy-5-methyl-4-isoxazole propionic acid) glutamate receptors play a major role in oligodendrocyte damage.

Below the level of SCI motor function, pain sensation, and temperature sensation are lost, while touch, proprioception (sense of position in space), and sense of vibration remain intact in anterior SCI. Posterior cord syndrome can also occur, but is very rare. Damage to the posterior portion of the spinal cord and/or interruption to the posterior spinal artery causes the loss of proprioception and epicritic sensation (e.g.: stereognosis, graphesthesia) below the level of injury. Motor function, sense of pain, and sensitivity to light touch remain intact. This kind of injury is not common in road side accidents. Brown-Séquard syndrome usually occurs when the spinal cord is hemisectioned or injured on the lateral side. True hemisections of the spinal cord are rare, but partial lesions due to penetrating wounds (e.g.: gunshot wounds or knife penetrations) are more common. On the ipsilateral side of the injury there is a loss of motor function, proprioception, vibration, and light touch. Contralaterally there is a loss of pain, temperature, and crude touch sensation.

The work presented in this thesis has been done in collaboration with Dr. Dena Howland. This model of partial spinal cord injury has already been used by her using cats (Doperalski et al. 2011; Jefferson et al. 2011) and human subjects (Fox et al. 2010; Behrman et al. 2008). Her research focuses on understanding the response of the spinal cord to injury and identifying approaches to enhance repair, plasticity and motor recovery. Therefore, we have used spinal hemisection model in our experiments due to

ease of managing cats post injury (no respiratory, cardiac or bowl control complications) quick recovery and expertise provided by our collaborator to perform the surgeries in animals used in our studies. In addition, this asymmetrical, incomplete surgically precise injury gives us an opportunity to preserve both ascending and descending tracts in one half of the spinal cord. Therefore, we can understand the anatomical and physiological basis of any observed motor deficit observed in cats with chronic LSH.

1.6 Aims, Objectives and Hypothesis

The main Aim of our study is to evaluate any changes or reorganization of inhibitory force feedback patterns between hind limb ankle extensors in decerebrate cat following chronic SCI. This aim is proposed to further validate the use of force feedback measurements from muscles after partial SCI for obtaining insight into alterations of proprioceptive network in spinal cord. Our data indicate that in chronic lateral spinal hemisection inhibitory force feedback appears to be enhanced and repatterned/redistributed in comparison to control data from decerebrate animals without SCI. We therefore hypothesize that reduced weight support and balance control following chronic LSH is due in part to enhanced and redistributed inhibitory force feedback. Understanding how the inhibition is redistributed following SCI will help us understand how the mechanical properties of the limb are changed in the injured state. We hypothesize that heterogenic force feedback pathways remain inhibitory following SCI however; their strength and directionality or pattern may alter as a result of SCI. we will verify that inhibitory responses observed are indeed due to force feedback from Golgi tendon organs by evaluating the latency of the inhibition. Since clasp-knife inhibition has

a much longer latency than force feedback, the two sources of inhibition should be distinguishable.

The second aim of our study is to determine the time of onset of possible altered neuromuscular interaction following SCI and their relationship to posture control. After chronic partial spinal cord injury (SCI), various sensorimotor functions can recover, ranging from simple spinal reflexes to more elaborate motor patterns, such as locomotion requiring posture control. However, complete posture control is never regained in animals. We propose that in acute animals when the spinal networks are not yet subjected to plastic changes (Ditunno et al. 2004; Valero-Cabre et al. 2004), we might get different results than in chronic animals. Comparing neuromuscular interactions in chronic and acute SCI between hind limb extensors can help us determine the time of onset of any intermuscular interactions and their relationship to poor posture control in SCI. If we get different results in acute and chronically spinalized animals it will prove that the neural control of posture and balance control as well as weight support during locomotion involve different mechanisms and different neural structures. We are interested to see if any redistribution or change in strength is the result of an adaptive process following LSH. We propose that any alteration in intermuscular force feedback interactions can affect inter joint coordination required for posture control following SCI. We hypothesize that different pathways may be involved in posture control during locomotion and quiet standing. This is because cats with chronic LSH can walk, exhibit good weight support and maintain balance control during locomotion. On the other hand they fail to maintain posture when exposed to certain perturbation. If we get different results in chronically spinalized static animals used in our study from earlier studies in decerebrate locomoting

cats (Ross and Nichols 2009), it will prove that the neural control of posture and balance control during locomotion involve different mechanisms and different neural structures.

The third aim of our study is to determine the directionality or gradient of distribution of force feedback between extensor muscles in the hind limb of decerebrate cat. The main purpose of this aim is to understand and establish the intermuscular interactions that have either not been studied or quantitatively analyzed earlier or have limited data. We are interested to revisit Daley's hypothesis (Daley and Biewener 2007) to ascertain whether force feedback could provide the substrate for regulating the stiffness of the distal limb, and in order to broaden our understanding about the amount and direction of inhibitory force feedback between muscles of the hind limb in animals (decerebrate) under static condition. We are particularly interested to study interactions of flexor hallucis longus (FHL) with gastrocnemius (GA), soleus (SOL), plantaris (PLT) to obtain a complete picture of inter- muscular interactions for muscles crossing the ankle. We have used this as control data in addition to the control data from earlier work in our laboratory to compare with our data from cats with spinal injury. We hypothesize that the ability of the neuromuscular system to maintain a pattern or directionality of inhibitory force feedback is task dependent and important to maintain posture in response to perturbations. This ability is lost in LSH. In chapter two we have described our observations regarding intermuscular inhibitory heterogenic force feedback in decerebrate animals.

The fourth aim of our study is to determine which possible descending pathways might be involved in altered intermuscular interactions following SCI. In chapter three

and four we have described our observations regarding these intermuscular force feedback interactions in a comparative manner in chronic LSH, acute LSH and dorsal LSH (preliminary data). We propose that ventral or ventromedial spinal pathways may be involved in regulating the pattern and strength of force feedback, as also suggested by recent findings that the strength of force feedback is regulated through signals deriving from neck and vestibular afferents (Gottschall and Nichols 2007) in decerebrate cats. We also propose that pontine reticulo- spinal and vestibulospinal pathways are important to maintain postural control. To test this hypothesis we have compared force feedback interactionsour between FHL and GA in LSH data with dorsal hemisection (DSH) data in chapter 3. However, we have limited evidence of existence of this mechanism between other muscle combinations.

The automatic postural response control mechanism appears to exist in the spinal cord. This system is insufficient following SCI and can affect the animal's ability to maintain balance control stability in the absence of central drive. Cats that have been chronically spinalized can be trained to stand and step with full weight support (Barbeau and Rossignol 1987; Carter and Smith 1986) however these chronic cats have poor balance control if exposed to postural perturbations. Since interlimb coordination is required during locomotion, we propose that interlimb coordination is preserved after SCI. We hypothesize that following LSH whatever neuromuscular alterations appear in spinal cord should be seen bilaterally (both on injured and uninjured side). This is due to the bilateral distribution of pathways and interconnections of neurons at the level of the spinal cord/ CPG. To test our hypothesis we have compared data in both hindlimbs of each cat in our study in chapter 2, 3 and 4.

The results of these experiments are clinically significant, especially for the rehabilitation of spinal cord injured patients. To effectively administer treatment and therapy for patients with compromised spinal reflexes, a complete understanding of the spinal circuitry is required.

Chapter 2 explains in detail the patterns of heterogenic force feedback between ankle extensors in decerebrate non-locomoting cats with intact spinal cord. This chapter details control data for our study. Chapter 3 describes detailed analysis of intermuscular force feedback patterns between GA and FHL. This chapter explains in detail all the characteristics of intermuscular force feedback interactions between ankle extensors that have already been observed in cats with intact spinal cord. The main purpose of this chapter is to determine any change in force feedback patterns following LSH (both acute and chronic SCI). This chapter also compares injured side limb with intact side limb force feedback patterns. In addition analysis of force feedback is done across animals. Chapter 4 represents force feedback interactions between SOL, PLT and FHL following both chronic and acute SCI. The data is analyzed in a comparative manner to observe force feedback patterns across hind limbs in each cat and across animals. Chapter 5 explains the possible anatomical, mechanical and physiological explanations of force feedback patterns in decerebrate cats (non-locomoting and locomoting) both with intact spinal cord as well as in cats following SCI.

CHAPTER 2

PATTERNS OF HETEROGENIC FORCE FEEDBACK BETWEEN ANKLE EXTENSORS IN DECEREBRATE CATS

2.1 Introduction

During upright stance while animals are suspending their body above the ground by means of legs, the controlling neuromuscular system must maintain posture against de-stabilizing internal (Breathing, heartbeat, neural noise, muscle tremor) and external (gravity, changes in support, pushes to the body, sudden obstacles) perturbations. In order to preserve equilibrium, the CNS must take these actions quickly and in a precisely calibrated manner. Therefore the brunt of the active muscle work has to be carried by the physiological limb extensor (‘anti-gravity’) muscles, which once active also provide most of the stiffness. Sensory feedback from muscles to spinal cord plays an integral role in standing and locomotion (Pearson 1995; Prochazka 1996; Duysens et al. 2000; Sinkjaer et al. 2000; Stein et al. 2000). Given the substantial role of Proprioreceptive feedback to the generation of ankle extensor activity, it is important to identify the individual contributions from each intermuscular interaction in maintaining ankle stability.

The cat hindlimb muscles have been traditionally classified into extensors and flexors muscles that act outside the sagittal plane. Physiologically, muscles are also classified into proximal and distal categories on the basis of their relative anatomical origin and insertion (Delay et al. 2007). Grossly, muscles acting at more proximal joints (hip and knee) in hindlimb are referred to as proximal muscles while those acting at

comparatively distal joints (ankle, tarsometatarso-phalangeal joints) are classified as distal muscles. This proximo-distal gradient was observed in the control of avian running (Daley et al. 2007), in reflex responses of squirrel monkey (Lenz et al. 1983), and in human motor performance and perception (DE Domenico and McCloskey 1987; Gandevia and Kilbreath 1990; Hall and McCloskey 1983; Tan et al. 1994). Daley proposed a proximo-distal gradient in joint control that is vital for maintaining whole limb mechanics for postural control. Long fibered proximal muscles modulate limb and body work, whereas short-fibered distal muscles with long tendons favor more economical force generation and elastic energy savings (Biewener and Roberts 2000). Since the distal joints are the most directly affected by interaction with the ground, regulation of compliance of distal muscles is critical to determining how the limb will react to the ensuing disturbance.

Since ankle extensors play an important role in posture maintenance, they have been extensively studied in our laboratory in decerebrate cats over a wide range of background forces (Nichols 1989; Bonasera and Nichols 1994) and locomotion (Ross and Nichols 2009). The strength of this feedback was found to be force dependent, providing strong evidence that the feedback arises from Golgi tendon organs (Nichols 1999). We have learned from these studies that FHL, GA, SOL and PLT exchange predominately force dependent inhibitory intermuscular force feedback in decerebrate cats. This feedback has a well defined consistent pattern in locomoting cats with predominantly proximal to distal in gradient/strength of inhibition between GA and FHL, distal to proximal between FHL and PLT and bidirectional between FHL and SOL across preparations. Similarly as described in chapter 3 and 4 we indeed found evidence for a

well defined uniform pattern of inhibitory force feedback in cats with SCI. We have observed a strong distal to proximal gradient of inhibitory force feedback between FHL, GA, SOL and PLT. However, we don't know the direction of inhibition between these muscle combinations in non-locomoting decerebrate cats.

Our main goal for the study presented in this chapter was to quantitatively analyze intermuscular inhibitory force feedback in decerebrate non-locomoting cats to determine if there is a well define gradient/ pattern of heterogenic force feedback among GA, PLT, SOL and FHL in decerebrate cats. Our aim was to obtain a complete pattern of feedback in each animal. Since these patterns can be variable, it is not sufficient to pool data from different animals. Proximal and distal ankle extensor is a relative term used in our study. We have classified proximal and distal muscles on the basis of their relative anatomical origin in hindlimb. We propose that the loss of ability of an animal to alter heterogenic inhibitory connections in response to perturbations could be responsible for poor posture control in SCI. We further propose that the inhibitory intermuscular force feedback connections could have variable patterns across animals with an intact spinal cord representing different motor states.

2.2 Methods

2.2.1 Preparation

We used the mechanographic technique to evaluate the distribution of force feedback from muscle receptors, which has been previously described (Nichols 1987), thus only a brief description will be presented here. All protocols are in complete

accordance with the guidelines of both the Federal and Institutional Animal Care and Use Committee of Georgia Institute of Technology.

Briefly, ten cats ranging from 4 to 4.5 kilograms were used that were housed in the same environment in animal house at Georgia Institute of Technology. They were not given any locomotor or behavioral training prior to the terminal experiments. Each cat was deeply anesthetized using isoflurane gas. A tracheotomy was performed, loosened sutures were placed around the carotid arteries, and a cannula was inserted into the external jugular vein to administer intravenous fluids during the experimental procedure. Withdrawal responses were monitored, and the level of anesthetic was adjusted accordingly.

Both hindlimbs were shaved and bone pins were inserted in the femur and tibia respectively. The animal was placed in the stereotaxic frame, supported above a static frame. Then both hindlimb were immobilized by clamping to the static trademill frame, while maintaining the knee at a 110^{o} angle and ankle at 90^{o} angle (mid-stance). The muscles were dissected, carefully removing associated connective tissue to minimize mechanical coupling, yet preserving the blood supply and nerve innervation. The muscles, namely GA (with a fragment of calcaneus), SOL (with a fragment of calcaneus), PLT, and FHL of both hindlimbs were dissected. Both PLT and FHL were cut near their insertion onto FDB and FDL respectively. Each muscle was attached via its tendon to individual clamps. These tendon clamps were placed in series with myographs using strain gauges in a half bridge configuration, and four linear motors (attaching two muscles in each limb at one time to the motors). Normal sailne was used to ensure that

the muscles stayed moist. Hook or cuff electrode was placed around tibial nerve in each limb. Figure 2.1 depicts this experimental setup.

An intercollicular decerebration was performed in each animal after the muscle dissection was complete as depicted in figure 2.2. All brain tissue rostral to the transection. Gelfoam and cotton were placed on the base of the cranium to minimize bleeding. Anesthesia was then titrated down slowly and withdrawn.

Data collection was started once good muscle tone was returned in forelimbs. Data were acquired while the muscles were quiescent as well as when they were activated by the crossed-extension reflex (XER). The stretches were of 2 mm with a rise period of 50 ms and a hold phase of 100 milliseconds (ms). Amplitude of 2 mm was chosen to fall generally in the range of active lengthening during locomotion. The rise time of 50 ms was rapid enough to provide a sufficiently large prereflex force for reliable measurement of the intrinsic mechanical response of the muscle. This measurement was useful to detect the presence of mechanical artifacts. The trials with mechanical artifact were not included in data analysis. At the end of each experiment, the animal was euthanized with an overdose of Nembutal followed by a pneumothorax.

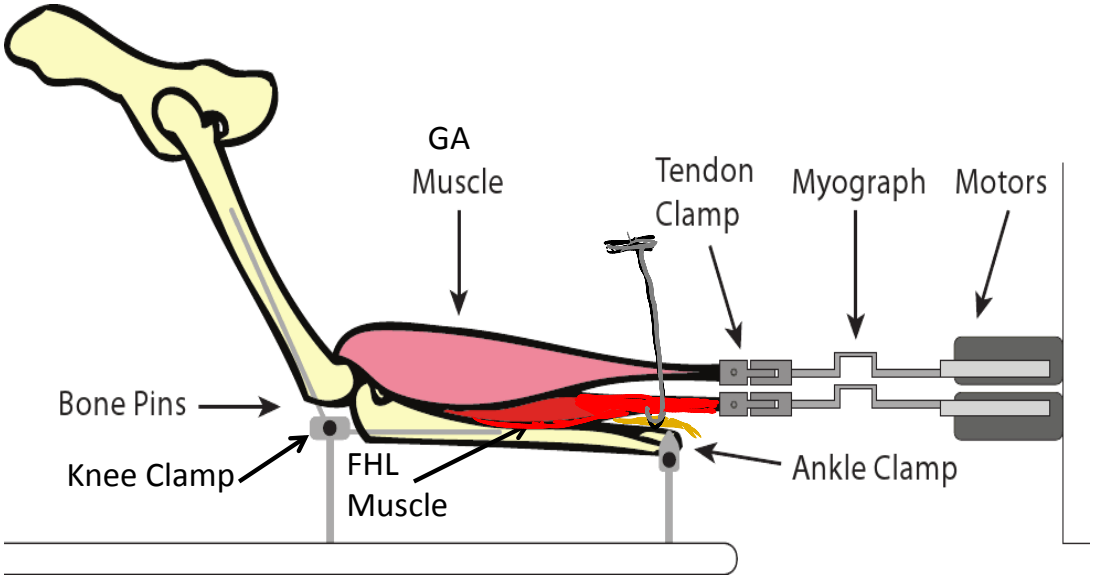

Figure 2.1 Experimental setup for GA (Pink) and FHL (Red) muscle puller experiment. Each muscle is attached to a myograph and linear motor in series. Tibial nerve (yellow) is stimulated with an electrode for XER.

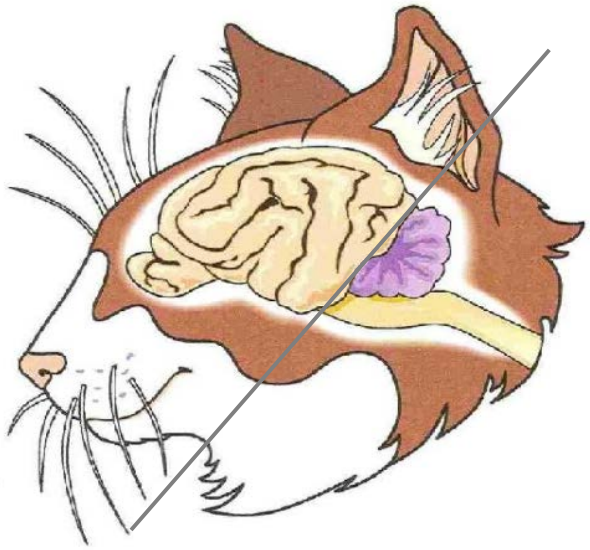

Figure 2.2 Diagrammatic representation of an intercollicular decerebration in cat. All brain rostral to transaction (grey line) removed.

2.2.2 Data Acquisition

The motors used in these experiments were Parker 406LXR linear motors with an encoder resolution of 0.1 microns, maximum acceleration of approximately 50 m/s^2, and maximum load capacity of 180 Kgf. Each of the 4 linear motors were mounted on a custom-built aluminum frame and could be adjusted in the horizontal, vertical, and diagonal directions to achieve proper alignment with the appropriate muscle in different cats with different heights. The four individual frames were mounted on a rigid, outer frame.

The motors were controlled using a 6000 series Gemini servo drive and dSPACE board, and Simulink program. Data was acquired digitally through the dSPACE board at a sampling rate of 1000 Hz. The typical paradigm was a 2 mm stretch at a velocity of 0.04 m/s, 100 ms hold period, and 2 mm release. In each trial stretches of the recipient were performed alone (state 1) in alternation with stretches of both donor and recipient muscle (state 2). Two groups of records resulted from this protocol, namely, one with stretch of the recipient only and one with stretch of both muscles. Heterogenic reflex effects were detected by changes in the magnitude of the reflexes in the recipient muscle from state 1 to state 2. Force responses in state 1 were purely autogenic, and responses in the state 2 consisted of autogenic and heterogenic components (compound responses). Finally, calculating the voltage outputs with no load and with a 1 kg load completed a two-point calibration of the strain gauges (both at the start and end of an experiment).

2.2.3 Data Analysis

Force measurements were used to determine intermuscular heterogenic feedback pathways when muscles were alternatively stretched. Measured forces of the recipient muscle in state 1 and state were divided in three time points namely, mechanical (10 ms following the beginning of the stretch), dynamic (50 ms following the beginning of the stretch) and static (100 ms following the beginning of the stretch). Each file contained data for a particular muscle combination (i.e. GA and FHL or PLT and FHL or SOL and FHL), consisted of 40 to 60 stretches, where half of the stretches occurred in state one and half in state two. Force output and length input of muscles in each trial was recorded. Software in Matlab version 7.01 was then used to analyze the data. A baseline was then fit to the 10 ms prior to stretch and the 10 ms following the return to the initial position to account for a shifting baseline. The baseline was constructed by performing a linear interpolation from the mean force response just prior to the stretch to the mean force after the end of the release. The entire baseline was then subtracted from the overall force response and the resulting baseline subtracted force data was used for further data analysis.

To evaluate the strength and sign of heterogenic force feedback between muscles during a trial, force responses of recipient muscle for a specific time point are plotted as a function of its background force. Each data point represents a response of the recipient muscle obtained when the muscle was either stretched alone (filled squares in Figure 2.1) or response of the recipient muscle when it was stretched with another muscle (circles in Figure 2.1), and individual responses represent an individual stretch at a given time point.

Polynomial fits and 95% confidence intervals were fit to each population of data for a given time point (mechanical, dynamic, static).

Additionally, the amount of heterogenic inhibition in Newton (N) was calculated by subtracting the individual force responses in state 1 from state 2 at a given time point with approximately matching background forces. Polynomial were fit to each population of data for a given time point (mechanical, dynamic, static). Additionally, this inhibition in N was converted into percent inhibition and Polynomial were fit to each population of data for a given time point. Statistics were performed using Statistica 6.0 and Excel to test the separation of the data populations. Multiple regression analysis was used to statistically prove that the two populations were distinctly different only if the P value of ≤ 0.01 was obtained. We chose $P \leq 0.01$ in accordance to the previous research work in our laboratory (Nichols 1989; Bonasera and Nichols 1994; Bonasera and Nichols 1999; Ross and Nichols 2009). The P value of ≤ 0.01 means that the likelihood that the phenomena tested occurred by chance alone is less than 1%. The lower the P value, the less likely the finding would occur by chance alone.

To understand the mechanisms underlying force dependent inhibition between FHL and other antigravity muscles in our study latency of recipient force response was calculated for each muscle combination. According to previous studies the reflex latency of the force dependent inhibition between FHL, GA, SOL and PLT occurred at 28 ± 4 ms (Bonasera and Nichols 1994).

2.3 Results

Previous data from our laboratory determined that the heterogenic feedback pathways among GA, SOL, PLT and FHL are predominately force dependent and inhibitory under conditions of constant force production (Bonasera and Nichols 1994; Nichols 1999). The purpose of these studies was to analyze the relative distribution of the force feedback patterns among ankle extensor muscles in the hindlimb in each cat. This chapter details results from ten experiments.

The main observation from these studies was that the heterogenic inhibition between GA, SOL, PLT and FHL is symmetric across limbs in each animal. However, the pattern/directionality of inhibition within each limb was variable across animals. We observed variable patterns of inhibitory force feedback among ankle extensors (proximal to distal, distal to proximal and symmetric). Specifically, the heterogenic inhibition between GA and FHL showed the most variable results. We concluded that the most common pattern of inhibitory force feedback between GA and FHL is a balanced bidirectional inhibition, however we also observed proximal to distal and distal to proximal pattern between these two muscles. We also observed modest bidirectional symmetric force feedback between FHL and SOL during XER (Nichols 1994). The heterogenic inhibitory force feedback between PLT and FHL was generally stronger from FHL (distal muscle) on to PLT (proximal muscle) across animals.

2.3.1 Force feedback inhibition between GA and FHL

The heterogenic force feedback between GA onto FHL was examined in ten total experiments using decerebrate non-locomoting cats. Of these experiments evaluating the interaction between GA and FHL, five demonstrated symmetric inhibition between GA and FHL (P value $\leq$ 0.01). Three preparations exhibited predominantly stronger inhibition of GA by FHL at P value < 0.01 in comparison to weaker inhibition from GA onto FHL with P value $\geq$ 0.01 as seen in SCI cats in chapter 3. However, the amount of inhibition of GA by FHL was smaller in amount in decerebrate cats with intact spinal cord in comparison to cats with SCI. The remaining 2 preparations demonstrated strong inhibition of FHL by GA at P value $\leq$ 0.01 and FHL inhibiting GA weakly at P value $\geq$ 0.01, as previously shown in both decerebrate locomoting and non-locomoting cats (Bonasera 1994; Ross and Nichols 2009). The directionality of inhibition was variable across cats however it stayed symmetric across limbs in each animal.

All ten experiments presented in this study exhibited heterogenic inhibition between GA and FHL. We observed 5/10 cats (50%) exhibiting balanced/ symmetric inhibitory feedback (5 to 10 observations per cat). We observed that the inhibition was either bilaterally significant at P value $\leq$ 0.01 (clearly separate confidence intervals) or bilaterally insignificant at P value $\geq$ 0.01 (overlapping confidence intervals) between GA and FHL. Our criterion for balanced inhibition between muscles was that we considered it symmetrical if the difference between the two directions of inhibition was less than 5%, considering it could be due to mechanical artifacts. The second type of heterogenic inhibitory interaction between GA and FHL was from proximal muscle/GA onto distal muscle/FHL. This type of inhibition was observed in 2/10 cats (20%) usually 5 to 10

observations per cat. The third type of heterogenic inhibitory force feedback pattern of predominantly distal to proximal inhibition was observed in 3/10 cats (30%).

Figures 2.3 and 2.4 depict representative raw data from part of a single trial in each figure, consisting of alternating state one and state two stretches in a decerebrate non-locomoting cat. Figures 2.3a and 2.4a depict the force output of GA while Figures 2.3b and 2.4b represent length input respectively of GA (proximal muscle) in a trial. Figures 2.3c and 2.4.c depict the force output of FHL while Figures 2.3d and 2.4d represent length input of the FHL muscle (distal muscle) respectively in the same trials. Additionally, the blue dashed lines indicate state 2 where recipient muscle was stretched along with donor muscle during XER. State one response in Figures 2.3 and 2.4 is shown without the dashed blue lines. In this particular example we observed balanced pattern of inhibition between GA and FHL.

Figure 2.5 through Figure 2.7 depict representative examples of three patterns/directionality of heterogenic inhibition observed between GA and FHL in a decerebrate non-locomoting cat in individual trials consisted of 40 to 60 stretches each. The left half of each figure (Figure 2.5, Figure 2.6, Figure 2.7) represents the inhibition of FHL by GA while right half of each figure (Figure 2.5, Figure 2.6, Figure 2.7) represent inhibition of GA by FHL at mechanical, dynamic and static time points from above downwards respectively. Heterogenic inhibition is not due to a purely mechanical event (Figures 2.5a, 2.5d, 2.6a, 2.6d, 2.7a, 2.7d) and increases with increasing background force for the dynamic and static responses, as indicated by the divergence in the polynomial fits in Figure 2.5, Figure 2.6 and Figure 2.7.

The traces inset in each Figure 2.5 through Figure 2.7 are force responses of the recipient muscle in state one (solid black line) and state two (dashed grey line). The background force for both conditions was matched at the mean background force for each muscle combination in a given trial. Baselines were subtracted from both traces to better illustrate the magnitude and time course of the inhibition between GA and FHL. As shown by these traces, the magnitude of inhibition remains relatively equal during the stretch and hold period between GA and FHL in Figure 2.5. In this representative trial we observed 3.6N inhibition (25%) from GA onto FHL and 3.8N (26%) from FHL onto GA (averaged across trials) at $P < 0.01$.

Figure 2.6 depicts a representative example of stronger heterogenic inhibition from GA to FHL in a decerebrate non-locomoting cat. The magnitude of inhibition is relatively stronger from GA onto FHL (Figure 2.6e, Figure 2.6f) in comparison to inhibition from FHL onto GA (Figure 2.6b, Figure 2.6c). In this representative trial we observed 5.2N inhibition (44%) from GA onto FHL at P value < 0.01 and 2N (18%) from FHL onto GA (averaged across trials) at P value > 0.01. The third pattern of intermuscular inhibitory force feedback between GA and FHL is demonstrated in Figure 2.7. The magnitude of inhibition from FHL onto GA is stronger (Figure 2.7b, Figure 2.7c) in comparison to inhibition from GA onto FHL (Figure 2.7e, Figure 2.7f). In this case we observed 5.8N (48%) inhibition of GA by FHL at P value < 0.01 and 2.7N (13%) inhibition of FHL by GA at P value > 0.01.

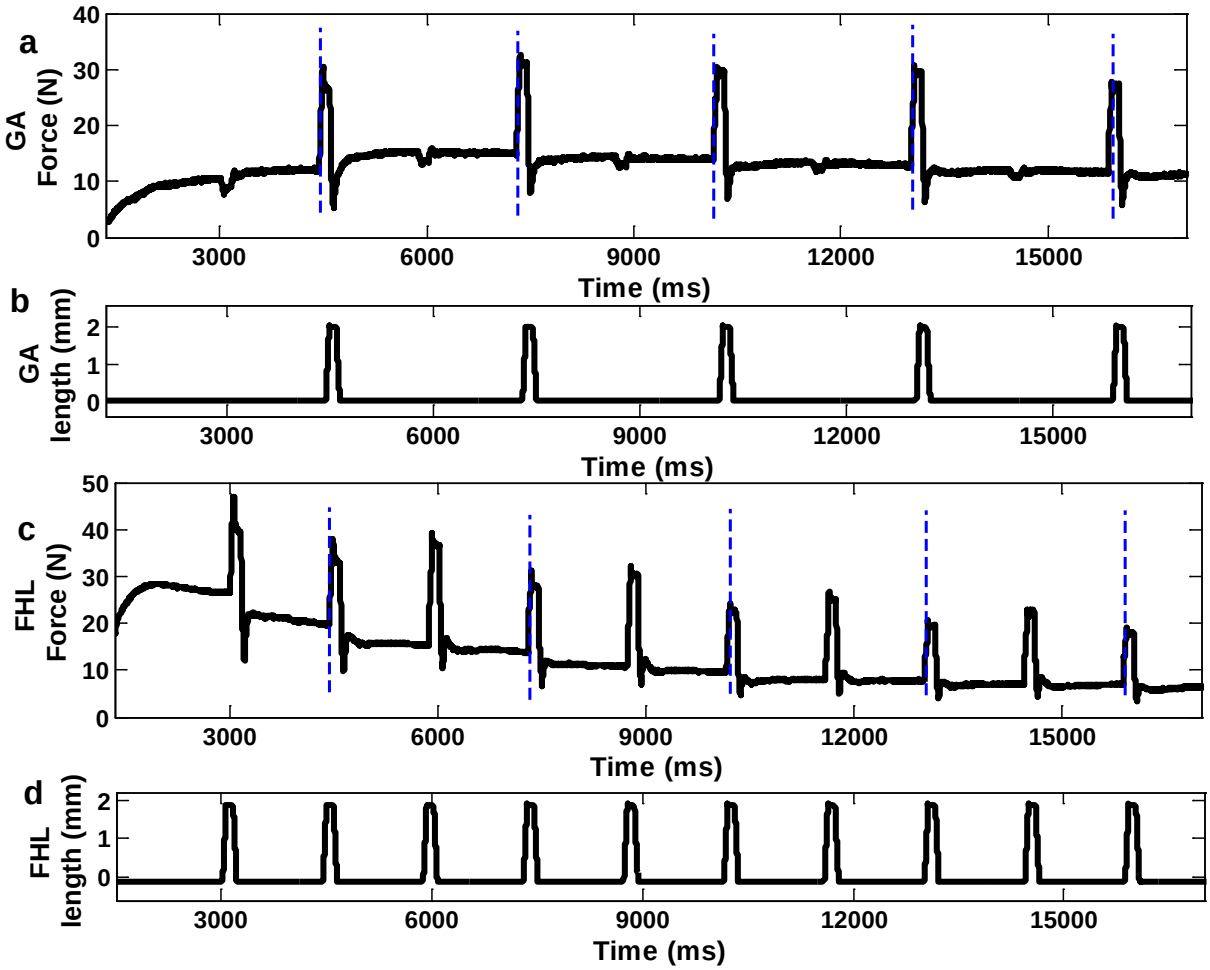

Figure 2.3 (a) Donor muscle (GA) stretch-evoked force response during XER. (c) Recipient muscle stretch-evoked force response during XER. Dashed blue lines on stretches indicate responses obtained when the donor muscle is stretched with recipient muscle at the same time in state 2. The y-axis is showing force response in N and x-axis is showing time in ms. Force responses without dashed blue lines indicate state 1, where recipient muscle was stretched alone. (b) Donor muscle (GA) length input to two-state stretch, where y-axis represent GA length in mm and x-axis represents time in milliseconds. (d) Recipient muscle (FHL) length input for two-state stretch. A two-state stretch is performed to ascertain strength and sign of feedback between recipient muscle (FHL) and donor muscle (GA). There is clearly some inhibition from GA onto FHL in state 2 (c). XER is done by stimulating tibial nerve in the left hindlimb in this example at 2T that evokes an increase in the background force of the recipient and donor muscles on the right hindlimb, GA and FHL respectively (a, c).

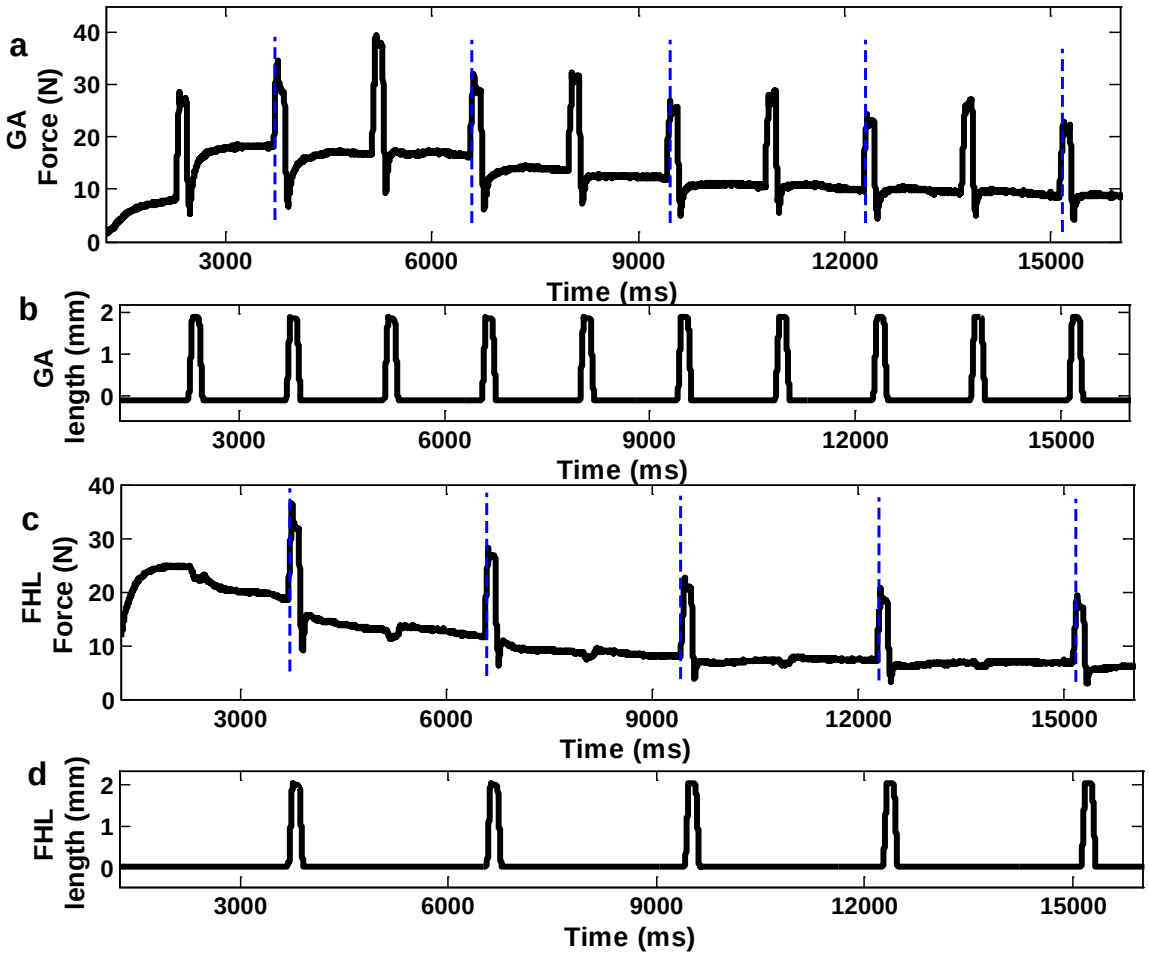

Figure 2.4 (a) Recipient muscle (GA) stretch-evoked force response during XER. (c) Donor muscle stretch-evoked force response during XER. Dashed blue lines on stretches indicate responses obtained when the donor muscle is stretched with recipient muscle at the same time in state 2. The y-axis is showing force response in N and x-axis is showing time in ms. Force responses without dashed blue lines indicate state 1, where recipient muscle was stretched alone. (b) Recipient muscle (GA) length input to two-state stretch, where y-axis represent GA length in mm and x-axis represents time in milliseconds. (d) Donor muscle (FHL) length input for two-state stretch. A two-state stretch is performed to ascertain strength and sign of feedback between recipient muscle (GA) and donor muscle (FHL). There is clearly some inhibition from FHL onto GA in state 2 (c). XER is done by stimulating tibial nerve in the left hindlimb in this example at 2T that evokes an increase in the background force of the recipient and donor muscles on the right hindlimb, GA and FHL respectively (a, c).

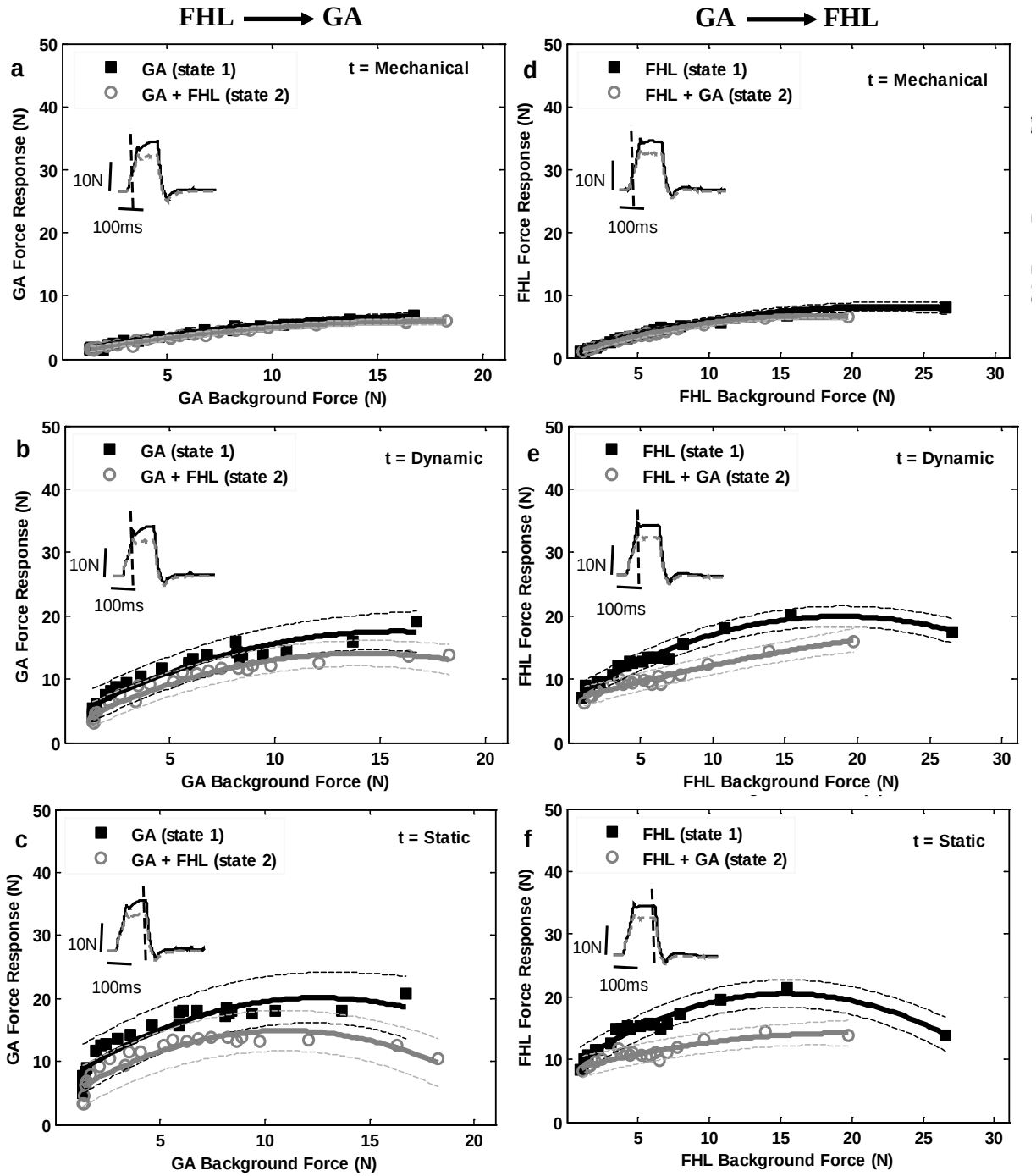

Figure 2.5 Symmetrical/bidirectional pattern of heterogenic inhibition between GA and FHL during XER for (a, d) mechanical phase, (b, e) dynamic phase, and (c, f) static phase. Black squares represent force responses of recipient muscle from stretches occurring in state one and grey circles in state two, respectively. Polynomials and 95% confidence intervals are fit to each population of data. The inserts in (a), (b), (c), (d), (e) and (f) shows two traces (state 1 black solid line, state 2 grey dashed line) matched at approximately mean background force of recipient muscle, superimposed to illustrate the magnitude of inhibition between GA and FHL, the vertical line indicates the sample time in each trace.

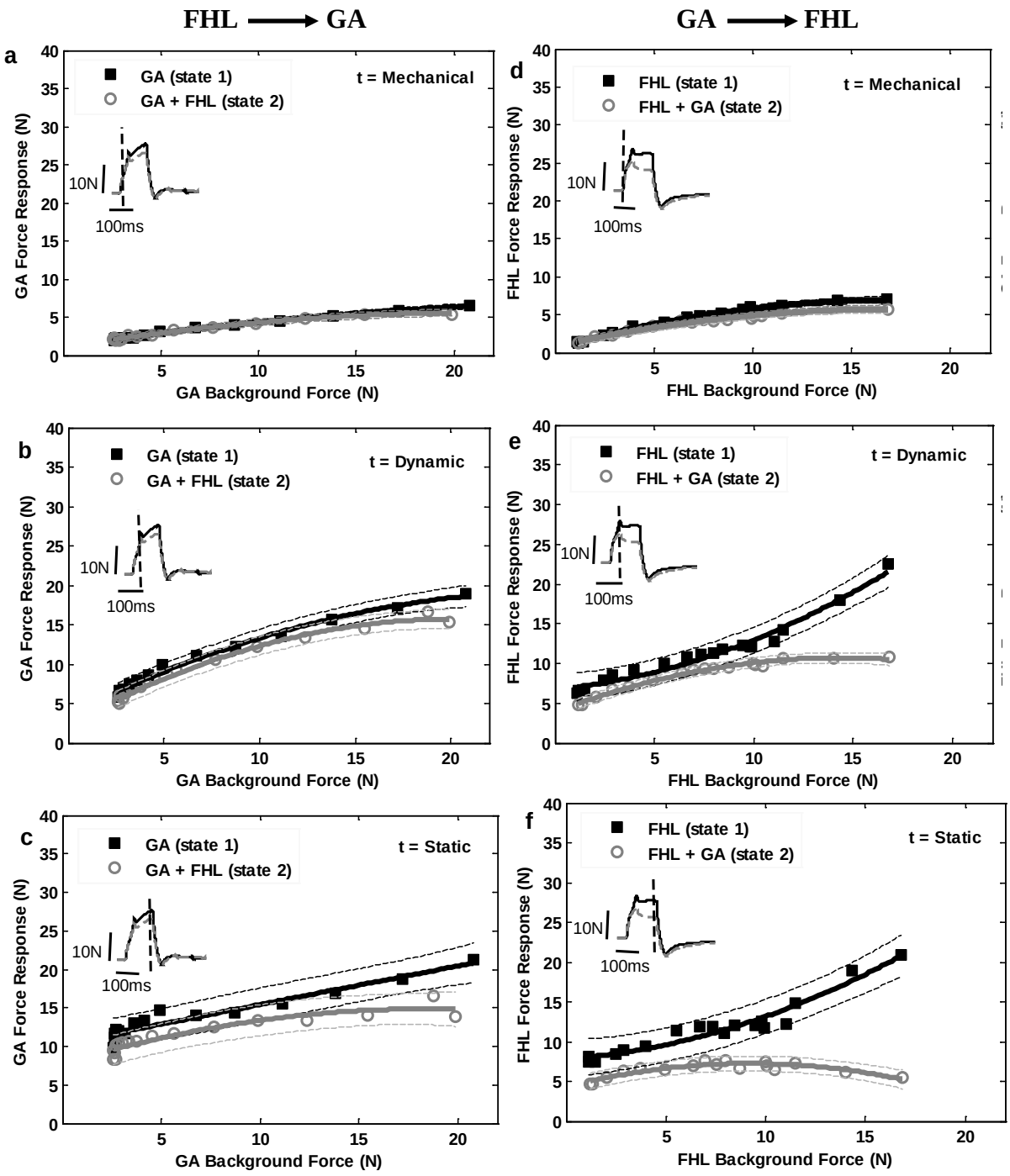

Figure 2.6 Proximal to distal pattern of heterogenic inhibition between GA and FHL during quiet stance with XER in a decerebrate cat in (a, d) mechanical phase, (b, e) dynamic phase, and (c, f) static phase. The same conventions as Figure 2.1 apply. GA is strongly inhibiting FHL at P < 0.01 (c, d, e, f).

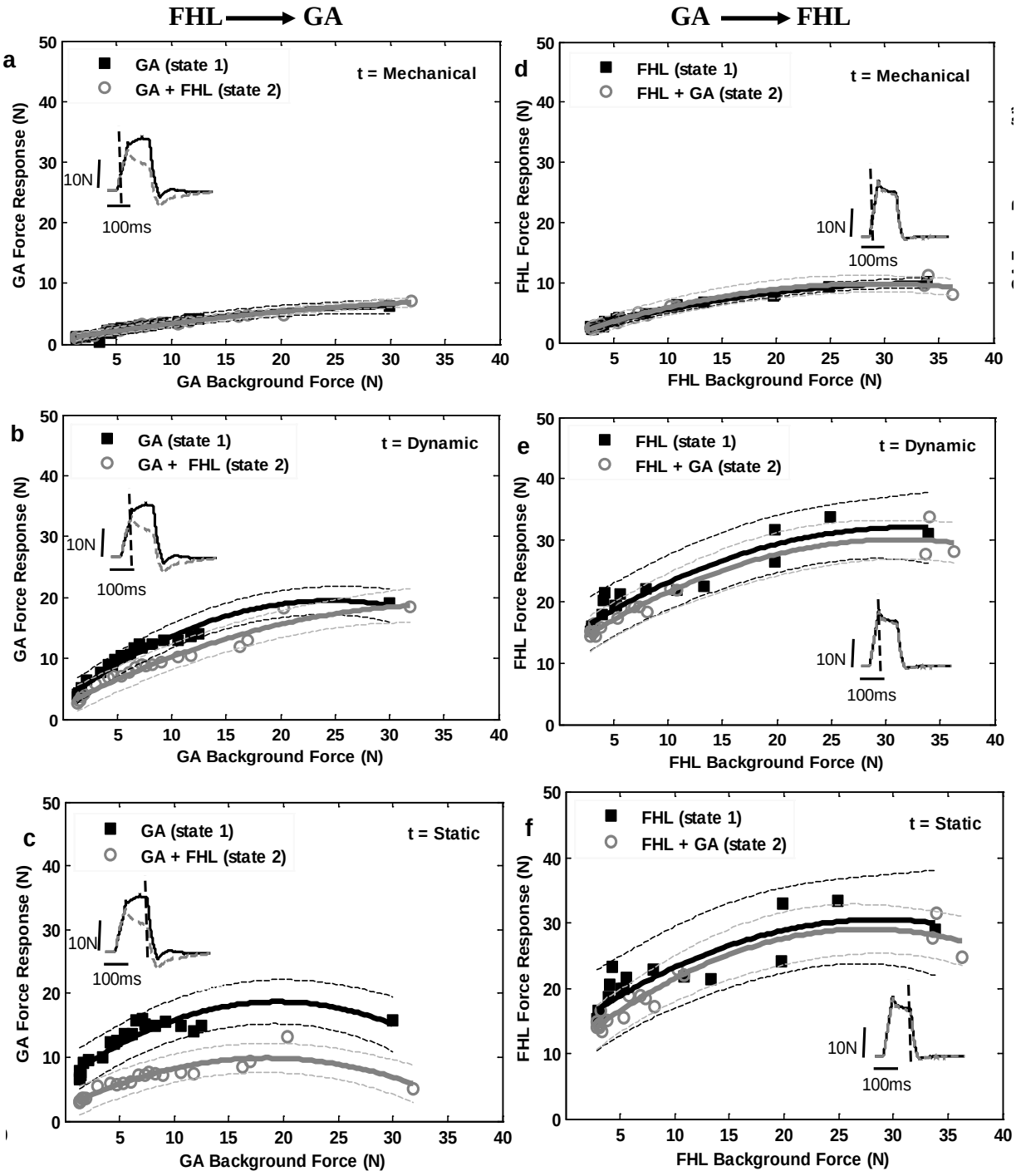

Figure 2.7 Distal to proximal pattern of heterogenic force feedback inhibition between GA and FHL during XER in a decerebrate cat for (a, d) mechanical phase, (b, e) dynamic phase, and (c, f) static phase. The same conventions as Figure 2.1 apply. FHL is strongly inhibiting GA at P < 0.01 (a, b, c).

2.3.2 Weak Inhibition is exchanged between FHL and SOL

The heterogenic feedback between SOL and FHL was examined in 5 decerebrate cats in both hindlimbs (10 limbs), 4 to 6 observations per cat. It has been previousely reported to exchange inhibitory force feedback with FHL during the cross extension reflex in non-locomoting cats (Bonasera and Nichols 1994; Nichols 1989). We observed bidirectional mutually symmetric inhibition between SOL and FHL in 5/5 cats (100%) at P value < 0.01. In most, but not all cases, this also corresponds to non-overlapping confidence intervals (data not significantly different). The inhibition in both directions (SOL onto FHL and FHL onto SOL) was weak though statistically significant at P value ≤ 0.01 in 70% of trials across animals. The range of inhibition was 3% to 21% (1-4 N) across animals.

Figure 2.8 illustrates a representative example of the heterogenic inhibitory force feedback that exists between FHL and SOL. The left half of figure 2.8 (a,b,c) depict inhibition of SOL by FHL and right half (d,e,f) inhibition of FHL by SO. In this example, the confidence intervals are separate for the two populations of data, confirming that there is significant heterogenic inhibition between SOL and FHL. Additionally, multiple regression analysis yielded P value < 0.01 in both directions (SOL onto FHL and FHL onto SOL), thus statistically proving that these populations are distinctly different. The inhibition is less than 2N in both directions.

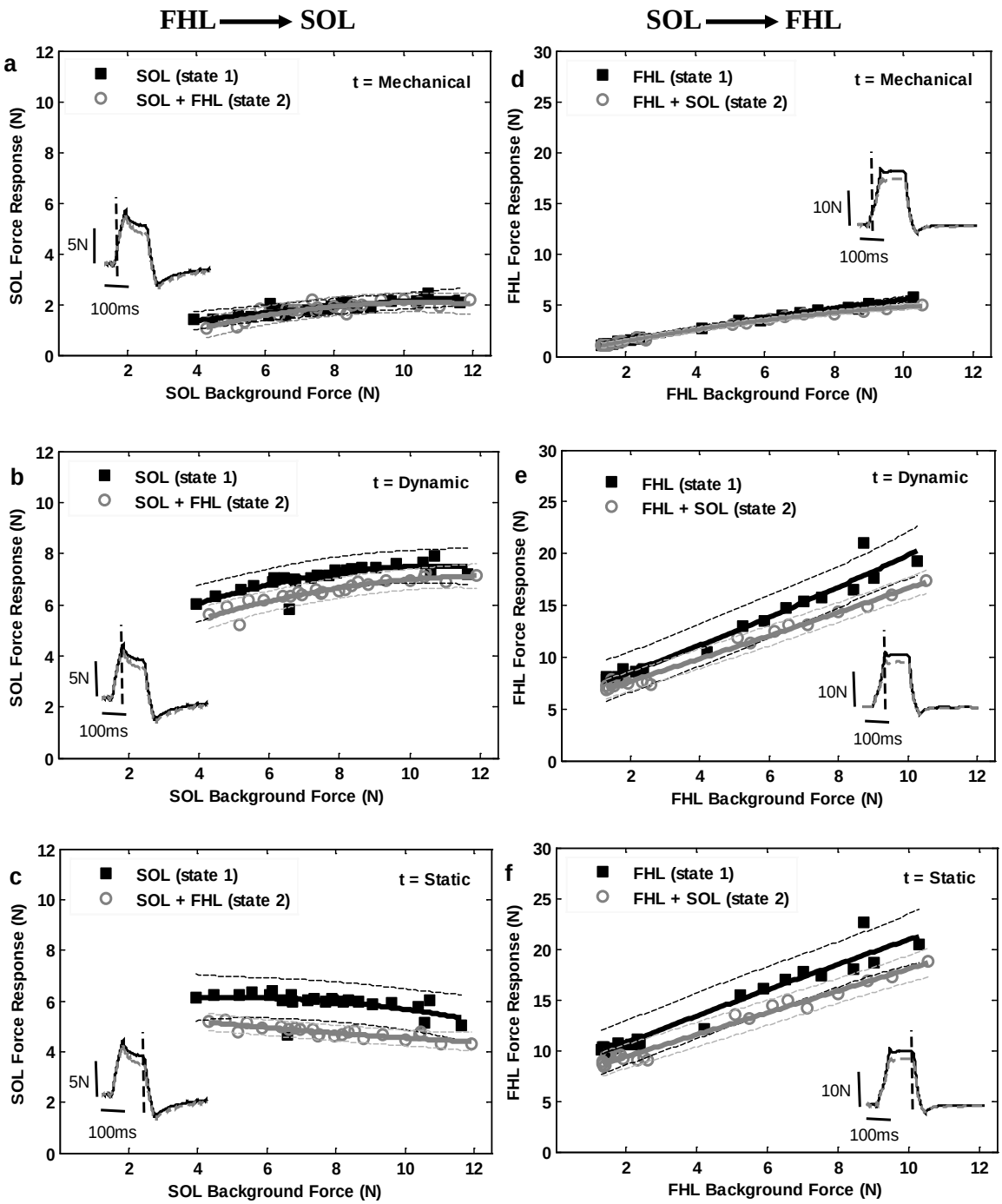

Figure 2.8 Symmetric/ bidirectional pattern of heterogenic inhibition between SOL and FHL during XER in a decerebrate cat in (a, d) mechanical phase, (b, e) dynamic phase, and (c, f) static phase. Black squares represent force responses of recipient muscle from stretches occurring in state one and grey circles in state two, respectively. Polynomials and 95% confidence intervals are fit to each population of data. The inserts in (a), (b), (c), (d), (e) and (f) shows two traces (state 1 black solid line, state 2 grey dashed line) matched at approximately mean background force of recipient muscle, superimposed to illustrate the magnitude of inhibition between SOL and FHL, the vertical line indicates the sample time in each trace.

2.3.3 FHL contributes inhibition to PLT

The heterogenic feedback between PLT and FHL was examined in four total experiments, three of which exhibited good XER. Of these experiments evaluating the interaction between PLT and FHL during quiet stance, three demonstrated stronger inhibition from FHL onto PLT than in the opposite direction. Our results are consistent with those reported earlier in both static as well as locomoting cats (Bonasera and Nichols 1994; Ross and Nichols 2009). While we observed a slight overlap in the confidence intervals at the lower background forces indicating small inhibition of PLT by FHL, a P value < 0.01 indicates that these populations are distinctly different. Also, the inhibition increases at higher background force of PLT.

Figure 2.9 illustrates the representative example of stronger inhibition of PLT by FHL (Figure 2.9a, b, c) and a comparatively weaker inhibition in the opposite direction (Figure 2.9d, e, f). Force traces inserts in the figure from state one (solid black line) and state two (dashed grey line) are matched at recipient muscle mean background force for each muscle combination in the given trial. It is evident that the magnitude of inhibition in case of PLT is increasing with increasing background force. There is slight overlap in the confidence intervals at the lower background forces in case of PLT inhibition by FHL (Figure 2.9 b, c) however at higher background force of PLT the two populations are distinctly different as shown by clear separation of confidence intervals.

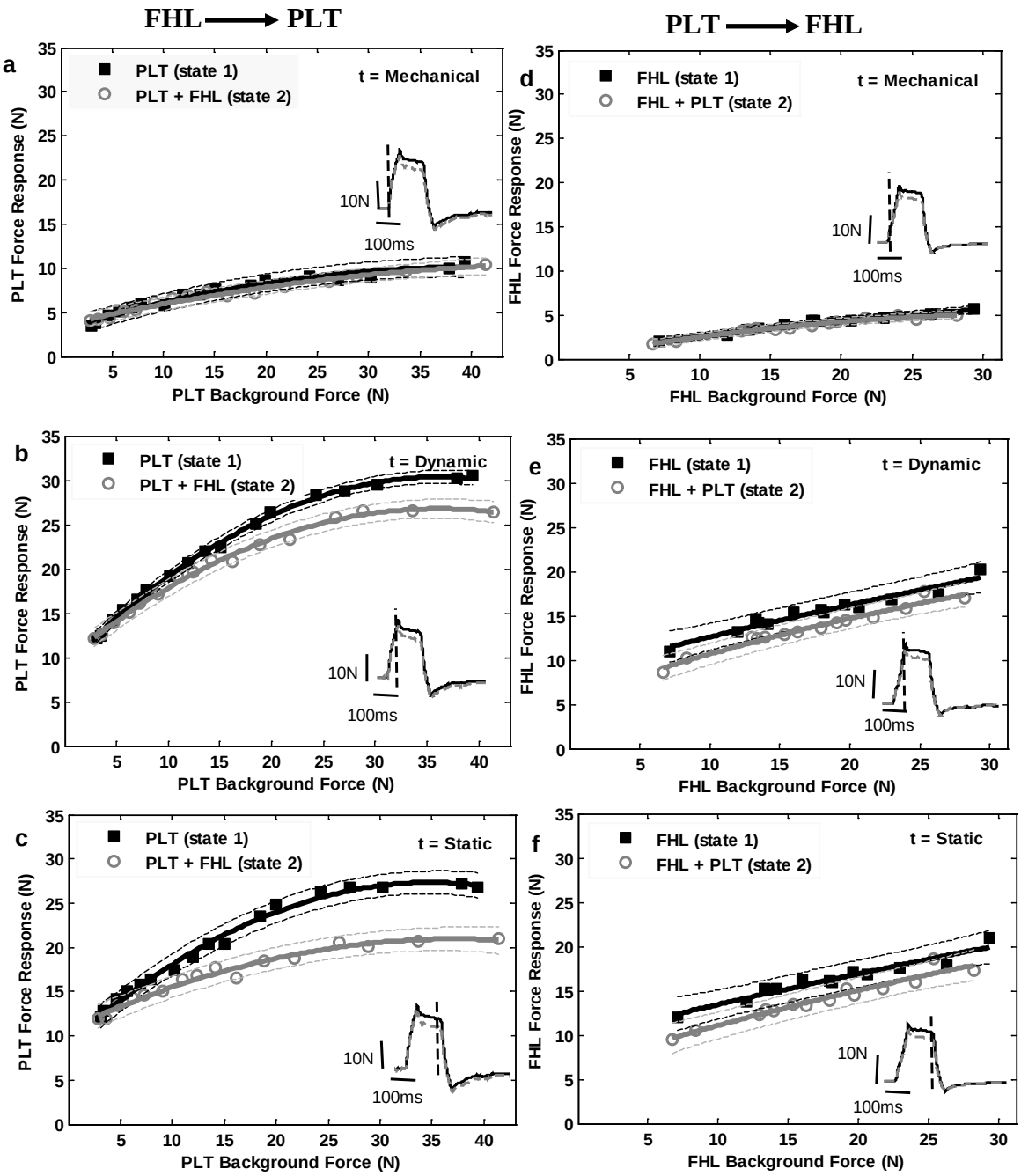

Figure 2.9 Distal to proximal pattern of heterogenic inhibition between PLT and FHL during XER for (a, d) mechanical phase, (b, e) dynamic phase, and (c, f) static phase. The same conventions as Figure 2.1 apply. The inserts in (a), (b), (c), (d), (e) and (f) shows two traces (state 1 black solid line, state 2 grey dashed line) matched at approximately mean background force of recipient muscle, superimposed to illustrate the magnitude of inhibition between PLT and FHL, the vertical line indicates the sample time in each trace. The left half of Figure (a, b, c) represents stronger inhibition of PLT by FHL, while right half (d, e, f) represents comparatively weak inhibition of FHL by PLT.

2.3.4 Latency of Reflex interactions

Reflex interactions between FHL/GA, FHL/PLT and FHL/SOL occurred at a latency of 28 ± 4 ms consistent with earlier reports (Bonasera and Nichols 1994). Therefore the Ib afferents from GTO's are likely to be responsible for carrying the information to spinal cord to produce the force dependent heterogenic inhibition observed in this study (Nichols 1989, Nichols 1992). An example of latency of reflex between FHL and GA is demonstrated in Figure 2.10.

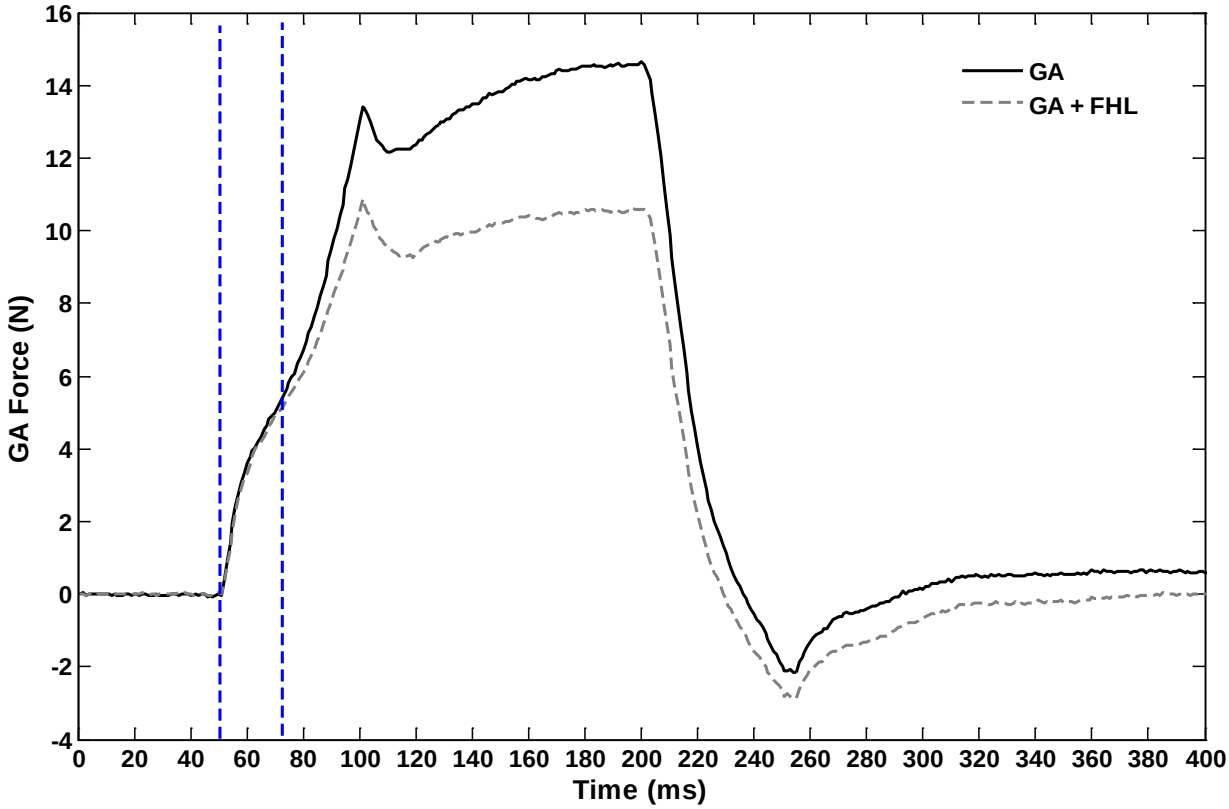

Figure 2.10 Reflex latency for the FHL/GA interaction was calculated at 28 ± 4 ms. Distance between the two blue dashed lines indicates latency of reflex.

2.4 DISCUSSION

In this study, we have attempted to address the organization of heterogenic force feedback between ankle extensors, namely FHL, GA, SOL and PLT in the intercollicular decerebrate cat (non-locomoting) for a wide range of background forces. We found that inhibitory heterogenic feedback linking ankle extensor muscles does not exhibit a uniform pattern across cats/subjects. Specifically, the most variable directionality of force-dependent inhibition was observed between GA and FHL. Furthermore, the patterns for force feedback linking FHL to SOL and FHL to PLT showed most consistent results. Specifically, we observed week inhibitory feedback bilaterally between FHL and SOL and a predominantly distal to proximal direction of inhibition between FHL and PLT, across cats and limbs. Despite the variability of inhibitory force feedback interactions among ankle extensors in our current data across animals, the results remain consistent for each muscle combination across limbs in each cat. The following discussion addresses these results from neural, anatomical and functional perspective, and evaluates the possible functions of heterogenic inhibition during posture maintenance.

There are several physiological and anatomical explanations at muscular level for our current results. First, GA is a two joint muscle, primarily composed of fast, high-threshold, fatigable motor units (Burke et al. 1973). It has short muscle fibers (Sacks and Roy 1982), a longer tendon than SOL (Walmsley and Proske 1981) and a high maximum isometric force and maximum velocity of shortening (Spector et al. 1980). It is mainly extensor and a weak abductor of ankle. FHL is predominantly a fast twitch muscle that inserts into tendon of FDL and can cause flexion of metatarsophalangeal joints. It is an

extensor and an adductor of ankle. A consistent pattern of strong inhibition of FHL by GA and a week inhibitory interaction in the opposite direction has already been reported in locomoting decerebrate cats (Ross and Nichols 2009). GA, specifically the MG, generates the greatest non-sagittal moment as a large abduction torque about the joint. This non-sagittal component could play an important role in stability during locomotion and induce stability by increasing the base of Support during locomotion.

Now the question arises why we have a variable pattern of inhibitory force feedback inhibition between these two muscles (FHL and GA) in non-locomoting cats? Basically both muscles are extensors yet the correct placement of foot requires the right amount of force production by appropriate muscles in appropriate direction during any motor task. During quiet stance a balance between adduction and abduction at ankle is required to prevent sway too. Therefore, we can have a variable intermuscular interaction between FHL and GA during quiet stance. We propose that the architecture of GA and FHL makes it possible for them to quickly respond to any perturbation during quiet stance. GA and FHL interactions therefore, show variable patterns of inhibitiory force feedback interaction during animal's attempt to maintain balance in response to both internal and external perturbations that needs quick adjustment. It could be task and state dependent too (Nichols et al. 2014).

We observed consistent results for force feedback interactions between SOL and FHL in this study across cats. One possible explanation for this consistent result could be the anatomical attributes of the muscle. SOL is a single joint muscle, primarily composed of slow, low-threshold, fatigue-resistant motor units (Burke et al. 1974) and has relatively

long muscle fibres (Sacks and Roy 1982), a relatively short tendon (Walmsley and Proske 1981) and a low maximum isometric force and maximum shortening velocity (Spector et al. 1980). These properties might be linked to the consistent pattern of weak intermuscular force feedback interactions with FHL during both quiet stance and locomotion. Also, it is the only uniarticular muscle used in our study therefore, we propose that the variability of force feedback patterns might be physiologically linked to multiarticular fast twitch muscles (GA, PLT) that might be required for quick maintenance of interjoint co-ordination and posture control during any motor task (quiet stance, locomotion). SOL is functionally a strong non fatigable muscle that needs to be contracted constantly during quiet stance to maintain weight support and balance. Therefore, even though the state of the animal constantly changes during mid-stance due to internal and external perturbations, the SOL muscle force feedback interaction pattern with FHL stays the same throughout mid stance.

PLT has properties that appear to be intermediate between those of SOL and GA. PLT has about the same percentage of fast motor units as GA (Baldwin et al. 1984; West et al. 1986). Its physiological cross-sectional area, mass and the maximum isometric force are larger than those of SOL and smaller than those of GA (Herzog et al. 1992; Sacks and Roy 1982). PLT spans the knee and ankle. Also, PLT is partly attached to the tendon of the flexor digitorum brevis (FDB) and, therefore, can cause flexion in the metatarsophalangeal joints. FHL also inserts into tendon of FDL and can cause flexion of metatarsophalangeal joints and is predominantly fast twitch muscle. We have observed stronger inhibition of PLT by FHL than in the opposite direction. The Same pattern of inhibition with stronger inhibition from FHL onto PLT has already been reported in

locomoting cats (Ross and Nichols 2009). Functionally, PLT is a weak ankle abductor and FHL is an ankle adductor. Considering that the direction/gradient of inhibition is consistent across different states (locomotion, quiet stance), we propose that inhibition of PLT by FHL maintains balance between adduction and abduction at ankle and foot and hence maintain torque at ankle.

The observation of different patterns of force feedback in stepping premammillary animals (Ross and Nichols 2009) and our intercollicular decerebrate animals adds to the evidence that the upper brainstem can regulate proprioceptive circuits in the spinal cord. This notion is corroborated by reports demonstrating that simultaneous stimulation of upper and lower brainstem regions enhance the lower brainstem effects on postural tone (Mori 1987). Therefore, most probably the neuromuscular interaction is state dependent and therefore it is different in locomotion than in static animals where the animal is trying to prevent any sway constantly. Based upon these observations and earlier suggestions (Ross and Nichols 2009), we propose that the spinal cord and brain stem house the appropriate circuitry to produce some of the key elements of postural control including directionally appropriate muscle activation.

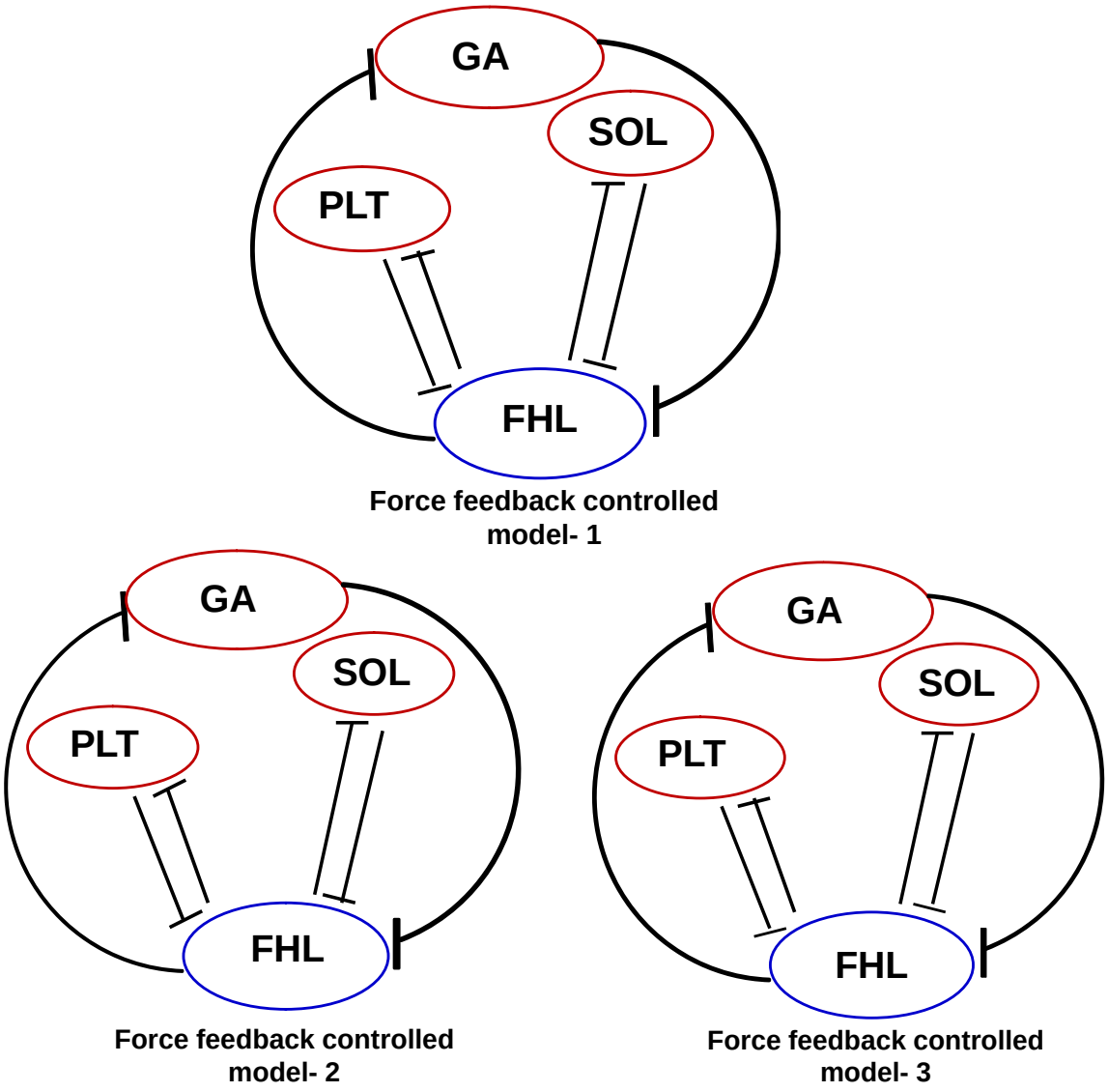

Figure 2.11 Summary diagrams of the three models of heterogenic inhibition observed among ankle extensors in the non-locomoting cats during XER. (Model-1) shows the most common type of interactions among ankle extensors. There is similar strength of Heterogenic inhibition between GA and FHL as well as between SOL and FHL. The inhibition between SOL and FHL is much weaker though in comparison to the balanced inhibition between GA and FHL. Inhibition between PLT and FHL shows distal to proximal pattern. (Model-2) represents proximal to distal pattern of inhibition between GA and FHL, bidirectional/ mutually equal amount of inhibition between SOL and FHL and a distal to proximal pattern between PLT and FHL. (Model-3) represents distal to proximal pattern of inhibition between FHL and GA as well as PLT and FHL, while the pattern of inhibition between SOL and FHL is bidirectional/mutually equal.

Over the years, the spinal reflex effects of group Ib afferents from Golgi tendon organs have turned out to be much more complex than originally thought. These effects are state dependent, that is, dependent on the context and task of motor acts. This task dependence is reflected in different group Ib reflex effects during both quiescent states and the locomotor stance. Ib afferents from ankle extensors in normal walking cats shows that these afferents have a high level of activity during the stance phase and a strong covariation with ongoing muscle activity (Prochazka and Gorassini 1998). Ib afferents connect GTO's to α-motoneurons neurons (Hultborn 2006; Jami 1992; Jankowska 1992; Marchand-Pauvert et al. 2005), Ib interneurons (mutual inhibition), group II interneurons, ventral spinocerebellar tract, dorsal spinocerebellar tract, primary sensory afferents (Jami 1992; Jankowska 1992; Schomburg 1990). Length feedback from muscle spindles on the other hand projects mainly to parent motoneurons and close synergists and is thought to regulate muscular stiffness (Nichols and Houk 1976) and enhance force output during stance (Stein et al. 2000; Mazzaro et al. 2006). Additionally, length feedback depends on background force independently of task. We therefore, propose that due to complicated connections of Ib afferents from GTO's at multiple levels in spinal cord different intermuscular interactions are possible according to task and postural requirements of the animal (Nichols et al. 2014).

CHAPTER 3

ALTERED PATTERNS OF INTERMUSCULAR FEEDBACK BETWEEN HINDLIMB ANKLE EXTENSORS FOLLOWING CHRONIC SPINAL CORD INJURY IN THE CAT

I. GASTROCANEMIUS AND FLEXOR HELLUCIS LONGUS

3.1 Introduction

Excitatory length feedback from muscle spindle is known to regulate stiffness of synergist muscles acting at the same joint, whereas inhibitory force feedback from Golgi tendon organs links muscles across different joints to promote interjoint coordination (Nichols 1994). This interjoint coordination is vital to maintain posture and balance during any motor act. Thus, the relative strength of length and force feedback within and across muscles collectively regulates the mechanical properties of the limb as a whole (Ross and Nichols 2009). This has been established earlier in our laboratory that inhibitory force feedback exists between extensor muscles of hind limb in cat (Bonasera and Nichols 1994; Wilmink and Nichols 2003). In decerebrate non-locomoting animals the symmetry of the force feedback distribution was not quantitatively established earlier. Therefore in chapter 2 we evaluated the strength and distribution of heterogenic force feedback among hindlimb ankle extensors in each of the ten decerebrate preparations. In order to understand the influence of SCI on proprioceptive pathways we then sought to compare the organization of intermuscular force feedback in control animals with those with SCI/LSH.

We expected the SCI to influence force feedback interactions between ankle extensors because SCI influence inhibition (Eccles and Lundberg 1959). We hypothesize that following SCI there is reorganization of the postural limb reflexes driven by stretch and load receptors (muscle spindle and GTO's), due to changes within the spinal cord (Rossignol and Frigon 2006; Rossignol and Frigon 2011). These changes are due to abnormal descending input produced by spinal cord injury or supraspinal disorders that gradually changes the spinal cord. Normal descending influence guides development of spinal cord reflexes early in life and throughout later life produces spinal cord plasticity that contributes to skill acquisition and maintenance. The spinal cord plasticity produced by peripheral and descending inputs affects input connections, interneuronal pathways, and motoneurons. Thus loss of its effect on spinal circuitry can alter intermuscular interactions post SCI.

Previous research work and our current data from control animals has proved that control decerebrate non-locomoting animals exhibit inhibitory force feedback among the hind limb extensor muscles. However, we observed that there is no set pattern/directionality of this inhibition and it differ from animal to animal. It could exhibit three different types of patterns across animals. There could be proximal to distal pattern consistent with Dailey's hypothesis (Daley et al. 2007), distal to proximal pattern consistent with Ross and Nichols (Ross and Nichols 2009) or balanced in the strength of inhibitory force feedback among the hind limb muscles consistent with previous studies in decerebrate locomoting cats (Ross and Nichols 2009; Daley et al. 2007). We propose that a predominantly proximal to distal distribution of force feedback promote maintenance of balance by reducing stiffness of the distal joints. The reduced distal joint

stiffness in turn mediates interface with the ground and therefore regulates distal limb compliance during any motor task. We hypothesize that the spinal cord loses its ability to maintain this task dependent neuromuscular response following SCI that could be one of the contributing factor for poor balance and weight support required for any motor task.

Since SCI results in loss of balance and weight support, we propose that pathways mediating the inhibitory force feedback may remain inhibitory after SCI but their strength and directional predominance may change resulting in a loss of posture control. To test our hypothesis muscles exchanging predominately force-dependent inhibition (Eccles et al. 1957; Nichols 1989), extensively studied in our laboratory previously in both static and locomoting cats were chosen for these experiments, namely GA (Gastrocnemius) and FHL (Flexor hallucis longus). We have observed a consistent pattern of strong statistically significant distal to proximal inhibition in chronic SCI both across limbs and across animals for these two muscles. To strengthen our claim we have conducted comparative studies in this muscle group on cats with acute LSH (chapter 5) and chronic LSH (chapter 3) as well as without LSH (chapter 2).

The purpose of these studies was to determine the distribution of the force feedback among ankle extensor muscles in the hindlimb of the cat following SCI. We also conducted these studies to determine how and when these intermuscular interactions changes after SCI. We choose spinal hemisection paradigm because post-operative care is easier in these animals during recovery period with less chance of muscle atrophy, ulcers/wound infection, better bowl and bladder control. Also, due to a clean surgical

hemisection it is possible to study the effect of SCI on different spinal tracts and their possible association with the poor weight support, posture control and locomotion.

Previous studies using SCI were conducted using training, drugs (Cote and Gassard 2003; Cote and Gassard 2004; Ichiyama et al. 2011; Lyalka et al. 2008) and electrical stimulation (Musienko et al. 2010), have shown improvement of reflex activity and locomotion behavior. There is still little information about load responses using natural/physiological stimuli mimicking clinical/natural environment. Therefore, studies using muscle stretch (natural stimulus) should answer some of these questions.

The main objective of this study was to understand the role of spinal cord in posture maintenance by understanding the altered intermuscular interactions following SCI. Preliminary accounts of these results have been published (Niazi et al. 2012; Niazi, Nichols and Howland 2012; Lyle et al. 2014; Niazi et al. 2014). We propose that a detailed understanding of the distribution and functional utility of proprioceptive networks, and how they are modulated by spinal injury both immediately and in long term requisite to exploit the full potential of sensorimotor training and effective management of SCI in clinical set up.

3.2 Methods

3.2.1 Preparation

The results depicted in this study were drawn from experiments on six healthy adult female cats weighing 4–4.5 kg to evaluate intermuscular reflex pathways. The studies were conducted on both legs so each muscle is represented twice per preparation

(12 legs from 6 chronic LSH cats). This approach also gave us an opportunity to compare the intact side leg with injured side leg in LSH in the same animal.

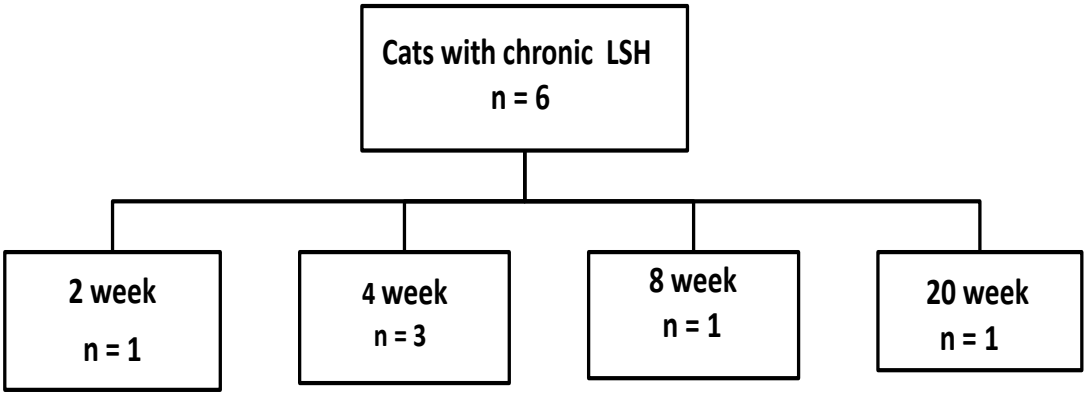

Figure 3.1 Division of cats with chronic LSH according to time of terminal surgery post SCI. Total number of animals used in our study were 6. Terminal experiments performed at 2, 8 and 20 weeks post SCI using one animal at each time point and at three animals at 4 weeks post SCI.

A versatile and physiologically robust method is essential for comprehensively mapping proprioceptive neural networks and examining neuromodulatory factors including spinal injury. Therefore, we have used mechanographic technique (Bonasera and Nichols 1994; Wilmink and Nichols 2003; Nichols 1987), which involves recording muscle force responses while stretching cat hindlimb muscles in isolation (autogenic/state 1) and in pair-wise combinations (Heterogenic + Autogenic/ state 2). This preparation has been used extensively as a model system for studying vertebrate motor control in our laboratory (Nichols 1987) thus only a brief description will be presented here. This approach uses decerebrate cats which exhibit similar reflex responses and walking patterns as intact cats and negates the need for anesthesia that can potentially influence

reflexes. Importantly, the decerebrate cats respond to postural perturbations (Honeycutt et al. 2009; Honeycutt and Nichols 2010; Gottschall and Nichols 2007) and exhibits naturalistic walking (Musienko et al. 2012; Ross and Nichols 2009) similar to intact cats. All protocols are in complete accordance with the guidelines of both the Federal and Institutional Animal Care and Use Committee of Georgia Institute of Technology.

Chronic Spinal hemisection was performed in the 6 cats by Dena R. Howland at university of Florida and University of Louisville, under general anesthesia and aseptic conditions described earlier (Jefferson et al. 2011) thus only a brief description will be presented here. The LSH was performed in each cat at T10 spinal level (Figure 3.2) after carefully performing laminectomy and opening up the dura matter covering spinal cord using iridectomy scissors. Penicillin G procaine (40,000U/kg body weight, i.m.) was given starting a day before to a day following SCI to prevent any infections. All animals were regularly monitored by a registered veterinarian at university of Florida. Cats were housed in large individual cages with food and water. Foam mattresses in the cages were used to prevent peripheral nerve compression, pressure sores, and skin breakdown. Behavioral studies were performed on these animals both before and after chronic LSH while histological studies were done after terminal experiments (Georgia Institute of Technology) at university of Florida. Terminal experiment with decerebration at 2, 4×3, 8 and 20 week post surgery were performed at Georgia Institute of Technology in Nichol's lab after they resumed walking following LSH. At the end of each experiment, the animal was euthanized with an over dose of Nembutal followed by pneumothorax.

We used the same procedure to perform acute LSH in three animals in our laboratory to obtain data to compare with chronic LSH data. This was done before muscle dissection in each animal to give appropriate time to animal for recovery from spinal shock. The acute animals were used to investigate the time of onset of any change in intermuscular interactions that is expected to appear in chronic SCI. In addition we performed an experiment using acute dorsal hemisection (DSH). In acute dorsal spinal hemisection we followed the methods of Cleland and Rymer (Cleland and Rymer 1990). Following lamanectomy and opening up the dura matter covering spinal cord DSH was performed in each cat at T10 spinal level by teasing apart dorsal columns and both dorsolateral funiculi with Dumont forceps, to the approximate level of the denticulate ligaments. In acute animals we performed terminal experiment immediately following injury (acute LSH or acute DSH).

At the end of each experiment, the animal was euthanized with an overdose of Nembutal followed by a pneumothorax. Dr Howland dissected and preserved spinal cord for histological study at the end of each experiment. First of all Heparin (1cc;1000U/i.v.) was administered followed by 1cc of 1% sodium nitrite IV after 20 minutes. Then immediately each cat was transcardially perfused with 0.9% saline, followed by 4% paraformaldehyde in 0.1M phosphate buffer (pH 7.4). The spinal cords were dissected, blocked, and post fixed in 30% sucrose and 4% paraformaldehyde (pH 7.4). Each dissected cord was transported back by Dr. Howland to her laboratory for detailed histological study to confirm spinal hemisection/ lesion magnitude in each cat.

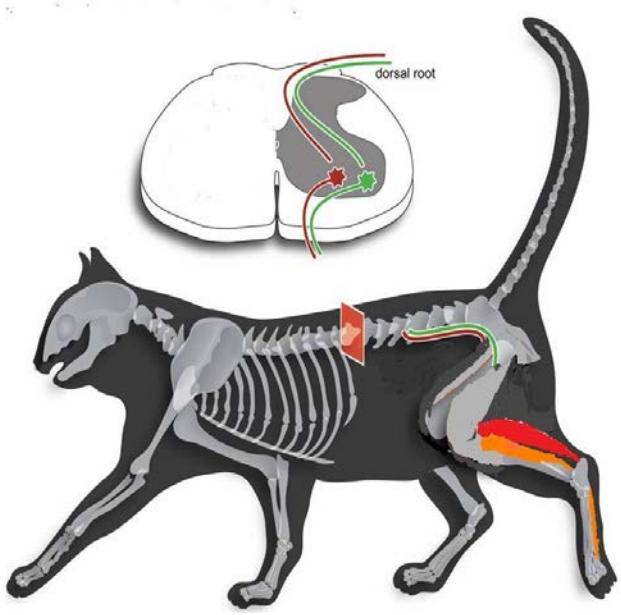

Figure 3.2 Diagrammatic representation of spinal cord LSH at T10 in a cat. FHL muscle is shown in orange color in left hindlimb and GA in red color.

Each cat was deeply anesthetized for our terminal experiment using isoflurane gas while the animal was kept on heating pad regulated at 37^0C to maintain body temperature homeostasis during data collection. A tracheotomy was performed, loosened sutures were placed around the carotid arteries and an intravenous flexible catheter was inserted into the external jugular vein to administer intravenous fluids during the experimental procedure and allow for the administration of concentrated pentobarbital upon the termination of the experiment. Later both legs and head were carefully shaved in each animal and bone pins were inserted in femur and tibia in each leg, hemostasis maintained by using bone wax. In acute SCI experiments we performed SCI before inserting bone pins.

After placement into a sterotaxic device supported over a table, limb fixation was accomplished with bone pins into femur and tibia being clamped to a static table frame. This was done to maintain the position of the limb as it is in natural posture at end of stance by keeping knee at 110^0 and ankle at 90^0 angles respectively. Figure 2.1 in chapter 2 depicts this experimental setup, whereby the dissected muscles of both immobilized hindlimbs were attached in series with myographs and linear motors. The position of each motor was adjusted according to the height of animal in each experiment.

The crossed extension reflex was used to activate the test limb muscles by stimulating the contralateral posterior tibial nerve at 2 times threshold (2T) and 40 HZ for its threshold for stimulation. Following each trial using XER the nerve was given at least 2-5 minutes rest before starting a new trial with XER to prevent nerve fatigue. We used cuff or hook electrodes for nerve stimulation. The tibial nerve was kept moist by using normal saline solution.

The FHL, GA and tibial nerves were carefully dissected and separated from surrounding connective tissue and muscles in both limbs. FHL muscle was carefully separated from surrounding connective tissue and followed behind the medial malleolus until its tendon was cut near its insertion into Flexor digitorum longus tendon. The GA tendon was secured with a small piece of calcanium Figure 3.3 shows the anatomy of the two muscles used in this study. Each muscle was attached via its tendon to individual clamps. These tendon clamps were placed in series with myographs using strain gauges in a half bridge configuration, and four linear motors. Either hook or cuff electrodes were placed around tibial nerve for the cross extension reflex (XER).

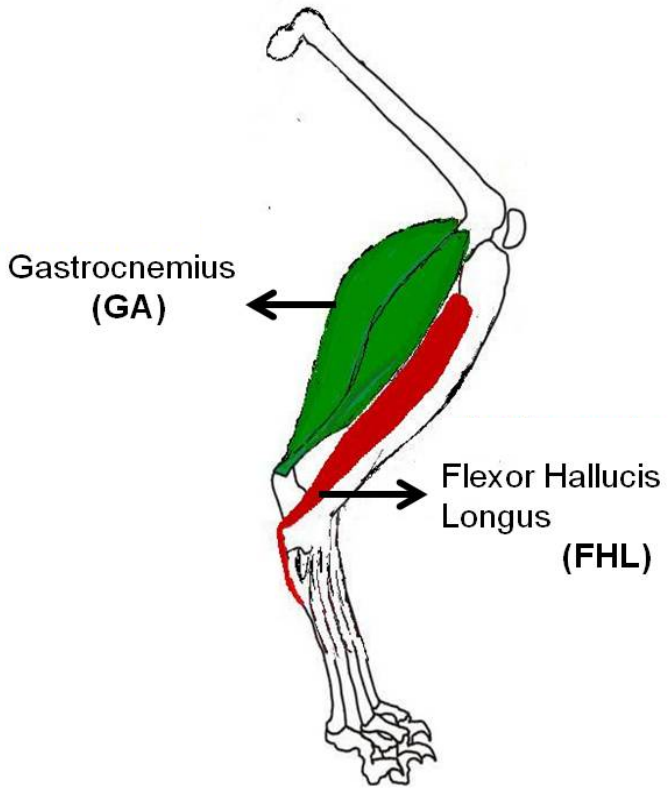

Figure 3.3 Anatomical representation of GA (green, proximal muscle) and FHL (red, distal muscle) in cat left hindlimb.

The strength and distribution of intermuscular pathways were determined from the force magnitude profile after 2 mm ramp and hold stretches (50 ms ramp stretch with velocity of 0.04 m/s, 100 ms hold, and 50 ms release). Intermuscular feedback effects were recorded across background forces by stretching a muscle denoted the "recipient" in isolation (state 1 or autogenic response) and then in combination with another muscle denoted the "donor" on alternate stretches (state 2 or heterogenic + autogenic response) with/without crossed extensor reflex (i.e. 45-60 stretch repetitions). The relative increase or decrease in the recipient force response when stretched in combination with the donor was reflected as intermuscular (heterogenic) feedback.

An intercollicular decerebration was performed in each cat, removing all brain matter rostral to the transaction and the anesthesia withdrawn slowly. Data collection was started after appropriate withdrawal responses and muscle tone assessment. Homeostasis after decerebration was maintained by packing the skull base with cotton balls and gel foam figure 2.2 in chapter 2 depicts the typical decerebration. In acute SCI experiments data collection was started after the animal was out of spinal shock indicated by good muscle tone in limbs, good XER reflex and background force as well as force response of muscles in hind limb.

3.2.2 Data Analysis

Force measurements were used to distinguish autogenic (intrinsic response to stretch0 and heterogenic (intermuscular reflex response) feedback pathways while muscles were alternatively stretched (state 1 and state 2) as described earlier in chapter 2. Data acquired during the experiments were organized by state, whereby state one corresponded to data obtained when the recipient muscle was stretched alone (black circles and lines in Figure 3.7), while state two represented those from stretching the donor and recipient muscles together (colored circles and lines Figure 3.7). Comparing recipient muscle force responses during state one with those during state two reveals the intermuscular force feedback contribution. Each trial contained data for GA and FHL muscle combination (45-60 stretches), where half of the stretches occurred in state one and half in state two (recipient muscle). Force output and length input of FHL and GA was recorded for each stretch (Figure 3.5).

The baseline was constructed by performing a linear interpolation from the mean force response just prior to the stretch to the mean force after the end of the release (Ross and Nichols 2009). The entire baseline was then subtracted from the overall force response. Figure 3.4a represent a sample force trace, the baseline calculation described above and the resulting baseline subtracted force data (Figure 3.4b and 3.4c). The baseline background force was subtracted from the total force profile of the given muscle to account for potential load dependent feedback gain (Ross and Nichols 2009). Force changes were plotted against the background force for each recipient muscle to check for load dependence.

Each force response was divided into three time points for data analysis as shown in Figure 3.4b and 3.4c. To characterize the strength and time course of intermuscular interactions, the force-time profile was analyzed taking into consideration the time course of applied stretch and intermuscular reflex latencies known to range between 16 to 24 ms (Bonasera and Nichols 1994; Wilmink and Nichols 2003). Specifically, the force value measured 10 ms following stretch onset was used to detect passive mechanical artifacts that could occur from incomplete separation of muscles during dissection that precedes reflex (Bonasera and Nichols 1994; Wilmink and Nichols 2003). If muscle force at this time point deviated during stretch of another muscle (state 2), these trials were discarded. Force responses that occurred 50 ms following the beginning of the stretch represented the dynamic phase of force feedback (Figure 3.4b and 3.4c). A similar analysis was done for the end of the hold period, corresponding to 100 ms following the beginning of the stretch, the static phase, as shown in Figure 3.4 similar to previous reports (Knikou et al. 2009; Grey et al. 2001; Wilmink and Nichols 2003; Ross and Nichols 2009).

Software in Matlab version 7.01 was used to analyze the data collected during these experiments. The raw data was further represented as stick figures to further demonstrate interemuscular interactions demonstrating both state 1 and state 2 for each time point for each trial for recipient muscle as shown in figure 3.6. This was done to visually recognize any intermuscular inhibition at three different time points across a trial before further analysis of our data. The force data analysis was then done using software in Matlab and statistical analysis was performed using Statistica 6.0 and Excel, within each time point (mechanical, dynamic and static) for both state1 and state 2, either with or without XER.

Populations of integrated values from the respective time points were plotted separately as a function of the background force of the recipient muscle obtained from the original force trace. Quadratic regression analysis was performed to test the overall separation of the populations of force responses (Ross and Nichols 2009). Figure 3.9 depicts the typical analysis, whereby force responses of recipient muscle in Newton (y axis) for a specific time point (mechanical, dynamic, static) are plotted as a function of the background force of the recipient muscle in Newton (x axis). Each data point (each circle) represents an individual force response of the recipient muscle from the recorded raw data when the muscle was either stretched alone (black circles) or response of the recipient muscle when it was stretched with another muscle (colored circles). Polynomial fits and 95% confidence intervals were fit to each population of data for a given time point at P value $\leq$ 0.01. P calculated using the following equation described earlier (McGraw-Hill Irwin: Boston; 2005). [F= ((SSE(Reduced) – SSE(Full)/ (DF(Full) –

DF(Reduced))/MSE(Full)]. Two regression models were fit to the data namely full model and reduced model as described earlier (Ross KT, Nichols TR. 2009, Kutner et al. 1996).

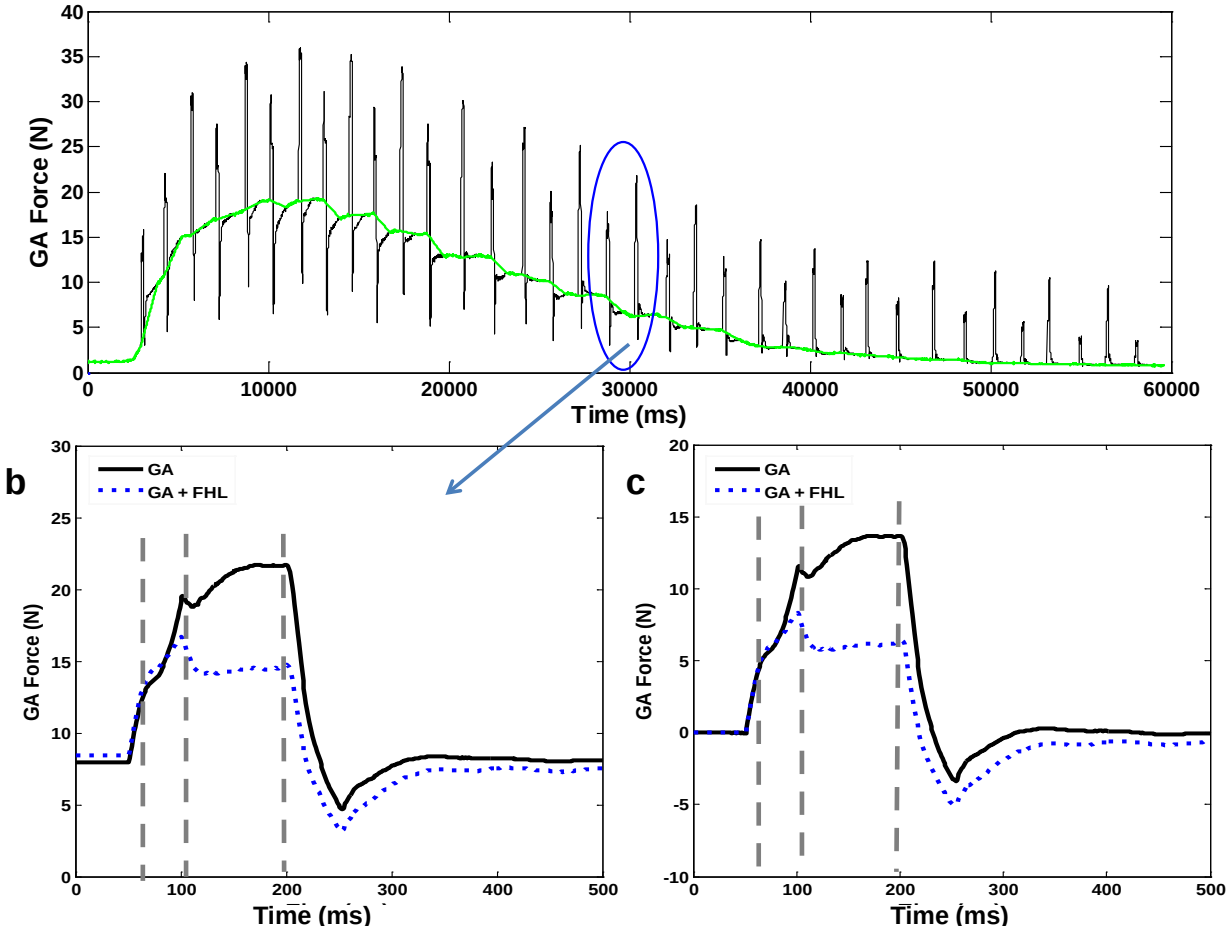

Figure 3.4 (a) Representative figure showing Recipient muscle (GA) stretch evoked force response during XER. The green line indicates the baseline that is calculated for each individual stretch by performing a linear interpolation between the first 10ms and last 10ms of data. (b) State 1 (black) and state 2 (blue) force responses in two consecutive stretches superimposed to show inhibition. The broken grey lines represent mechanical time point at 60ms, dynamic time point at 100ms and static time point at 200ms respectively. (c) Baseline subtracted force responses obtained after subtracting baseline from each individual stretch shown in Figure 3.6b.

Additionally, differences for both the dynamic and static time point force responses in the recipient muscle were calculated by calculating difference between state 2 and state 1 force responses and curve fits generated to determine the amount of inhibition at different time points during ramp and hold period of each individual trial, as shown in Figure 3.7d. This analysis enabled us to demonstrate weather the inhibitory intermuscular force feedback between GA and FHL changes over time during muscle stretch and hold in decerebrate cats or is different in chronic SCI.

The percent heterogenic inhibition is calculated by converting the amount of inhibition in Newton obtained by subtracting individual state 2 force responses from state 1 force response at each time point to percent change. The significance of this calculation is that we can compare data across limbs and animals if we normalize it to percent change. The amount of force response in Newton (N) varies across each trial and animal therefore it is more relevant to describe the change in terms of the percent change. Each consecutive pair wise combination (state 1 and state 2) has been normalized to the isolated muscle stretch response (recipient) so that the relative strength can be expressed as a percentage change from the autogenic response. Comparisons were made to determine the influence of SCI on the strength and distribution of intermuscular proprioceptive feedback.

A detailed statistical analysis was conducted to calculate the mean change in force response of recipient muscle, the standard deviation, range (maximum and minimum change) and percent change between autogenic and heterogenic states were also calculated. If $P \leq 0.01$ it is considered significant and documented as box plots for each

time point for every individual trial as demonstrated in figure 3.8. Data was compared across state, limbs and cats to determine the effect of SCI on force feedback.

Data published by Nichols in 1989 using decerebrate cats indicate that the amount of inhibition in recipient muscle depends on the force of both the donor and recipient muscle (Bonasera and Nichols 1994). For this reason we further analyzed the recipient force response points against the donor background force to study the effect of SCI on the amount of inhibition in relation to the donor background force. We also plotted recipient muscle background force as a dependent variable against the donor muscle background force as an independent variable in the form of a simple scattered graph as shown in figures 3.16 and 3.17. The two distinct time points showing change in force response of the recipient muscle from state 1 to state 2 were used for further analysis of the data. They were identified at the end of the ramp (dynamic time point) and at the end of hold phase of muscle stretch (static time point). The populations of integrated values from the respective time points plotted separately as a function of background force of the donor muscle obtained from the original force trace. Multiple regression analysis was performed to test the overall separation of the populations of force responses (Wilmink and Nichol 2003).

To understand the mechanisms underlying force dependent inhibition between FHL and other antigravity muscles in our study latency of recipient force response was calculated for each muscle combination. According to previous studies the reflex latency of the force dependent inhibition between FHL, GA, SOL and PLT occurred at 28 ± 4 ms (Bonasera and Nichols 1994). This analysis helped us determine if the clasp knife

inhibition appeared after SCI in our data. The reflex latency in clasp knife inhibition is ≥ 80 ms (Nichols and cope 2001).

3.3 RESULTS

The main target of our studies was to determine the distribution of the force feedback between ankle extensor muscles in the hindlimb of the cat following chronic SCI. Our goal was to determine any possible connection between disturbed weight support/ balance support and intermuscular force feedback. According to our existing data feedback pathways among GA and FHL are predominately force dependent and inhibitory in non-locomoting (Bonasera and Nichols 1994; Nichols 1999; Wilmink and Nichols 2003) and locomoting cats (Ross and Nichols 2009). We choose FHL and GA muscles which have already been extensively studied in our laboratory in decerebrate cats in both static and locomotion based studies. We hypothesize that task dependent modulation of the relative patterns of intermuscular force feedback is a rapid spinal mediated neural mechanism that requires supraspinal input.

We used six cats with chronic spinal cord injury at different time points. This was done to determine the time of onset and any time related changes in intermuscular interactions following SCI as the animal recovers from injury. These cats did not receive any therapeutic management or training post SCI. We randomly selected cats at two, four, eight and twenty week post LSH periods. These cats were able to stand up and walk within a week following SCI (Jefferson et al. 2011). However, their ability to maintain

full body weight support with lateral stability/balance control remained compromised at least until 20 week post spinal cord injury in our study.

Uniformity of lesion magnitudes across cats was confirmed by Dr. Dena Howland laboratory. She used Cresyl violet and myelin stained sections through the lesion epicenters of each animal to determine the extent of tissue sparing and damage. Typically, complete disruption of the ipsilateral gray and white matter was seen in all six animals with chronic LSH. Contralateral gray and white matter was completely spared with the exception of some dorsal contusion in one out of six cats (one of the 4 weeks post SCI cats). Thus, lesion variability was minimal across animals.

We observed a consistent pattern of intermuscular inhibition between FHL and GA in all the cats with chronic SCI in contrast to variable pattern in control animals. The inhibition was always predominantly stronger from FHL (distal muscle) onto GA (proximal muscle) and weaker from GA onto FHL. Six out of six cats (100%) with chronic LHS showed this pattern with and without XER on both injured and uningured side limb (12/12 limbs, 100%). This is in contrast to variable results in control data as explained in chapter two where we observed three different patterns (predominantly proximal to distal inhibition, distal to proximal inhibition and a balanced inhibition) between GA and FHL in control static/non-locomoting animals.

The results presented in this chapter are divided in six main sections. The first Section (3.3.1) addresses in detail the inhibitory force feedback from GA on to FHL following chronic LSH. The second section (3.3.2) depicts data analysis in a chronic LSH

cat explaining detailed analysis of inhibitory force feedback from FHL on to GA. Section 3 (3.3.3) explains comparison of heterogenic inhibitory force feedback both across limbs (each animal) and cats used in this study with chronic LSH. Our experiments used partial SCI therefore this is an important section to demonstrate the effect of partial SCI on force feedback across limbs and its possible connection to the poor balance control in chronic LSH. This section reviews the comparative analysis of data from chronic LSH cats. Section four (3.3.4) addresses the recipient force response dependence on donor muscle background force and its significance. Section five (3.3.5) explains intermuscular force feedback between ankle extensors following acute SCI. This section is important to determine the time of onset of neuromuscular changes that might be responsible for the altered intermuscular force feedback interactions following SCI. Section six (3.3.6) explains clasp knife inhibition and the evidence of its presence or absence following LSH in our study.

3.3.1 GA weakly inhibits FHL following Chronic LSH

The intermuscular feedback interaction from GA onto FHL was examined in all six cats with chronic LSH. Our goal was to compare these results with results from control cats (without SCI) and determine if the LSH had any effect on reflexes. Six out of six cats (100%) with chronic LSH exhibited very week inhibition from GA onto FHL in all 12 limbs (6 of each injured and uninjured limbs) with $P \leq 0.01$ that was highly statistically insignificant.

Figure 3.5 depicts representative raw data from part of a single trial consisting of alternating state one and state two stretches, showing intermuscular interaction where GA

is inhibiting FHL in an animal 4 weeks following chronic LSH during XER. Figures 3.5a and 3.5b depict the force output and length input respectively of the donor muscle (proximal muscle) GA in a trial. Figures 3.5c and 3.5d depict the force output and length input respectively of the recipient muscle (distal muscle) FHL in the same trial. Additionally, the blue dashed lines indicate state 2 where recipient muscle FHL was stretched along with donor muscle GA during XER. State one response is shown in Figures 3.5a and 3.5c without the dashed blue lines. Figure 3.5 shows a small amount of inhibitory force feedback from GA onto FHL in state two. This pattern is observed in all six cats with chronic LSH. Clearly, the inhibitory force feedback from Ga on to FHL remains inhibitory even following SCI and it persists up to 20 weeks following SCI. Figure 3.5a also demonstrate small amounts of inhibition of GA (donor muscle) by FHL even when it is not stretched (isometric) during state 1. In addition we can see that at the end of stretch and hold period in each muscle stretch the muscle shows a drop in force before coming back to the baseline force value. This is because of the strong inhibitory feedback between FHL and GA that the time taken by the cross bridges in muscle to come back to the resting state.

Figure 3.6 further explains the inhibition of FHL by GA in the same trial shown in Figure 3.5. The data were divided into three time points to determine the part of the stretch where inhibitory force feedback appeared. Therefore all the stretches in this case each of the 42 stretches were divided into three time points explained earlier. Figure 3.6a shows the mechanical time point where no observable inhibition of FHL by GA is noted indicating a good surgical preparation in the given experiment. Figure 3.6b and 3.6c shows state 1 and state response of FHL in dynamic and static time point respectively.

We can see that the inhibition can be observed in both dynamic and static time point. Each circle represents a muscle stretch where, blue circles stand for state 2 and black circles for state one response. This trend of small inhibition of FHL by GA is seen in 6/6 cats (100%).

Figure 3.7 depicts a representative example of the intermuscular inhibition from GA onto FHL in chronic LSH. The data were analyzed at three different time points (t =mechanical, t=dynamic and t=static) during stretch and hold of the muscles. To evaluate the strength and sign of heterogenic feedback during XER, individual force responses at specific time points were obtained from the baseline subtracted force data, and background force was obtained from the original force trace shown in Figure 3.5. Figure 3.7 depicts the typical analysis, whereby force responses for a specific time point are plotted as a function of background force. Polynomial fits and 95% confidence intervals were fit to each population of data for a given time point.

There was no difference observed in mechanical time point between state 1 and state 2 demonstrating no mechanical artifact. Inhibition from GA onto FHL increases and then decreases with increasing background force for the dynamic as well as static responses consistent with data from decerebrate static and control cats. We therefore, concluded that following SCI the inhibition was force dependent as indicated by the divergence in the polynomial fits in Figure 3.7b and 3.7c. Each circle represents an individual stretch (colored circles for FHL force response in state 2 and black circles for FHL response in state 1). This increasing inhibition from dynamic to static stage is observed in all 6 cats (100%) both on injured side as well as uninjured side limbs of each

cat. Multiple regression yielded P value $\geq$ 0.01, thus statistically proving that the two populations (force responses of recipient muscle in dynamic and static time points) are not distinctly different.

Inserts in Figure 3.7a, Figure 3.7b and Figure 3.7c are force responses for state one (black lines and circles) and state two (blue lines and circles) for GA muscle. The background force for both conditions was matched at the average background force of approximately 11 N. Baselines were subtracted from both traces to better illustrate the magnitude and time course of the inhibition from GA onto FHL.

Figure 3.7d demonstrates the amount of heterogenic inhibition of FHL by GA in N at dynamic and static time points for comparison purposes. Each circle is obtained by subtracting state 2 force responses from state I force responses at approximate matched background force in Figure 3.7b and Figure 3.7c for dynamic and static time points respectively. We observed the polynomial fits for the static and dynamic time points had a lot of overlap suggesting that the two populations are not significantly different. The small inhibition trend was seen in 6/6 cats. The inhibition increased from dynamic to static time point, however it was always much weaker in comparison to inhibition of GA by FHL in each cat.

The detailed statistical analysis of data from also showed more inhibition in static as compared to dynamic state comparable to control data. Figure 3.8 provides a summary of the statistical analysis of a representative trial to calculate inhibition between GA and FHL at dynamic and static time point. Each black and blue box represents state 1 and 2

respectively. The whiskers of the box plot represent range of force response in each state including maximum and minimum values. The body of each box plot splits the data set into three quartiles 25^{th}, 50^{th}, and 75^{th} percentiles of the force responses in the same trial shown in Figure 3.7 through Figure 3.9. Within the box, the red line is drawn at the second quartile/ Q2/ 50^{th} percentile that stands for the median of the data set (state 1 or state 2). The mean change/inhibition is calculated by subtracting mean of force responses of state 1 from state 2. The amount of force response obtained in Newton is then converted into percent change. P value is calculated for evaluating the significance of percent change from state 1 to state 2 and it is considered statistically significant only if its value is $p \leq 0.01$. We observed weak inhibition of 10 % to 28% at t= static on injured side and 7.5% to 25% on uninjured side limb in chronic LSH across 6 cats as depicted in table 3.1. Therefore inhibition is observed bilaterally even after partial SCI. Also, this inhibition is not influenced by the time after SCI and is always a little less on the uninjured side in all 6 cats.

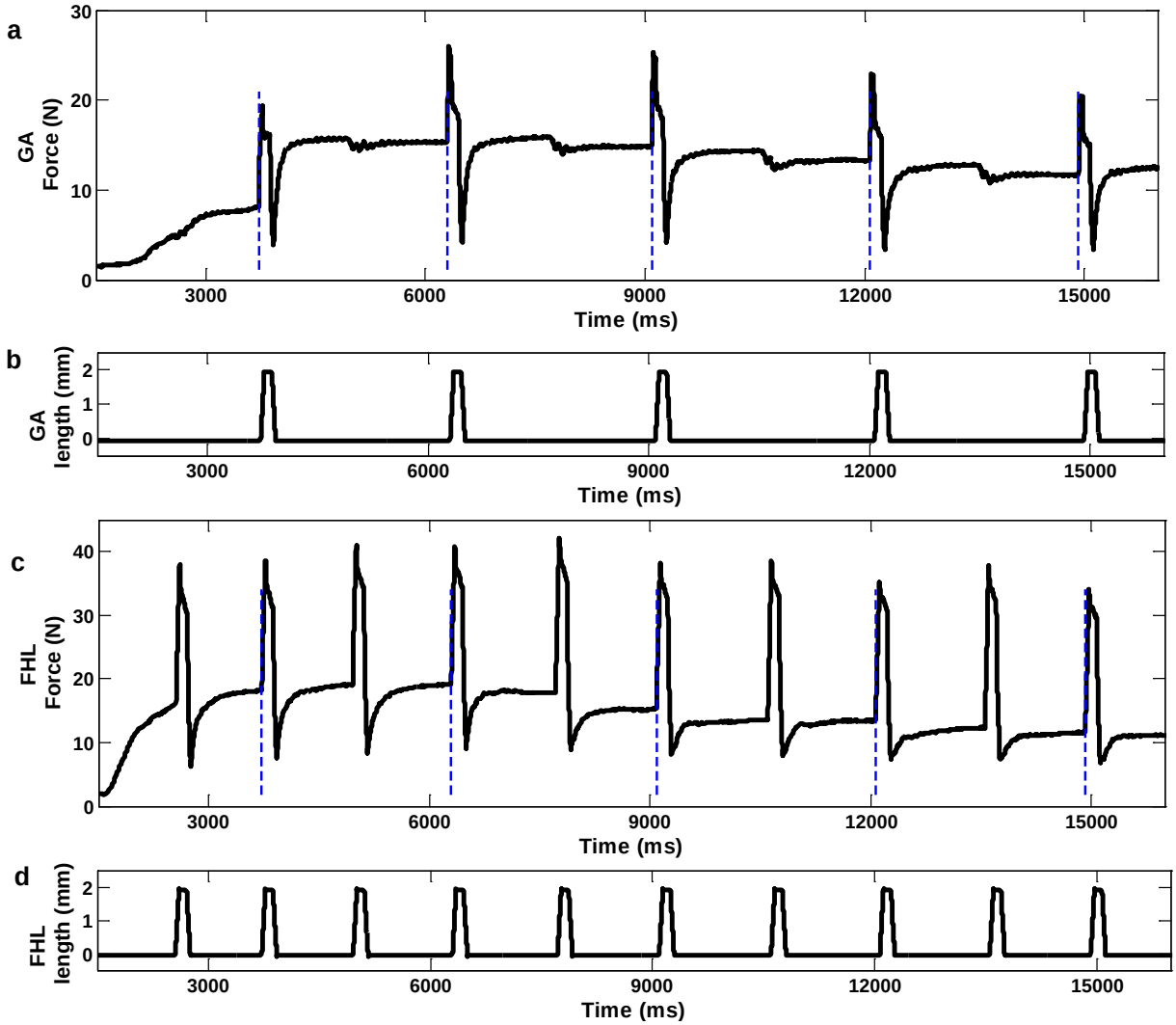

Figure 3.5 (a) Donor muscle (GA) stretch-evoked force response during XER. (c) Recipient muscle stretch-evoked force response during XER. Dashed blue lines on stretches indicate responses obtained when the donor muscle is stretched with recipient muscle at the same time in state 2. The y-axis is showing force response in N and x-axis is showing time in ms. Force responses without dashed blue lines indicate state 1, where recipient muscle was stretched alone. (b) Donor muscle (GA) length input to two-state stretch, where y-axis represent GA length in mm and x-axis represents time in milliseconds. (d) Recipient muscle (FHL) length input for two-state stretch. A two-state stretch is performed to ascertain strength and sign of feedback between recipient muscle (FHL) and donor muscle (GA). There is clearly some inhibition from GA onto FHL in state 2 (c). XER is done by stimulating tibial nerve in the left hindlimb in this example (the side without LSH) at 2T that evokes an increase in the background force of the recipient and donor muscles on the right hindlimb (injured side), GA and FHL respectively (a, c).

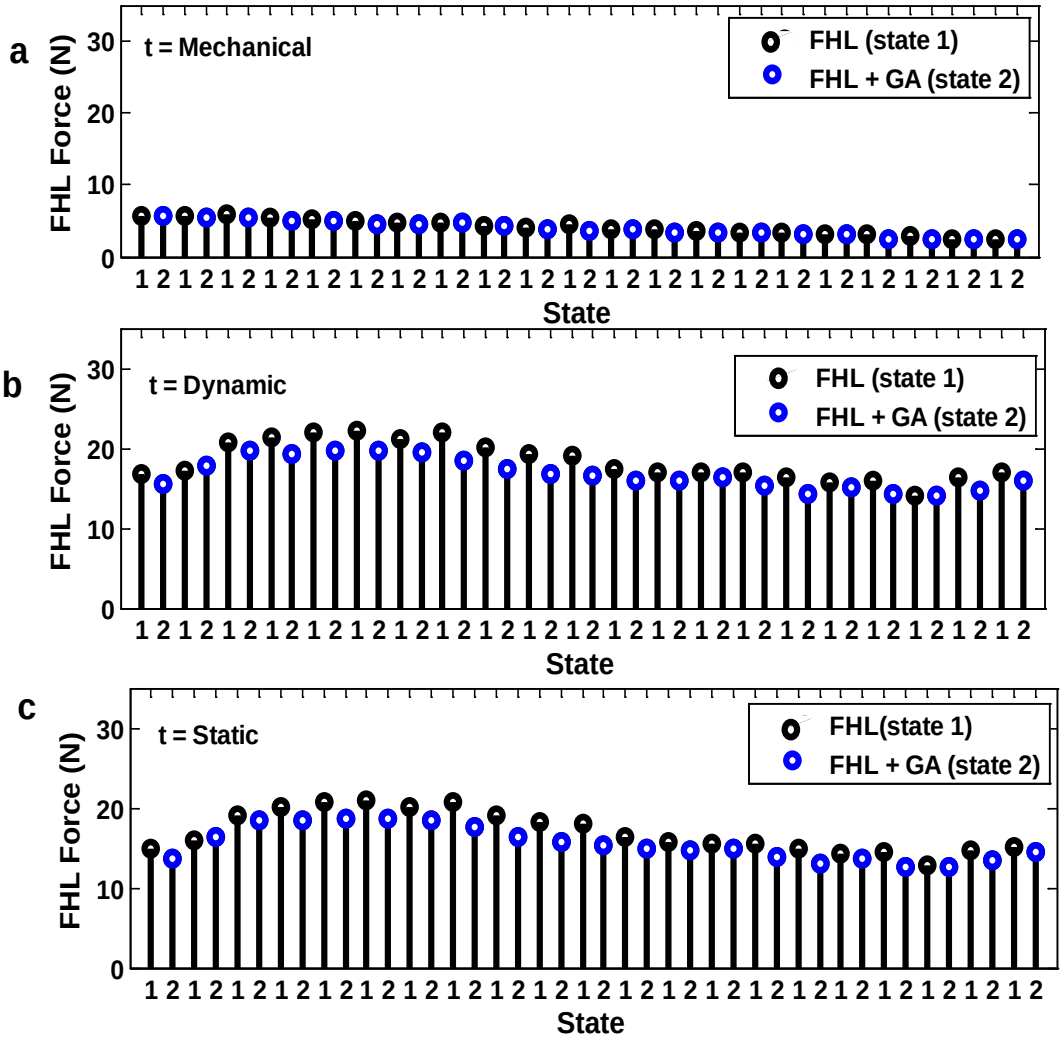

Figure 3.6 Recipient muscle (FHL) stretch-evoked force response during XER in (a) mechanical phase, (b) dynamic phase, and (c) static phase. Each individual circle represents FHL muscle stretch response where, blue circles indicate state 2 and black circles indicate state 1. Y-axis represent force response of recipient muscle (FHL) in N and X-axis represent state of the muscle during a muscle stretch. There is a small amount of inhibition of FHL by GA at dynamic and static time points during state 2 indicated by difference of heights of black and blue circles.

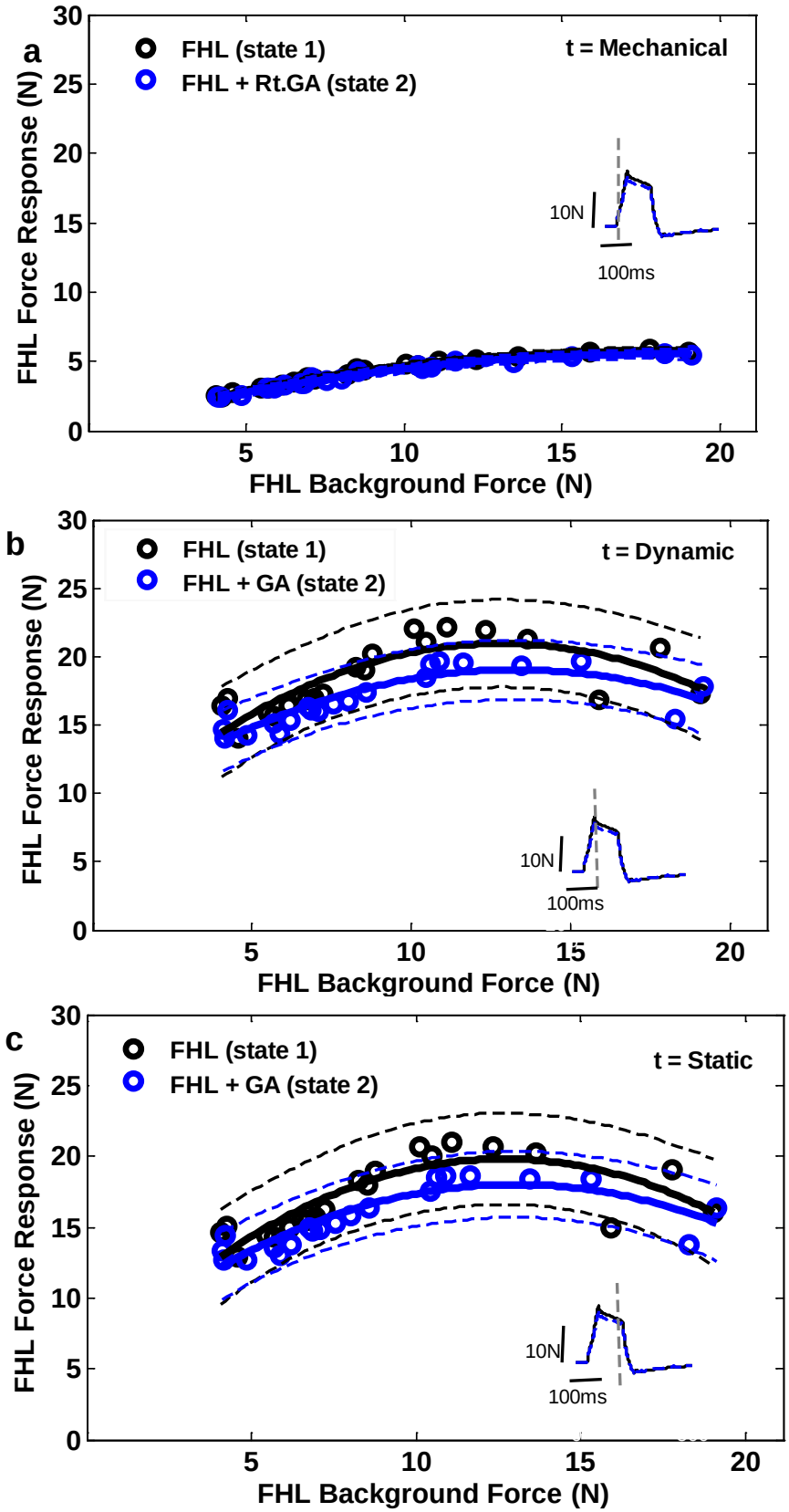

Figure 3.7 (continued)

Figure 3.7 (continued)

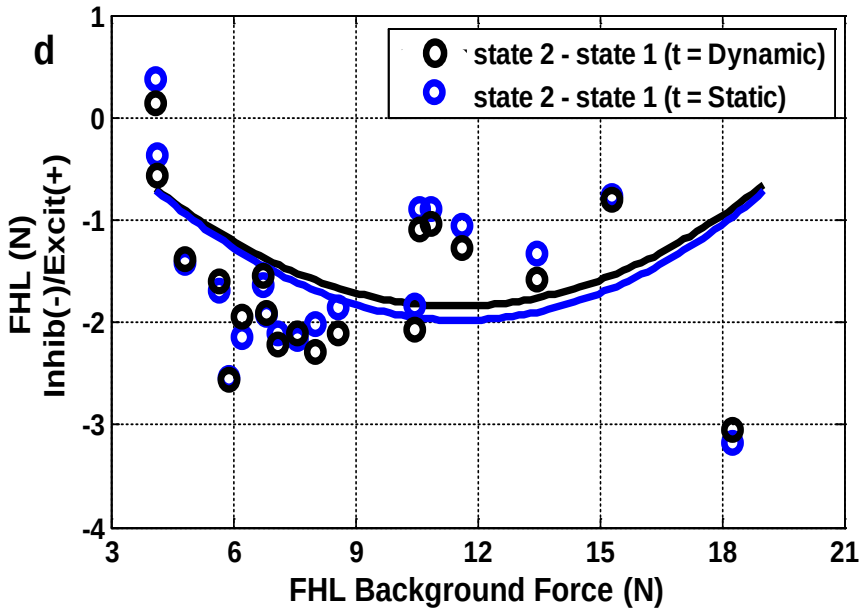

Figure 3.7 Heterogenic inhibition from GA (donor) onto FHL (recipient) during XER in a cat four weeks following chronic LSH at (a) mechanical phase, (b) dynamic phase, and (c) static phase. Black circles represent FHL force responses from stretches occurring in state one and blue circles in state two, respectively. Polynomials and 95% confidence intervals are fit to each population of data, and statistical tests reveal that the populations for the dynamic and static phases are not distinctly separated ($p \geq 0.01$). The inserts in (a), (b) and (c) shows two traces (state 1 black, state 2 blue) matched at approximately mean background force of 11 N for FHL, superimposed to illustrate the magnitude of inhibition from GA onto FHL during XER, and the vertical line indicates the sample time. The magnitude of force responses in FHL is higher during the static versus the dynamic time point. (d) Amount of inhibition of FHL by GA calculated in N for both dynamic (black lines and circles) and static time (blue lines and circles). Each circle represents force response of FHL as a result of single stretch. Difference is calculated by subtracting state 1 and state 2 force responses at an approximate matched background force and time. X-axis shows background force of FHL in N and y axis represent inhibition in N where – stand for inhibition and + for excitation. Polynomial fit is generated to each population of data for dynamic and static time point respectively.

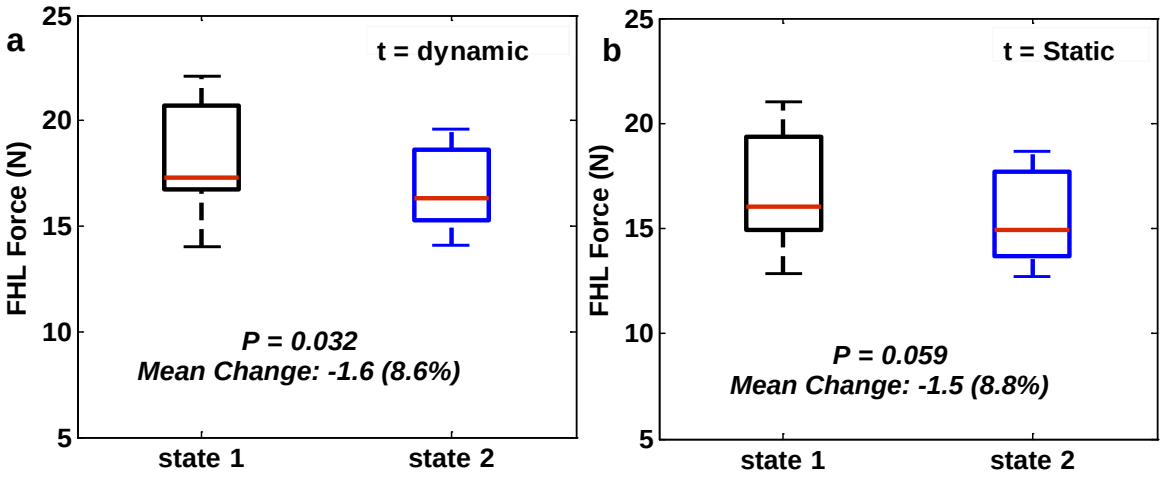

Figure 3.8 (a) Box plot representing statistical analysis of a representative trial showing inhibition of FHL by GA in (a) dynamic time point (b) static time point. State one is shown in black and state 2 in blue. Y-axis shows FHL force in a given trial for both state 1 and 2. The median force response is shown in red color across all FHL stretches in a trial at a given time point. The whiskers of the box plot represent range of force response in each state including maximum and minimum values. The P value, mean change, range of inhibition with SD and percent change is calculated for each time point to demonstrate the amount of inhibition.

3.3.2 FHL strongly inhibits GA following chronic SCI

The intermuscular force feedback interaction from FHL onto GA was examined in all six cats with chronic LSH. Our goal was to compare these results with results of intermuscular force feedback data from GA onto FHL to determine the predominant direction of inhibition between the two muscles post SCI at different time points. Our current data from these experiments has shown that there is predominantly strong inhibition from FHL to GA. Six out of six cats (100%) with chronic LSH exhibited very strong inhibition from FHL onto GA in all 12 limbs (6 of each injured and uninjured side) with $P < 0.001$ that was highly statistically significant across limbs and cats. We propose

that since GA is a strong force producing muscle therefore its strong inhibition could be one of the contributing factors for poor balance control and weight support post SCI.

Figure 3.9 depicts representative raw data from a trial showing intermuscular interaction between GA (recipient) and FHL (donor) from an animal four weeks following chronic LSH during XER. The representative trial consists of 46 stretches in recipient muscle (GA). Half of the stretches were done during state 1 alternating with the other half at state 2. The selection of the trial was done carefully by taking a trial with GA as a recipient muscle with the comparable range of background force with the trial shown in Figure 3.5 (FHL as recipient muscle) from the same animal. The force response in a muscle depends on background force therefore for comparing data it is important to choose the trials with comparable range of background force (Nichols 1989).

Figures 3.9a and 3.9b depict the force output and length input respectively of the recipient muscle (proximal muscle) GA while figures 3.9c and 3.9d depict the force output and length input respectively of the donor muscle FHL. Additionally, the blue vertical dashed lines indicate state 2 where the recipient muscle GA was stretched along with donor muscle FHL. State one is shown in Figures 3.9a and 3.9c without the dashed blue lines. Figure 3.9 clearly shows strong inhibitory force feedback from FHL onto GA in state two. This inhibition appears more pronounced at the end of stretch and hold (static time point). This trend was observed in all six animals on injured as well as uninjured side limb. The inhibition was smaller for the dynamic time point and larger for the static time point in all six animals (100%) irrespective of data collection time after LSH. If we compare figure 3.9 to figure 3.5, we can see a clear trend of predominantly strong

inhibition of GA by FHL and weak inhibition of FHL by GA. Therefore, as we proposed the inhibitory force feedback between the two muscles remain inhibitory after LSH, however its amount and directionality or gradient is altered. In our data it is a consistent distal to proximal directionality of inhibition in animals with chronic LSH.

Figure 3.10 shows the relative amount of GA inhibition by FHL at mechanical, dynamic and static time point in state 1 and state 2. Each individual stretch is divided into three time points to generate the figure. The inhibition is clearly seen in state two and is most strong at static time point consistent with data from control animals. We generated this plot to confirm the time of appearance of inhibition before proceeding on with further data analysis.

We further analyzed the data to look at this inhibition statistically by doing a multiple regression analysis as described earlier in the chapter in detail. Figure 3.11 depict the mechanical, dynamic and static phase of the force feedback from FHL onto GA during XER. While there is slight overlap in the confidence intervals at the lowest background force, approximately 5N, the two populations are clearly separated at higher background forces. Multiple regression yielded $P<<0.01$, thus statistically proving that these populations are distinctly different. Force responses in the recipient muscle, GA, for state one (black circles and lines) and state two (red circles and lines) are shown in Figure 3.11.

The insert in Figure 3.11 is generated by matching background force for both conditions (state 1 and 2) at average background force of approximately 11N across all the stretches in a representative trial. Baselines were subtracted from both traces to better

illustrate the magnitude and time course of the inhibition from FHL onto GA, grey dashed lines on trace represent time point of data analysis.

Figure 3.11a through Figure 3.11d to illustrate the magnitude and timing of inhibition from FHL onto GA. There was no observable separation of data during mechanical time point suggesting a good preparation with good muscle separation not shown here in all six cats across trials. Heterogenic inhibition increases with increasing background force as indicated by the divergence in the polynomial fits. Figure 3.11d shows the amount of inhibition in Newton comparing inhibition in dynamic and static time point across the whole trial at each individual stretch. Polynomial fit to each population of data for dynamic and static time point respectively done. We observed highly statistically significant inhibition of GA by FHL at $p<<0.01$.

Figure 3.12 represents the detailed summary of statistical analysis for the same trial shown in figure 3.13. The inhibition of GA is 59% in static state and 18% in dynamic time point. Same pattern/directionality and strength of force dependent GA inhibition by FHL was observed in 6/6 cats.

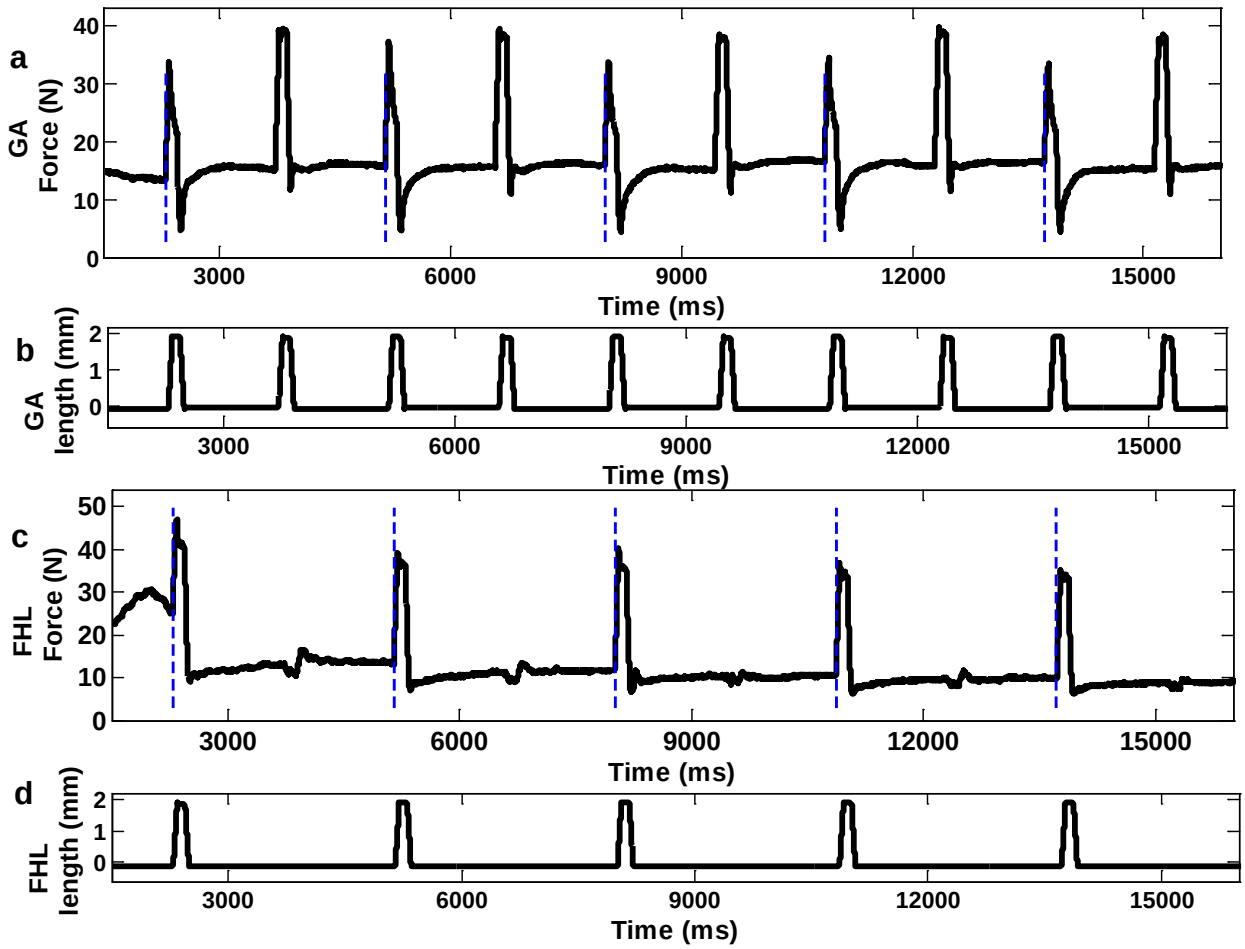

Figure 3.9 (a) Recipient muscle (GA) stretch-evoked force response during XER in a cat 4 weeks following chronic LSH. (c) Donor muscle (FHL) stretch-evoked force response during XER. (b) Recipient muscle (GA) length input to two-state stretch (d) Donor muscle (FHL) length input for two-state stretch. The same conventions as Figure 3.7 apply. A two-state stretch is performed to ascertain strength and sign of feedback between a recipient (GA) and donor muscle (FHL). There is clearly strong inhibition from FHL onto GA in state 2. XER is done by stimulating tibial nerve in the contralateral hindlimb (the side without LSH) at 2T evokes an increase in the background force of the recipient and donor muscles on the injured side hindlimb, GA and FHL respectively (a, c).

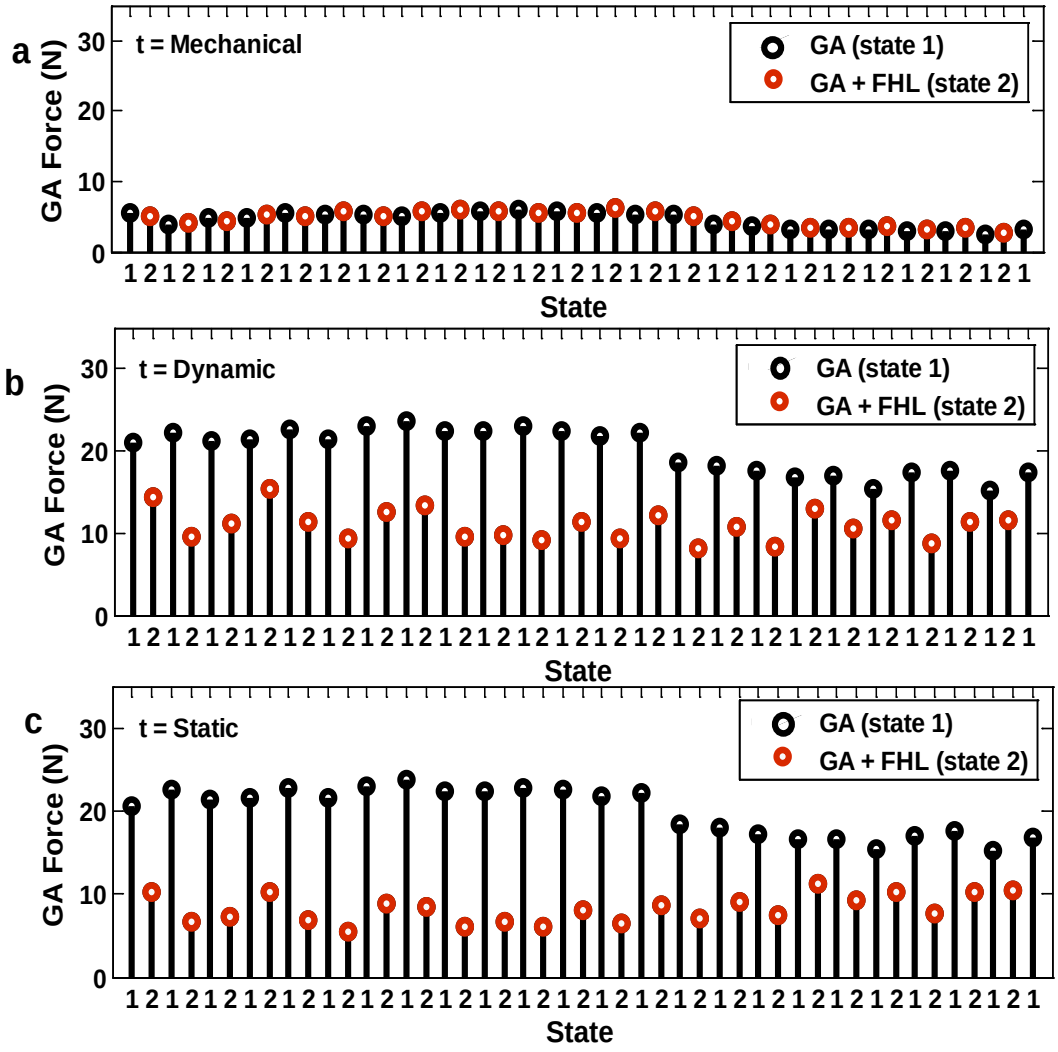

Figure 3.10 Recipient muscle (GA) stretch-evoked force response during XER in (a) mechanical phase, (b) dynamic phase, and (c) static phase. Each individual circle represents FHL muscle stretch response where, blue circles indicate state 2 and black circles indicate state 1. The same conventions as Figure 3.8 apply. There is a large amount of inhibition of GA by FHL at dynamic and static time points during state 2 shown by difference of heights of black and red circles. The inhibition of GA at static time point is larger than at dynamic time point.

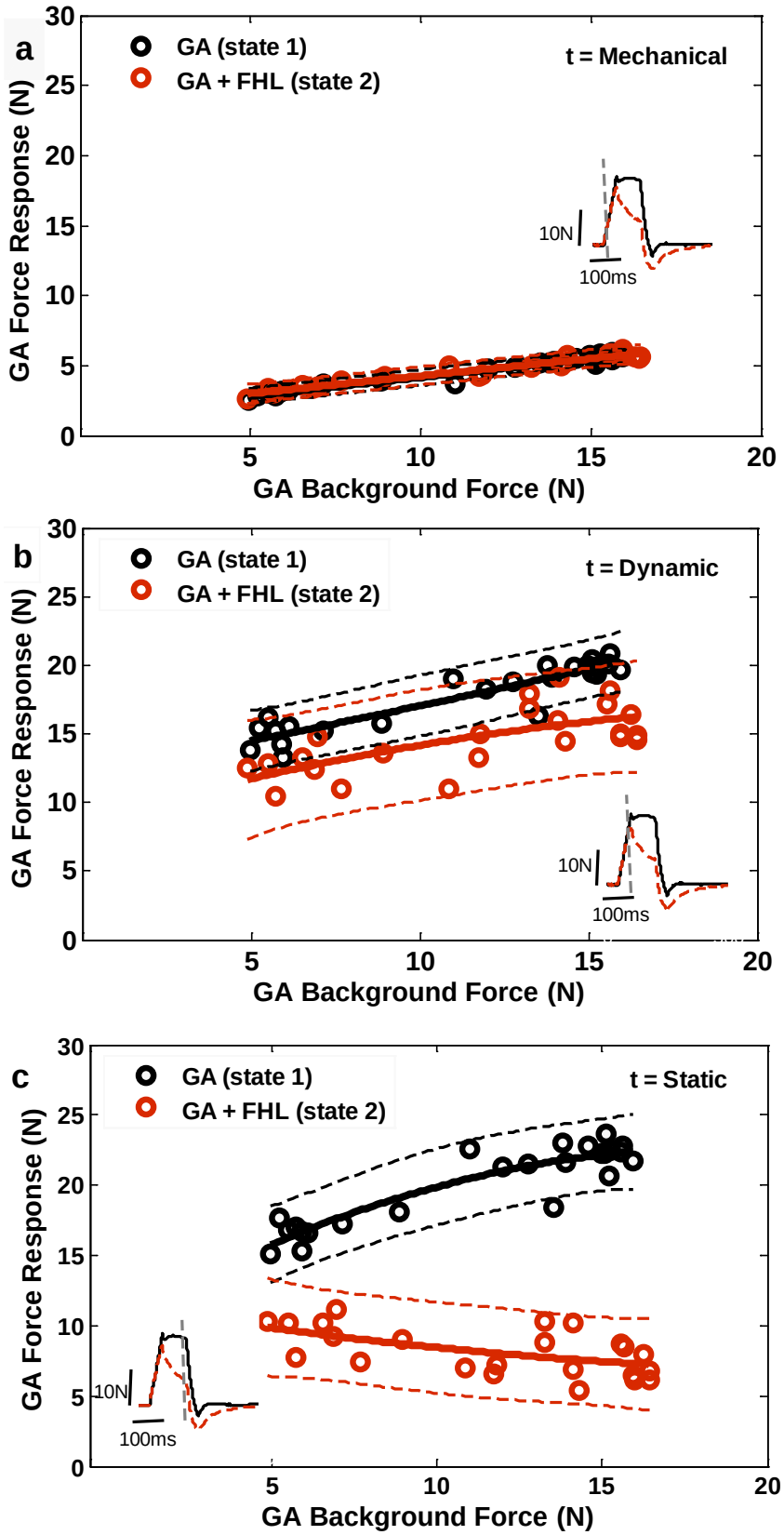

Figure 3.11 (continued)

Figure 3.11 (continued)

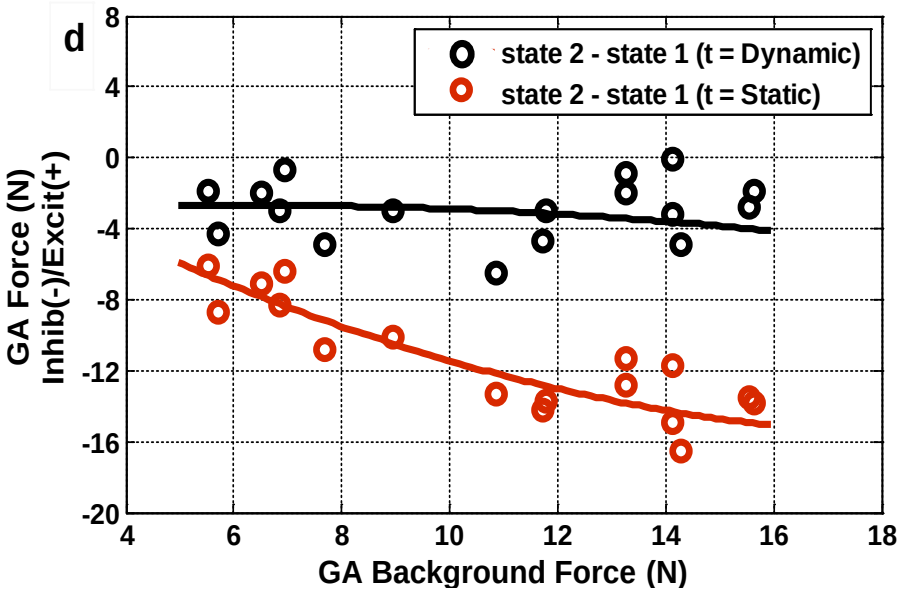

Figure 3.11 Heterogenic inhibition from FHL (donor) onto GA (recipient), during XER in a cat 4 weeks following chronic LSH for (a) mechanical phase, (b) dynamic phase, and (c) static phase. The same conventions as Figure 3.9 apply. Polynomials and 95% confidence intervals are fit to each population of data, and statistical tests reveal that the populations for the dynamic and static phases are distinctly separated ($p \leq 0.01$). The inserts in (a), (b) and (c) shows two traces matched at approximately 11N average background force in GA from state one (black line) and state two (red line) superimposed to illustrate the magnitude of inhibition from FHL onto GA during XER, and the vertical line indicates the sample time. The magnitude of force responses in GA is higher during the static versus the dynamic time point. (d) Amount of inhibition of GA by FHL calculated in N for both dynamic (black lines and circles) and static time (red lines and circles). Each circle represents force response of FHL as a result of single stretch. The same conventions as Figure 3.9d apply. Polynomial fit is generated to each population of data for dynamic and static time point respectively.

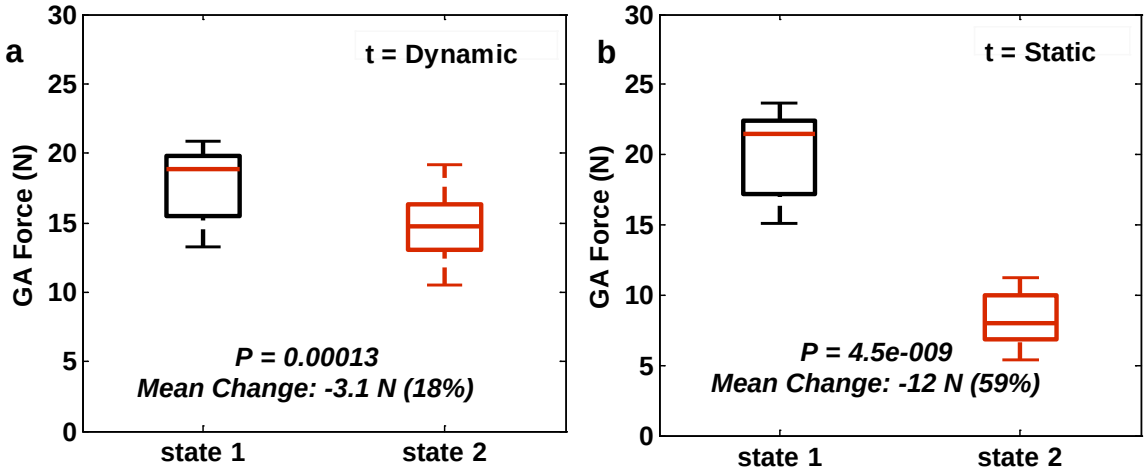

Figure 3.12 Box plots representing statistical analysis of a representative trial showing strong inhibition of GA by FHL following chronic LSH in (a) dynamic time point (b) static time point. State one is shown in black and state 2 in red. The median is shown in red color across stretches in a trial at a given time point. The P value, mean change and percent change are calculated for each time point to demonstrate the amount of inhibition across state and time point. The comparison clearly shows increase in inhibition from dynamic to static time point so, inhibitory interactions stayed inhibitory after LSH/SCI but their strength stayed strong from distal to proximal muscle.

3.3.3 The pattern of inhibitory force feedback across limbs and animals between GA and FHL following chronic LSH

We evaluated the strength and sign of feedback between GA and FHL across animals in both hindlimbs, to determine the relative contribution of inhibition between proximal and distal muscles in cats with chronic LSH. The force feedback between the GA muscle and FHL muscle was mainly inhibitory in all six cats. This was examined in all 6 experiments both with and without XER. Of these experiments, 6/6 exhibited strong inhibition from FHL onto GA across cats and limbs. Therefore, there is a definitive consistent pattern of inhibition between the two muscles following SCI. We therefore

conducted comparative quantitative analysis across limbs and cats. We observed very strong inhibition of 26.7% to 79% at t= static on injured side and 18% to 60% on uninjured side limb in chronic LSH across 6 cats as depicted in table 3.1. Therefore inhibition is observed bilaterally even after partial SCI (LSH). Although the inhibition is stronger in injured side limb in comparison to intact/uninjured side limb but preferred direction from FHL to GA is the same across limbs and animals. This inhibition was force dependent across limbs (12/12 limbs) and animals (6/6 cats). It increased with increasing background force over the time of stretch and hold (each stretch). The P value is $<<0.01$ for both dynamic and static time point.

An example of the inhibition between GA and FHL is shown in Fig. 3.13 from a cat with chronic LSH (4 week following LSH) comparing the two legs in the same animal. The data from injured side limb has been described earlier in detail in Figure 3.5 through Figure 3.12. Figure 3.13a shows the amount of inhibition in four representative trials, two for each limb representing inhibition between GA and FHL. When both muscles were stretched for state two, strong inhibition of GA by FHL was observed in both injured side limb and uninjured side limb. Each circle represents force response obtained by subtracting state 1 force responses from state 2 force responses at approximate matched background force for each muscle separately in Figure 3.13a. We then normalized the data by converting change in N to percent change for both limbs in each animal shown in Figure 3.13b. The polynomial fits for the injured and uninjured side for GA and FHL showed strong inhibition of GA by FHL. Since, the amount of force production by a muscle and its background force varies from one trial to the next the inhibition amount is

normalized to percent change to make comparisons across trials, limbs and animals more meaningful. The strong inhibition of GA by FHL was seen in 6/6 cats (100%).

The statistical results of the analyses across limbs and cats over different time points after the LSH are summarized in Table 3.1 and Table 3.2. Both tables include measurements for both limbs in each animal. The tables contain the range of maximum background force, range of inhibition, mean inhibition, SD and P value range in each limb observed across each of the six animals. Figure 3.14 demonstrate comparison across cats and limbs in all six animals. We selected trials with comparable background forces. It is obvious from the figure that inhibition from FHL onto GA is strong in all six animals irrespective of the time following LSH. Therefore we propose that this altered heterogenic inhibition between these two muscles appear in chronic LSH animals after injury and possibly stay there up to at least 20 week following LSH. It does not change with improvement in locomotor activity of the animal. Figure 3.15 represent the suggested model for intermuscular inhibition between FHL and GA following chronic LSH.

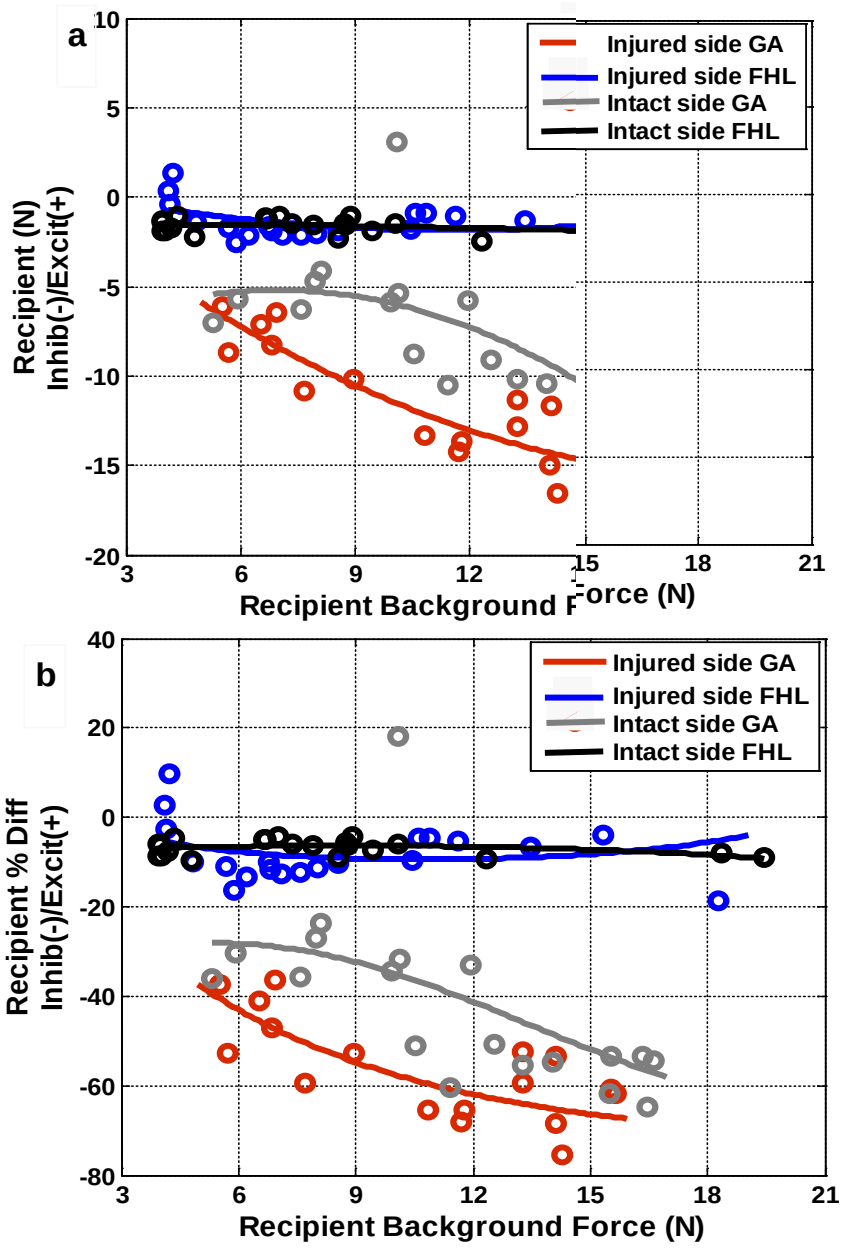

Figure 3.13 Comparison of inhibition between FHL and GA in a cat 4 weeks following chronic LSH across both hindlimbs (a) inhibition in N (b) percent change/inhibition. The trials were selected with comparable background forces of recipient muscles in a given animal. The FHL inhibition by GA is shown on injured side (blue circles) and uninjured side (black circles), while GA inhibition by FHL is shown on injured side (red circles) and uninjured side (grey circles). Each circle is calculated by subtracting state one force response from state 2 force response at static time point at a given time and background force of recipient muscle. Polynomials are fit to each population of data. The directionality of force feedback between GA and FHL is distal to proximal in both limbs post LSH with greater amount of inhibition on the injured side limb.

Table 3.1 Magnitudes of inhibition of recipient muscle FHL by donor muscle GA during XER in percentage change, range, SD and P values for each limb in cats following chronic LSH at 2, 4, 8 and 20 weeks. Inhibition is statistically significant if P<0.01. The data shown includes 3 to 6 observations in each limb in every cat each trial consisted of 42-60 stretches each.

RECIPIENT (FHL)	DONOR (GA)							
	Cats/weeks post LSH	Recipient Muscle Max Background force Range	Injured side limb			Uninjured side limb		
			%Δ (-) Range	% Δ (-) Mean ± SD	P value	% Δ (-) Range	%Δ (-) Mean ± SD	P value
	Cat1 = 2W	8 ~ 22	8~17	11.7 ± 3	≤ 0.01	14 ~16	14.8 ± 1	≤ 0.01
	Cat2 = 4W	20 ~ 30	12 ~ 16	14.0 ± 3	≤ 0.05	13 ~25	19 ± 8	≤ 0.01
	Cat3 = 4W	24 ~ 32	10 ~ 13	11.6 ± 2	≤ 0.01	6 ~ 11	7.9 ± 3	≤ 0.04
	Cat4 = 4W	15 ~ 25	7 ~ 16	11.2 ± 5	≤ 0.01	5 ~ 7	6.5 ± 1	≤ 0.05
	Cat5 = 8W	12 ~ 20	10 ~ 12	10.9 ± 1	≤ 0.05	9 ~ 14	11.6 ± 4	≤ 0.05
	Cat6 = 20W	9 ~ 30	17~25	20.7 ± 4	≤ 0.01	21 ~ 28	24.5 ± 5	≤ 0.01

Table 3.2 Magnitudes of inhibition of recipient muscle GA during XER between in percentage change, range, SD and P values for each limb in cats following chronic LSH at 2, 4, 8 and 20 weeks. Inhibition is statistically significant if P<0.01. The data shown includes 3 to 6 observations in each limb in every cat each trial consisted of 42-60 stretches each.

RECIPIENT (GA)	DONOR (FHL)							
	Cats/weeks post LSH	Recipient Muscle Max Backgrou-nd force Range	Injured side limb			Uninjured side limb		
			%Δ (-) Range	% Δ (-) Mean ± SD	P value	% Δ (-) Range	%Δ (-) Mean ± SD	P Value
	Cat1 = 2W	20 ~ 32	38 ~ 67	52.3 ± 15	< 0.001	25 ~ 29	27.3 ± 2	< 0.001
	Cat2 = 4W	7 ~ 30	41 ~ 57	49 ± 11	< 0.001	11 ~ 18	14.5 ± 5	< 0.001
	Cat3 = 4W	10 ~ 32	42 ~ 62	54.8 ± 9	< 0.001	36 ~ 60	48.3 ± 11	< 0.001
	Cat4 = 4W	18 ~ 42	41 ~ 44	42.5 ± 2	< 0.001	25 ~ 28	26.5 ± 2	< 0.001
	Cat5 = 8W	18 ~ 28	36 ~ 55	45.7 ± 13	< 0.001	30 ~ 37	33.5 ± 5	< 0.001
	Cat6 = 20W	6 ~ 9	41 ~ 45	42 ± 3	< 0.001	25 ~ 41	35.3 ± 11	< 0.001

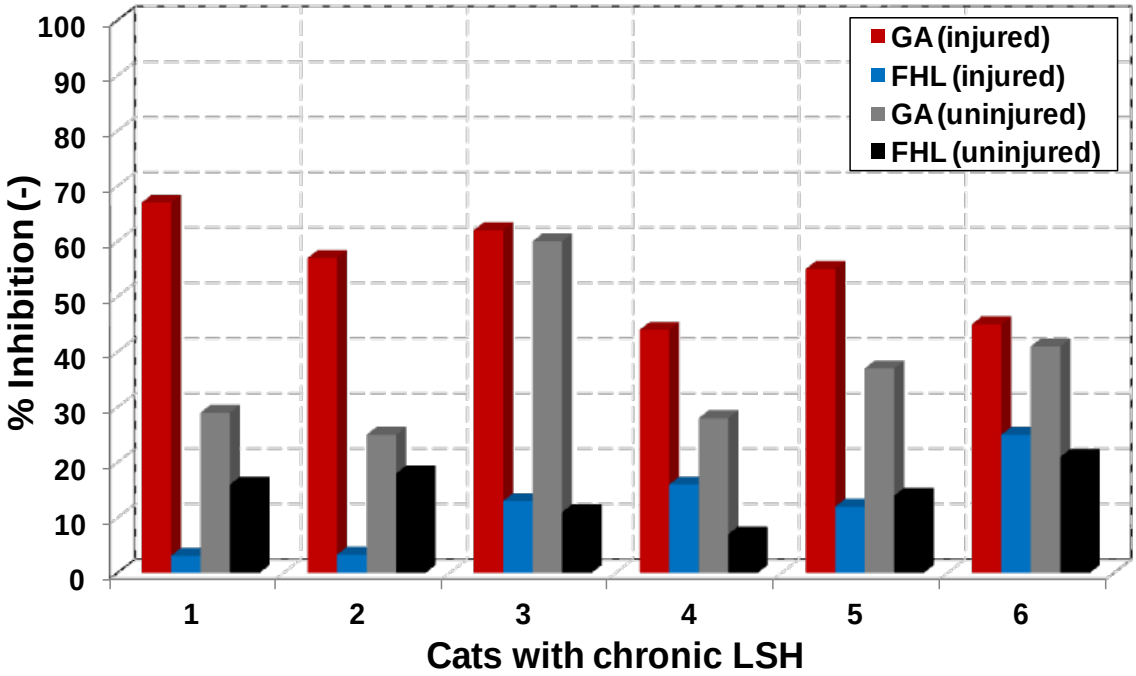

Figure 3.14 Comparison of heterogenic inhibition across limbs and cats in all six animals (chronic LSH) to show the trend or pattern of inhibition. X-axis represent cats numbered from 1 to 6(cat-1 is two weeks, cat-2 four weeks, cat-3 four weeks, cat-5 eight weeks and cat-6 twenty weeks post SCI). Y-axis represents inhibition in term of percent change. Each bar represents one trial in a given animal. Trials selected with comparable background forces and optimal inhibition for comparison across animals and limbs.

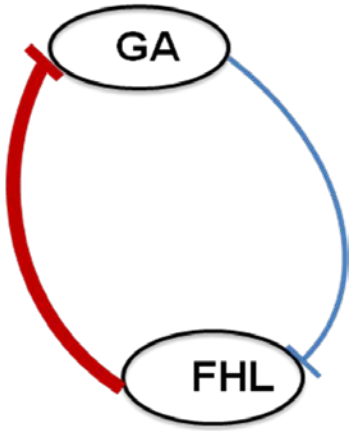

Figure 3.15 Summary diagram/proposed model of the heterogenic inhibition between ankle extensors FHL and GA following chronic LSH. Inhibition between GA and FHL has a greater strength in distal to proximal direction (red) in comparison to proximal to distal direction (blue).

3.3.4 Recipient muscle force response is correlated with the background force of the donor muscle across limbs and animals between GA and FHL following chronic LSH

Data published by Nichols in 1989 using decerebrate cats indicate that the amount of inhibition in recipient muscle depends on the force of the donor muscle. For this reason we further analyzed the recipient force responses against the donor background force to study the effect of SCI on the amount of inhibition in relation to the donor background force. We also plotted recipient muscle background force as a dependent variable against the donor muscle background force as an independent variable in the form of a simple scattered graph as shown in Figure 3.16a and 3.17a. R^2 values were calculated to determine the correlation between the two background forces. This was done to demonstrate that the two muscles compared for inhibition amount exhibited increasing background force increase over time in a comparable manner.

The stretches were divided into three distinct time points showing change in force response of the recipient muscle from state 1 to state 2 were used for further analysis of the data. The populations of integrated values from the respective time points plotted separately as a function of background force of the donor muscle obtained from the original force traces shown in Figure 3.5 and 3.9. Multiple regression analysis was performed to test the overall separation of the populations of force responses (Wilmink and Nichols 2003).

Figure 3.16 and Figure 3.17depict the typical analysis, whereby force responses of recipient muscle for a specific time point (mechanical, dynamic and static) are plotted as

a function of the background force of the donor muscle. Each data point (each circle) represents individual force response of the recipient muscle from the recorded raw data when the muscle was either stretched alone (black circles) or response of the recipient muscle when it was stretched with another muscle (colored circles). Polynomial fits and 95% confidence intervals were fit to each population of data for a given time point at P value $\leq$ 0.01.

We observed increase in force response of the recipient muscle along with increase in background force of the donor muscle consistent with the data from decerebrate animals.

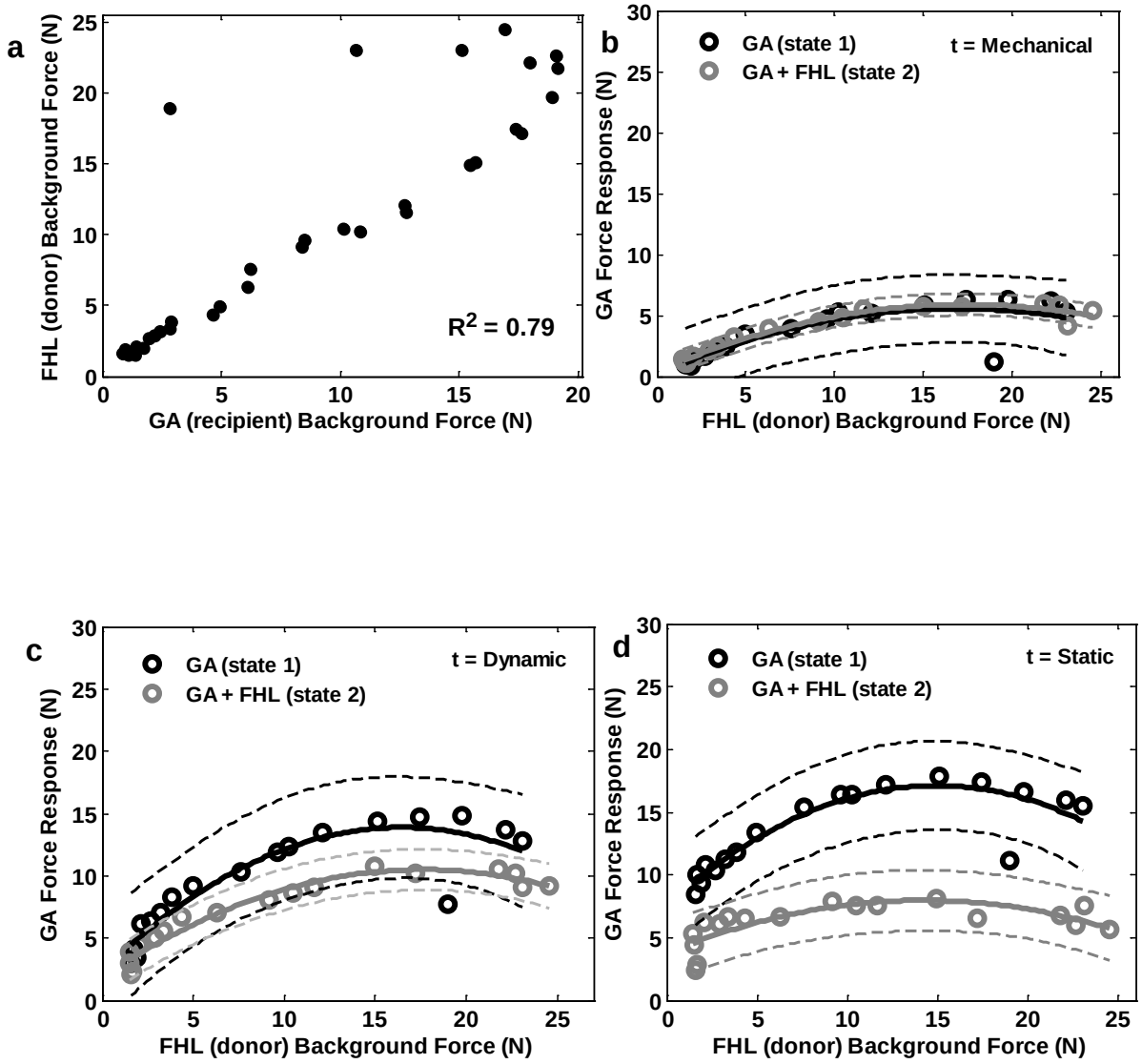

Figure 3.16 Heterogenic inhibition of GA (recipient) by FHL (donor) following chronic LSH. (a) Background forces of FHL and GA depicting the comparable increase in both muscles background force as a result of 2mm stretch at a highly statistically R^2 value of 0.79 (significant correlation). The state 1 force response of GA (black circles and lines) and state 2 response (grey circles and lines) demonstrated with donor background force on x-axis as an independent variable at (b) Mechanical time point. (c) Dynamic time point (d) static time point. Each set of force responses were fitted with quadratic polynomials and 95% confidence limits.

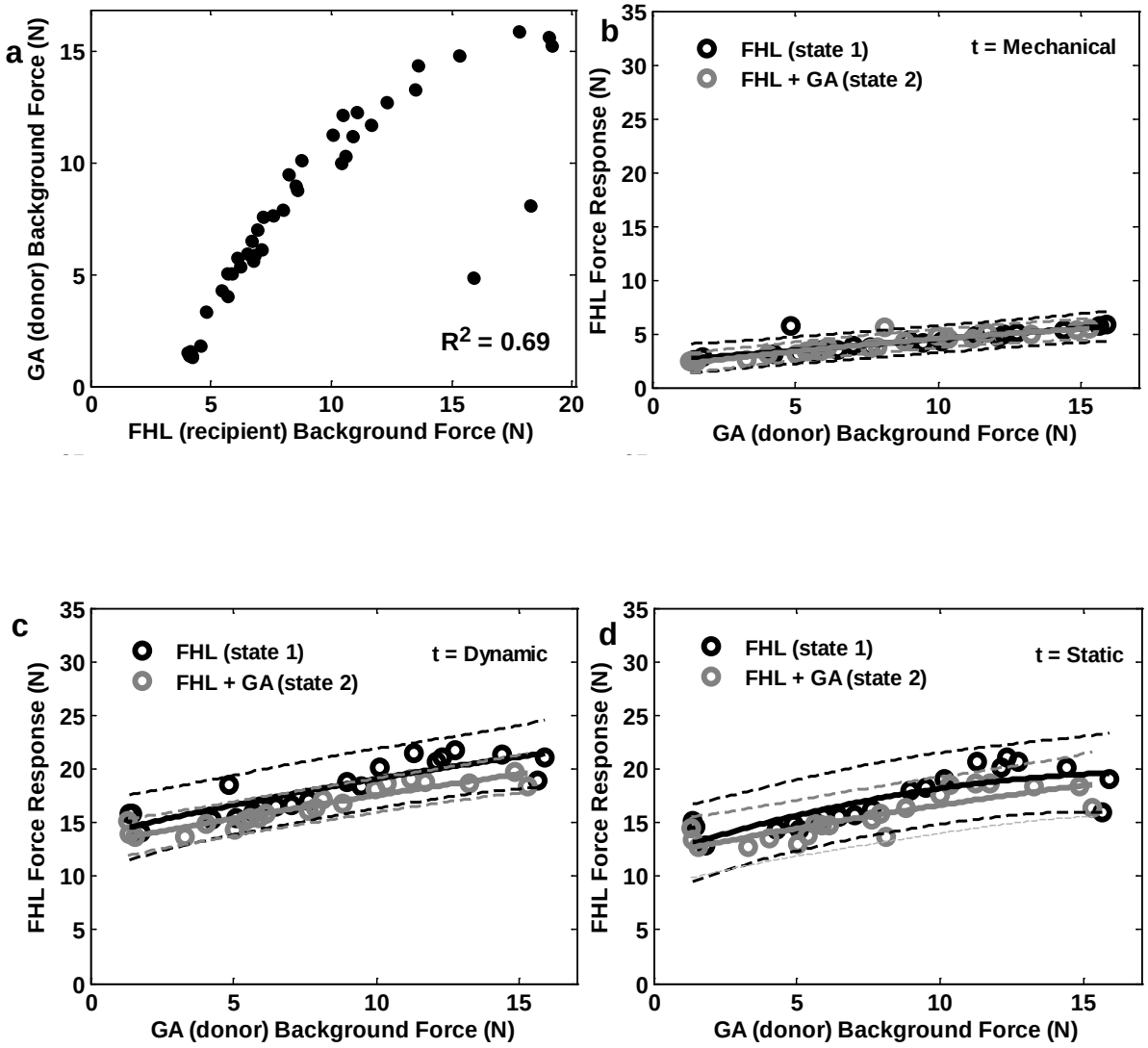

Figure 3.17 Heterogenic inhibition of FHL (recipient) by GA (donor) following chronic LSH. (a) Background forces of FHL and GA depicting the comparable increase in both muscles background force as a result of 2mm stretch at a highly statistically R^2 value of 0.69 (significant correlation). The state 1 force response of FHL (black circles and lines) and state 2 response (grey circles and lines) demonstrated with donor background force on x-axis as an independent variable at (b) Mechanical time point. (c) Dynamic time point. (d) Static time point. Each set of force responses were fitted with quadratic polynomials and 95% confidence limits.

3.3.5 Intermuscular force feedback interactions between FHL and GA in acute spinal cord injury in cat.

We studied intermuscular force feedback interaction between GA and FHL in acute SCI to determine the time of onset of altered intermuscular interactions observed in our study using chronic LSH. We used two types of acute SCI namely acute LSH and acute DSH. In this section I will describe the results from three cats with acute LSH and a brief summary of results from one cat with acute DSH. Our secondary purpose of this study was to determine which part of spinal cord might be involved in balance control (ventral half or dorsal half). We hypothesize that if the results from acute LSH and acute DSH are not similar then it means ventral half or vestibulospinal tract might be involved in posture control.

Figure 3.18 and Figure 3.19 depict representative examples of force feedback interaction between GA and FHL in cats with acute LSH. Figure 3.18 shows weak inhibition of FHL by GA comparable to our results in chronic LSH in Figure 3.7. The analysis was done at three time points (mechanical, dynamic, static) as shown in Figure 3.18 (a, b, c). The inhibition of FHL by GA increased from dynamic (figure 3.18b) to static (Figure 3.18 c) time point. The force responses of FHL was force dependent in all three animals and increased with increasing background force of FHL and donor muscle GA. The small separation of confidence intervals indicates weak inhibition of FHL by GA using XER in acute LSH. Figure 3.19 shows strong inhibition of GA by FHL consistent with our results shown in Figure 3.11 in chronic LSH. The wide separation of confidence intervals indicates strong inhibition of GA by FHL.

The inhibition between the two muscles is further explained in terms of percent change in Figure 3.20a. The detailed statistical analysis of the two trials representing inhibition of GA by FHL (72% inhibition) and FHL by GA (8% inhibition) at P value > 0.01 is explained in Figure 3.20b and Figure 3.20c respectively. We observed that the inhibition was stronger from FHL onto GA in 3/3 (100%) cats with acute LSH. We were not able to demonstrate this altered pattern in a cat with acute DSH instead we observed bidirectional/equal amount of inhibition between GA and FHL in acute DSH not shown here. However, we propose further detailed studies in acute DSH to confirm our findings.

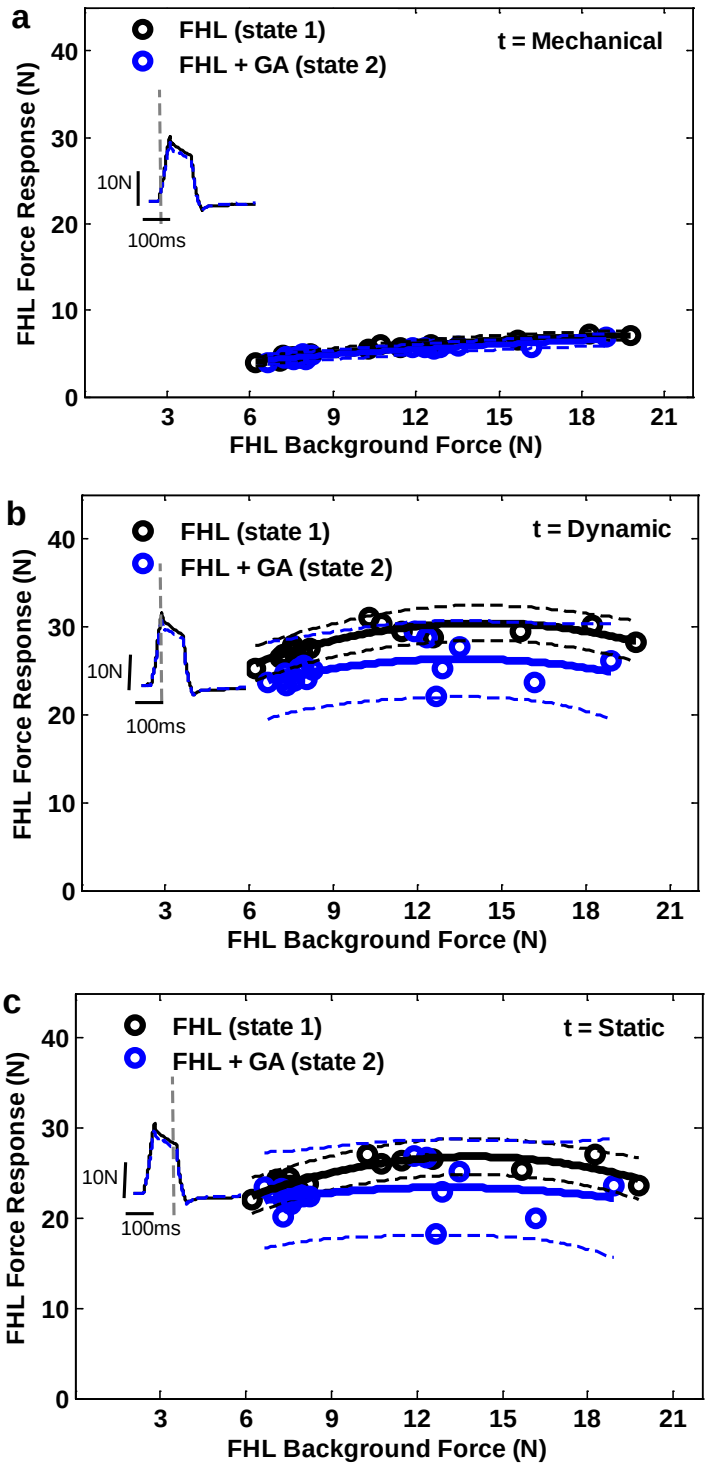

Figure 3.18 Heterogenic inhibition from GA (donor) onto FHL (recipient), during XER in a cat following acute LSH for (a) mechanical phase, (b) dynamic phase, and (c) static phase. The same conventions as Figure 3.11 apply. Polynomials and 95% confidence intervals are fit to each population of data. Each circle (blue for state 2 and black for state 1) represents force response of FHL as a result of a single stretch.

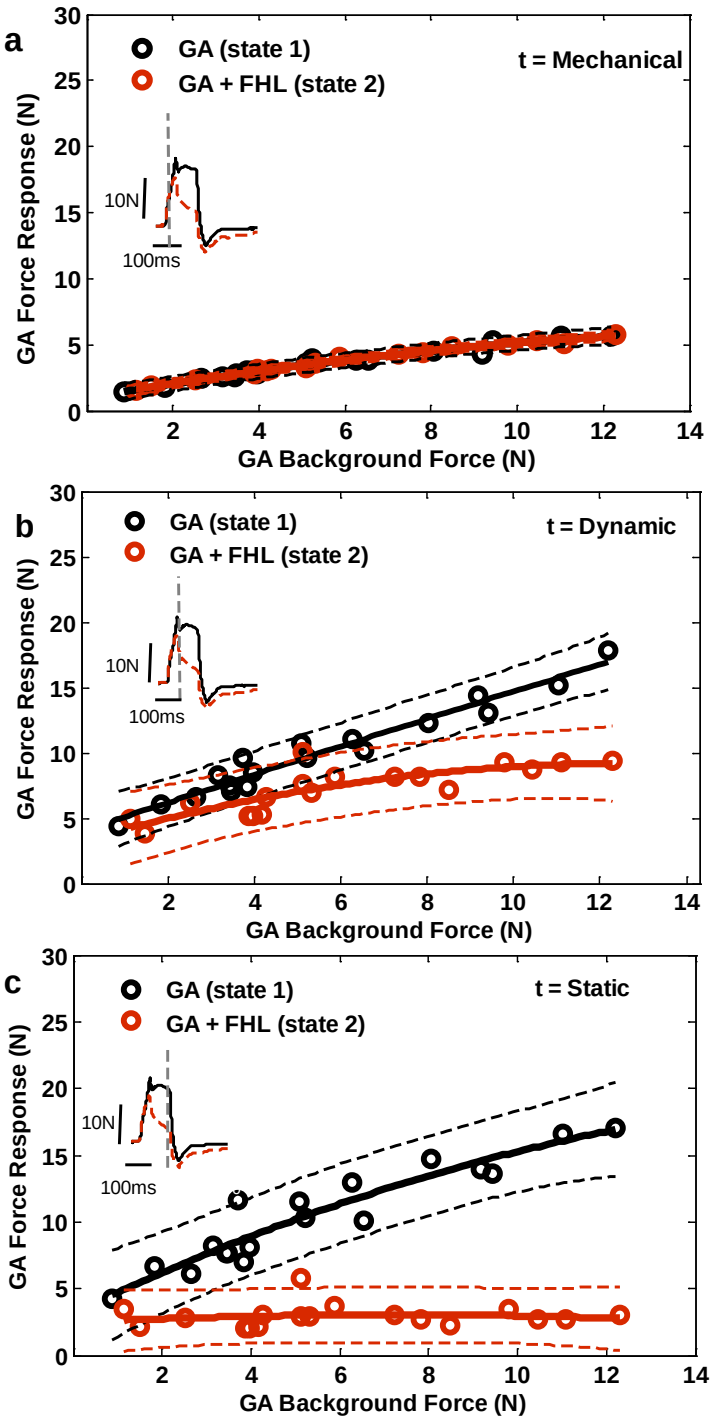

Figure 3.19 Heterogenic inhibition from FHL (donor) onto GA (recipient), during XER for (a) mechanical phase, (b) dynamic phase, and (c) static phase in a cat following acute LSH. The same conventions as Figure 3.11 apply. Polynomials and 95% confidence intervals are fit to each population of data. Each circle represents force response of GA as a result of single stretch. The clear separation of confidence intervals indicates strong inhibition of GA by FHL at P value > 0.01.

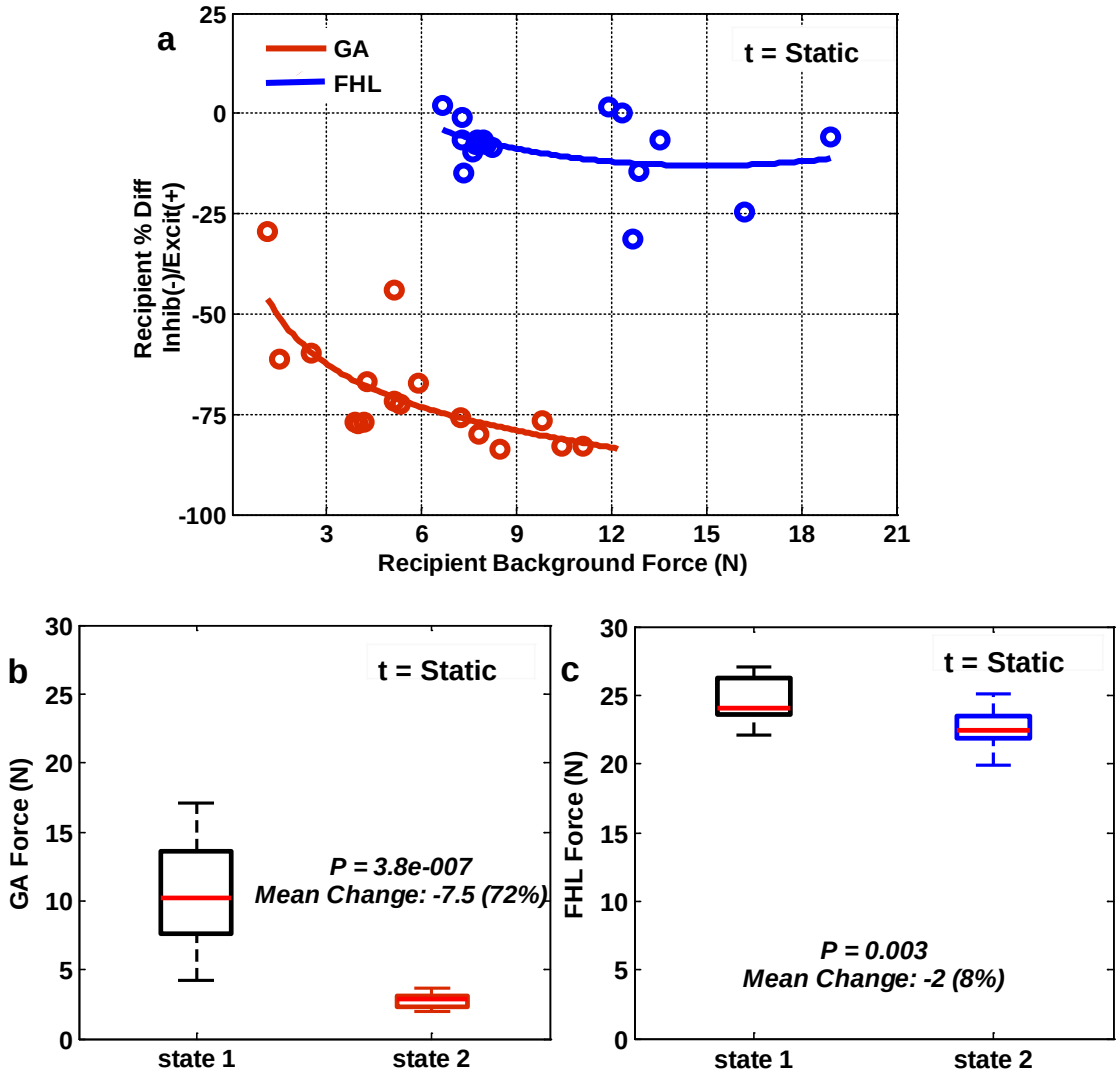

Figure 3.20 (a) Amount of inhibition of FHL by GA and GA by FHL is calculated in N (blue circles for FHL and red circles for GA) at static time point. Each circle represents force response of recipient muscle as a result of a single stretch. Difference is calculated by subtracting state 1 and state 2 force responses at an approximate matched background force and time and then converting the difference in N to %change/inhibition. X-axis shows background force of recipient muscle in N and y-axis represent inhibition in % where – stand for inhibition and + for excitation. Polynomial fit is generated to each population of data (each recipient muscle). (b and c) Box plots representing statistical analysis of a representative trial at static time point explaining force feedback inhibitory interactions between GA and FHL following acute LSH. State one is shown in black and state 2 in red for GA and blue for FHL. The median is shown in red color across stretches in a trial at a given time point. The P value, mean change and percent change are calculated to demonstrate the amount of inhibition between GA and FHL. The comparison of (b) and (c) clearly shows stronger inhibition from FHL onto GA.

3.3.6 Clasp knife inhibition

The hallmark of clasp knife inhibition after complete transaction of spinal cord has been described as a profound autogenic and heterogenic inhibition that occurs with the latency of more than 80 ms (Nichols and Cope 2001). The heterogenic inhibition is observed even at very low background forces of the recipient muscle.

In our study we did not observe any autogenic inhibition between GA and FHL following LSH. Figure 3.21 depicts a representative example of absence of clasp knife inhibition in animals with chronic LSH. There is no autogenic inhibition in state one (black line). The latency of reflex response is comparable to decerebrate cats with intact spinal cord described earlier in chapter 2, Figure 2.10 (28 ±4 ms). This latency is much smaller than the clasp knife inhibition reflex latency of more than 80 ms. Clasp knife inhibition between GA and FHL was also not observed in acute LSH. The sum of autogenic and heterogenic inhibition in state 2 was not strong enough to drop the force response of the recipient muscle to almost zero (Nichols and cope 2001). The absence of clasp knife inhibition was observed in 6/6 cats with chronic LSH (100%) and 3/3 (100%) cats with acute LSH in both hindlimbs.

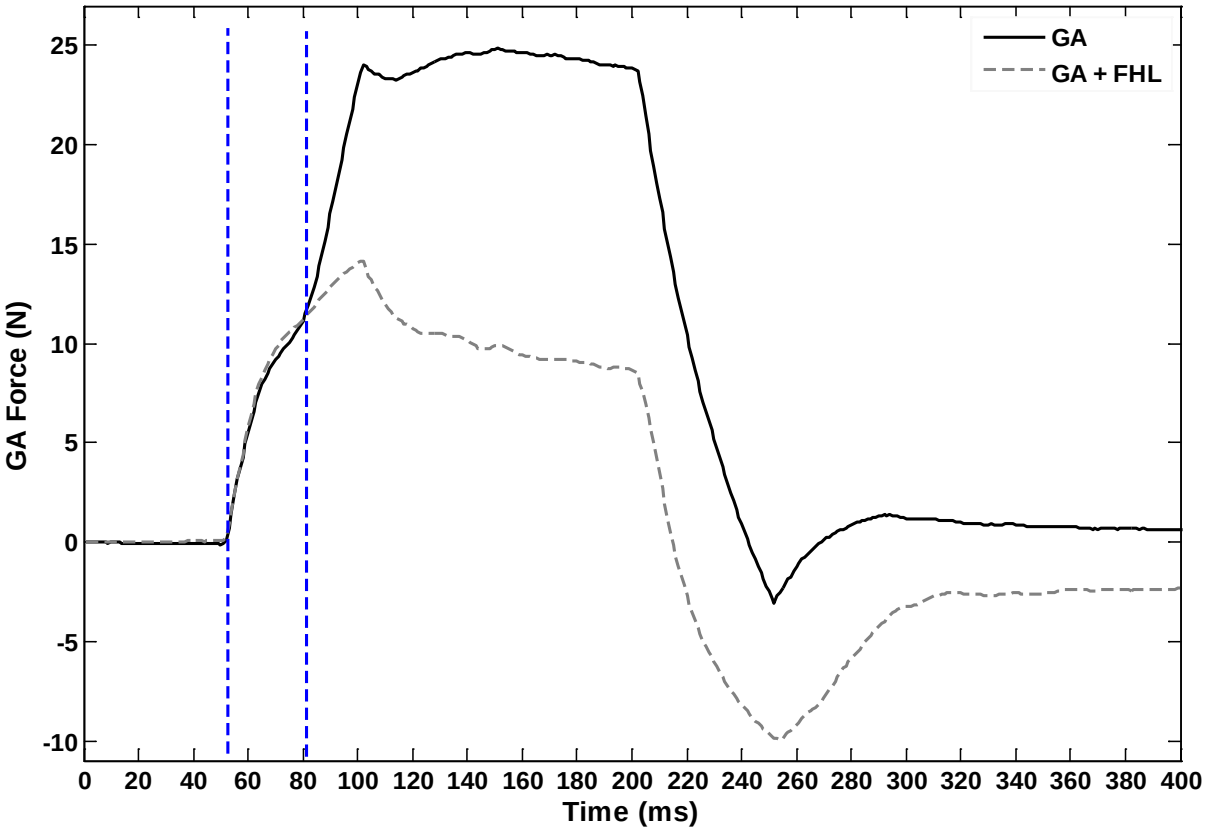

Figure 3.21 Reflex latency for the FHL/GA interaction was calculated at 28 ± 4 ms. Distance between the two blue dashed lines indicates latency of reflex. There was no evidence of autogenic inhibition in state 1 and the force of recipient muscle did not drop.

3.4 Discussion

In the present study, we describe changes in intermuscular reflexes over time using the chronic partial spinal lesion paradigm with a focus on comparison between hindlimb muscles using GA and FHL. We also compared our results to control animals and animals with acute LSH. The main motivation of this study was to understand the intermuscular interactions following incomplete SCI that is comparable to human contusion injury of spinal cord. The most common types of spinal cord injury in humans are contusions and compressions. Spinal contusion occur when the spinal cord is bruised, often causing inflammation and bleeding from blood vessels near the injury site. Spinal compressions occur when pressure is applied to the spinal cord by an outside source, such as bones, from a vertebral fracture, or blood, from an adjacent hematoma. Hence, clinically most spinal cord injuries in humans are incomplete in nature and consequently, studying the reorganization of reflex pathways after an incomplete SCI in cats could provide important clues as to their intrinsic organization, reorganization following partial SCI, and possible involvement in locomotor recovery and poor weight support.

Our results indeed showed that the intermuscular pathways are modified after a partial spinal lesion. Although, all the animals with chronic LSH were able to walk again within a week following SCI they all had poor balance control ability. The most likely explanation is that the spared pathways from supraspinal structures are most probably involved in reorganizing the spinal CPG during locomotor recovery in animals with chronic SCI. Since our experimental animals were able to walk it is possible that the spinal CPG in chronic SCI could have reached a stage where it could function more or less independently from descending supraspinal inputs at the time of terminal

experiments involving decerebration either due to sprouting of neurons in spinal cord or reorganization of CPG in response to altered central and sensory/proprioceptive input. It is unlikely that the locomotive recoveries in hindlimbs despite of altered intermuscular interactions that occur over multiple weeks are dependent only upon the descending contralateral spared corticospinal pathways. More likely, plasticity of descending and/or spinal circuitry, in combination with spared pathways, plays a significant role in the changes seen. In addition following incomplete SCIs in rodents, substantial increases in collateral sprouting of the corticospinal tract have been reported during the first 2 months post-injury (Bareyre et al. 2004; Li et al. 1994). This is supported by study in cats showing direct anatomical evidence of interneuronal sprouting in the cat (Fenrich and Rose 2009). We propose that the sprouting and new connection formation in spinal cord is not a perfect phenomena and may involve many new circuits formation that are not perfect resulting in incomplete or faulty recovery of balance control following SCI.

We propose that balance control and weight support appear to be more complex motor task that could not be totally controlled at spinal level and instead need perfect supraspinal input. We observed strong inhibition emanated exclusively from FHL onto GA and weak inhibitory interactions were found in the opposing direction in all six animals irrespective of the time past SCI. It was observed from 2 to 20 week post chronic SCI. The results remained consistent across animals and limbs. We were able to see the same results in acute LSH. Thus, proving that the intermuscular interactions are altered immediately following LSH and the changed are maintained up to 20 weeks. During this period locomotion is recovered however, balance control is never fully recovered. The

changes are therefore at spinal level independent of any repair process in decending pathways.

Another explanation for altered intermuscular interactions following LSH is that there could be a central mechanism for deciding the relative strengths of these force-dependent feedback pathways that are possibly disturbed in SCI. There are functional consequences of altered inhibition, namely poor interjoint coordination. While GA and FHL both have mechanical actions at the ankle, GA generates the greater non-sagittal moment due to large abduction torque about the ankle joint. This could play an important role in stability by increasing the base of support during any motor task requiring stabilizing effect. Therefore, strong inhibition of GA may interfere with ankle stability and balance control. FHL on the other hand has a smaller ankle torque; it also produces an adduction torque and acts on the MTP and distal interphalangeal (IP) joints (Goslow et al. 1972; Lawrence and Nichols 1999). Strong inhibition of GA reduces stability at ankle by increased planterflexion and abduction. Previous studies in locomoting animals also indicated a persistent pattern of force feedback gradient during locomotion between GA and FHL (Ross and Nichols 2009). Therefore, we propose that the interactions between GA and FHL are vital in maintaining normal motor activity in cat. Since, animals have shown three different intermuscular interactions between GA and FHL in decerebrate cats we propose that the animal loses its ability to change the appropriate task dependent muscular interactions between these two muscles following LSH needed for different task performance.

Since we have observed strong inhibition of GA by FHL in our experiments we propose that the weak inhibition of FHL by GA disturbs the net torque and interjoint as well as cross-axis coupling that, in some cases, parallels the mechanical coupling of biarticular muscles (Nichols 1994) required for stability at ankle joint. We propose that an imbalance between adduction and abduction at ankle resulting from altered interactions between GA and FHL could be one of the reasons for poor stability during standing and walking in SCI. Additionally, inhibition, in combination with excitatory muscle length feedback, contributes to the regulation of whole-limb stiffness (Nichols and Houk 1976; Nichols et al. 1999). Therefore net result of this strong distal to proximal gradient between GA and FHL not only effects stability at ankle joint but will also result in poor whole limb stiffness. In addition, GA is a major force producing muscle in hind limb and its strong inhibition could result in failure to maintain posture against gravity and other perturbations.

Partial spinal lesion (LSH in our study) primarily disrupts the anatomical organization of spinal cord on one side. Therefore, one might expect to observe changes on the damaged side only. However, there is crossing over of spinal tracts (medial vestibulospinal tract, pontine reticulospinal tract and ventral corticospinal tract) therefore we see some changes on the uninjured side limb too. Our data showed increased inhibition of a major force producing hind limb muscle GA from FHL bilaterally in each animal. This pattern was seen in all animals in both limb but it was asymmetric in amount across limbs in each animal. There was stronger inhibition of GA by FHL on injured side that might be there to offer more compensatory inputs on the damaged side. Conversely intermuscular force feedback rearrangement from the undamaged side could have

emerged to offset losses on the damaged side. Previous studies (Bonasera and Nichols 1994) suggested that inhibition increases from dynamic to static time point in decerebrate animals. We have observed the same trend in our study. Therefore, even after SCI the heterogenic inhibition stayed time dependent. We have also observed increase in force response of recipient muscle as a result of increase in background force of donor muscle.

It is an interesting fact that there is a variable pattern of inhibition between GA and FHL across animals in non-locomoting decerebrate cats however, in locomoting premamillary cats GA always strongly inhibits FHL (Ross and Nichols 2009). Therefore, there is a well defined pattern of inhibition in locomotion and SCI. Physiologically, muscles can also be classified into proximal and distal categories on the basis of their relative anatomical origin and insertion (Delay et al. 2007). Grossly, muscles acting at more proximal joints (hip and knee) in hindlimb are referred to as proximal muscles while those acting at comparatively distal joints (ankle, tarsometatarso-phalangeal joints) are classified as distal muscles. The same principle can be applied to the muscles acting at the same joint, for example; GA is a proximal muscle in comparison to FHL at ankle joint.

The animals in our study were able to walk a week following SCI without any training or other medical intervention. They however, exhibited poor lateral stability and balance control when exposed to any perturbation. Inhibition converging on the distal musculature (Delay et al. 2007) may be useful in some motor tasks like stabilizing from a fall but overall this could disrupt posture by inhibiting large force producing muscles in the hindlimb. Following LSH we observed only distal to proximal pattern of inhibition

between proximal and distal ankle muscles. We propose that the poor balance control in our cats following LSH could be attributed to the loss of proximal to distal pattern/directionality of inhibition proposed by Delay et al. However, we did not study proximal joint muscles therefore further experiments are required to support the idea of gradient of inhibition between hind limb musculature. We were not able to observe this altered pattern of force feedback between GA and FHL in cats following dorsal LSH. However, it was reported in only one experiment therefore requires further studies to prove the difference in the two types of SCI.

Clasp knife inhibition is the most common clinical sign observed in patients following SCI. We did not observe any clasp knife inhibition in our study in animals with LSH (Figure 3.21). However, clasp knife inhibition has already been reported in complete transaction of spinal cord in cat (Nichols and Cope 2001) and in cats with DSH (Cleland and Rymer 1990). We therefore, propose that the dorsal column damage might be responsible for clasp knife inhibition. In our study the dorsal column was intact on one side of the spinal cord therefore the cats with LSH did not exhibited clasp knife inhibition. Clinically we observe it more often due to the fact that most of the SCI in humans is a contusion injury that can compress or affect multiple tracts in spinal cord. Our results suggest that clasp knife inhibition can be present in some SCI cases depending upon the parts of spinal cord affected by the injury. This is clinically a very important observation that can help clinicians to identify the parts of the spinal cord affected by injury or accident. Thus they can plan treatment and rehabilitation accordingly.

CHAPTER 4

ALTERED PATTERNS OF INTERMUSCULAR FORCE FEEDBACK BETWEEN HINDLIMB EXTENSORS FOLLOWING CHRONIC SPINAL CORD INJURY IN THE CAT

II. SOLEUS, PLANTARIS AND FLEXOR HELLUCIS LONGUS

4.1 Introduction

Antigravity muscles, usually the extensors, provide support by generating the force against the ground that keeps the limb extended and the center of mass at the appropriate height. A cat stands with its limbs in a semi-flexed posture and extensor muscles are tonically activated to prevent the joints from collapsing into flexion. However, bipeds and quadrupeds are inherently unstable and their bodies sway during quiet stance and require complex patterns of muscle activation produce direction-specific forces to control the body's center of mass. We propose that there is a widespread reorganization of intermuscular force feedback following SCI between ankle extensors that ultimately affect animal ability to maintain posture and wait support.

The purpose of the results from experiments reported here in this chapter was to obtain further insights into the intermuscular force feedback mechanisms among the ankle extensors in the chronic LSH cat. To meet this objective, we extended our study to Soleus (SOL) and Plantaris (PLT) muscles that allowed us to develop a model of intermuscular force feedback in cats with SCI. We asked whether the reorganization of force feedback following SCI is limited only to FHL and GA or it extends to other ankle extensors too. We also wanted to know if the redistribution of inhibitory heterogenic

force feedback is limited to multiarticular muscles or it can affect uniarticular muscles like SOL too. To test our hypotheses, we analyzed data from cats with chronic SCI at different time points using PLT, SOL and FHL muscles.

Numerous investigations in our laboratory have already demonstrated that inhibitory force feedback exists between SOL and FHL as well as between PLT and FHL during walking (Ross and Nichols 2009) and quiet stance (Bonasera and Nichols 1994). Our most recent data has proved that this inhibitory force feedback has no specific directionality in decerebrate cats (chapter 2) particularly between GA and FHL. It varies from one animal to the other and therefore we propose that it could be state dependent (chapter 2). An important issue, therefore is to establish the contribution of each of these muscles in intermuscular and interjoint co-ordination following SCI.

We observed a consistent pattern and amplification of intermuscular force feedback between PLT, SOL and FHL following SCI in cats with chronic LSH (2week to 20 week post SCI). We propose that following SCI the animal loses its ability to adjust to different perturbations in its environment and hence exhibits only one kind of intermuscular interaction between muscles. We also propose that following SCI the strong force producing muscles like SOL, GA and PLT are strongly inhibited by more distal muscles like FHL thus ankle compliance is lost.

4.2 Methods

4.2.1 Preparation

The methods used to determine the strength and sign of intermuscular force feedback in chronic LSH cats have been described previously (see chapter 3). The results depicted in this chapter are drawn from experiments on six healthy adult female cats weighing 4–4.5 kg to evaluate intermuscular reflex pathways using FHL, SOL and PLT muscles from hindlimb of cats. The studies were conducted on both legs so each muscle is represented twice per preparation (12 legs from 6 chronic LSH cats). Comparative studies were performed across legs and animals to determine the effect of SCI on these intermuscular interactions. All protocols were in complete accordance with the guidelines of both the Federal and Institutional Animal Care and Use Committee.

Chronic Spinal hemisection was performed at the T9-T10 level (Figure 3.2) using iridectomy scissors in 6 cats at university of Florida under general anesthesia and aseptic conditions described earlier (Jefferson et al. 2011) as explained earlier in chapter 3. Behavioral studies were performed on these animals both before and after chronic SCI while histological studies were done post terminal experiments (Georgia Instute of Technology) at university of Florida. Terminal experiment With decerebration at 2, 4, 8 and 20 weeks post surgery done at Georgia Institute of Technology in Nichol's lab after they resumed walking following SCI. At the end of each experiment, the animal was euthanized with an overdose of Nembutal followed by a pneumothorax. Acute LSH was performed in Nichol's laboratory at Georgia Institute of Technology.

The mechanographic technique was used to evaluate the pattern, distribution and contribution of intermuscular force feedback from muscle receptors (Nichols 1987). Each animal was surgically prepared by performing a tracheotomy following anaesthesia with isoflourine, preparing carotid arteries for ligation, and cannulating the external jugular vein for fluid replacement. Withdrawal responses were monitored, and the level of anesthetic was adjusted accordingly. Both hindlimbs were immobilized using bone pins insertion into the femur and tibia bones, and the legs were clamped to maintain the knee at 110^{o} angle (mid stance position). The animal was placed in the stereotaxic frame, supported above a table/ rigid frame while maintaining the core temperature at 37^{o}C.

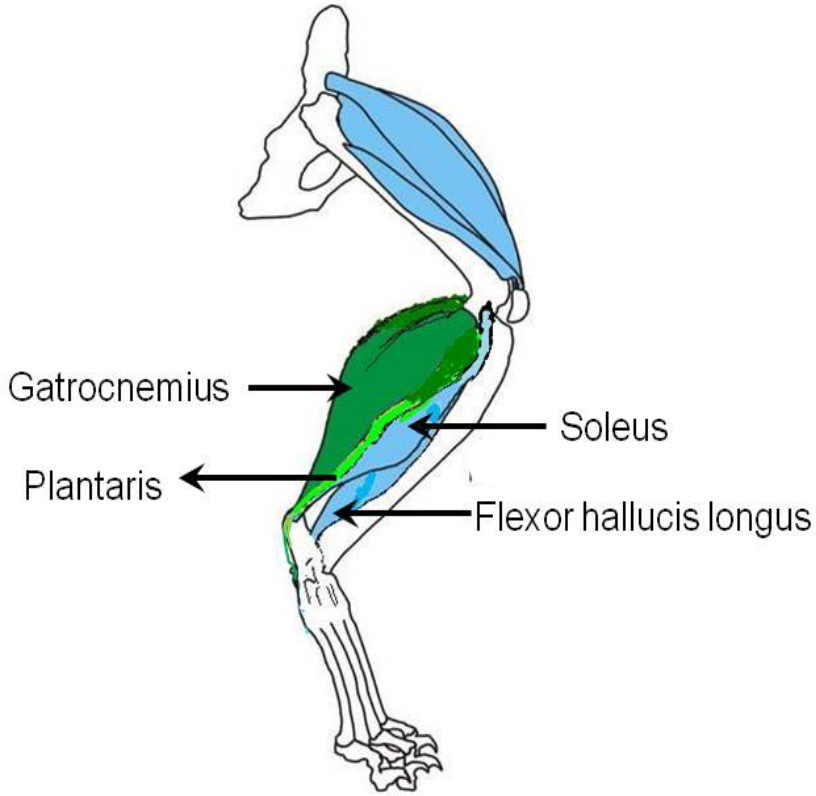

Figure 4.1 Anatomical/diagrammatic representation of ankle extensor muscles in cat hindlimb. GA (green), PLT (light green), SOL (blue) and FHL (blue).

The PLT, SOL, and FHL muscles of both right and left hind limbs were dissected after being immobilized. Both Plantaris (PLT) and Soleus (SOL) were cut near their insertion after careful separation from GA and surrounding connective tissue. As PLT tendon passes through Achilles tendon, special care was taken to separate it and was cut near its connection with flexor digitorum brevis in sole of foot where it broadens opposite the distal end of calcaneous. The soleus tendon was secured with a small piece of calcanium. FHL muscle was carefully separated from surrounding connective tissue and followed behind the medial malleolus until its tendon was cut near its insertion into Flexor digitorum longus tendon. All three muscles were attached via their respective tendon to myographs and linear motors.

An intercollicular decerebration was performed in each cat, removing all brain matter rostral to the transaction as explained earlier (chapter 2, 3). Anesthesia withdrawn slowly and data collection is started after appropriate withdrawal responses and muscle tone assessment. Once baseline data without any nerve stimulation were obtained, XER was elicited with electrical stimulation of the contralateral (muscles of one limb and nerve stimulation of the other limb) posterior tibial nerve at 2 times threshold to collect further data.

4.2.2 Data Acquisition and Analysis

The Parker 406LXR linear motors used in this study that were mounted on a custom built aluminum frame and could be adjusted in the horizontal, vertical, and diagonal directions so that the motors could be properly aligned with the appropriate muscle. Data was acquired digitally through the dSPACE board at a sampling rate of

1000 Hz described in detail earlier (Bonasera and Nichols 1994, Wilmink and Nichols 2003, Nichols 1987). As described earlier (chapter 2 and 3) the typical paradigm was a 2 mm stretch at a velocity of 0.04 m/s, 100 ms hold period, and 2 mm release. Intermuscular effects were recorded across background forces by stretching a muscle denoted the "recipient" in state one and two as described in chapter 2 and 3 both with/without crossed extensor reflex (i.e. 40-60 stretch repetitions).

Software in Matlab version 7.01 was used to analyze the data. Briefly, the background force of the muscle was calculated as an average of the force 10 ms prior to the beginning of the stretch, during the isometric hold period. A baseline was constructed by performing a linear interpolation from the mean force response just prior to the stretch to the mean force after the end of the release. The entire baseline was then subtracted from the overall force response. To evaluate the strength and sign of feedback individual force responses at three specific time points described in chapter 2 and 3 (mechanical, dynamic, static) were obtained from the baseline subtracted force data, and background force was obtained from the original force trace. The polynomial fits (95% confidence interval) for force responses obtained at each time points were plotted as a function of recipient background force.

Additionally, differences for the recipient muscle force response were calculated by subtracting the force responses at each background force and polynomial fits were calculated using matlab. Statistics were performed using Statistica 6.0 and Excel to test the separation of the data populations at each time point across limbs and cats. The 95%

confidence intervals represent the validity of the polynomial fit to the data points; a P value < 0.01 from the statistical test statistically proves that the two populations of data are distinctly different.

Additionally, differences for both the dynamic and static phases force response in the recipient muscle were calculated as the difference between state 2 and state 1 force responses and curve fits generated to determine the amount of inhibition at different time points during ramp and hold period of each individual trial. Percent difference was also calculated on the basis of this calculation between state 2 and state 1 force response of recipient muscle for each time point**.** Each pair wise combination has been normalized to the isolated muscle stretch response (recipient) so that the relative strength can be expressed as a percentage change from autogenic to autogenic plus heterogenic response. Comparisons were made to determine the influence of SCI on the strength and distribution of intermuscular proprioceptive feedback. Mean change in force response of recipient muscle, standard deviation, range (maximum and minimum change in force response of recipient muscle) and percent change between state 1 and state 2 was calculated. If P value $\leq$ 0.01 it is considered significant and documented as box plots for each time point for every individual trial as demonstrated in figure 4.7.

To understand the mechanisms underlying force dependent inhibition between FHL and other antigravity muscles in our study latency of recipient force response was calculated for each muscle combination. According to previous studies the reflex latency of the force dependent inhibition between FHL, GA, SOL and PLT occurred at 28 ± 4 ms (Bonasera and Nichols 1994). This analysis helped us determine if the clasp knife

inhibition appeared after SCI in our data. The reflex latency in clasp knife inhibition is ≥ 80 ms (Nichols and cope 2001). We did not observe any clasp knife inhibition between GA and FHL described earlier in chapter 3 in animals following LSH.

4.3 Results

The purpose of studying force feedback interactions between SOL, PLT and FHL was to further determine the distribution of the feedback interactions among ankle extensor muscles in the hindlimb of the cat with chronic LSH. Force feedback pathways between these muscles are inhibitory under conditions of quiet stance (Bonasera and Nichols 1994; Nichols 1999; Wilmink and Nichols 2003) that has already been studied extensively in our laboratory. Our main goal was to determine how SCI effects these interactions in these animals with poor balance control. We also wanted to confirm that the reorganization of intermuscular interactions in LSH is not limited to GA and FHL as described in detail in chapter 3.

We hypothesize that if the reorganization of intermuscular interactions is widespread among ankle extensors as a result of SCI that could be one of the contributing factors for a poor support capability in SCI. This chapter details results from six cats with chronic LSH at different time points (2 to 20 weeks post SCI). The results were compared with control static animal data (chapter 2) and locomoting animal data (Ross and Nichols 2009) to develop a model of force feedback in cats with partial SCI (LSH).

Uniformity of lesion magnitudes across cats was confirmed by Dr. Dena Howland laboratory. She used Cresyl violet and myelin stained sections through the lesion epicenters of each animal to determine the extent of tissue sparing and damage. Typically, complete disruption of the ipsilateral gray and white matter was seen in all six animals with chronic LSH. Contralateral gray and white matter was completely spared with the exception of some dorsal contusion in one out of six cats (one of the 4 weeks post SCI cats). Thus, lesion variability was minimal across animals.

The results presented in this chapter are divided in seven main sections. The first Section (4.3.1) addresses in detail the inhibitory force feedback between SOL and FHL following chronic LSH. The second section (4.3.2) depicts data analysis in a chronic LSH cat explaining detailed analysis of inhibitory force feedback between FHL and SOL limbs in each cat. Section 3 (4.3.3) explains comparison of heterogenic inhibitory force feedback across cats used in this study with chronic LSH. Section four (4.3.4) addresses the inhibitory force feedback between PLT and FHL following chronic LSH. Section five (4.3.5) explains intermuscular force feedback between ankle extensors PLT and FHL across limbs. Section six (4.3.6) describes force feedback interaction patterns between FHL and PLT across cats. Section seven (4.3.7) explains clasp knife inhibition and the evidence of its presence or absence following LSH in our study among FHL, PLT and SOL.

4.3.1 FHL strongly inhibits SOL, while SOL very weakly inhibits FHL following chronic SCI

The strength of the increase in inhibition of SOL by FHL during SCI was examined in three out of total six experiments. All of the animals used in these experiments exhibited stepping behavior within a week following SCI and poor balance control/weight support irrespective of the time post SCI. We did not collect data from SOL muscle in the initial two experiments of the project while the third one was rejected due to broken/damaged soleus tendon and poor XER activation. Of the three remaining experiments evaluating the force responses in SOL and FHL during XER, 3/3 (100%) demonstrated strong inhibition in 6/6 legs (100%) from FHL onto SOL (distal to proximal pattern/directionality of inhibition).

Figure 4.2 and Figure 4.3 each shows raw data from a single trial. Figure 4.2 depicts a representative example of the strong inhibition of SOL by FHL in a chronically injured cat with LSH. Figure 4.3 is a representative example of weak inhibition of FHL by SOL in the same animal with chronic LSH. Figures 4.2a and 4.3a depict force output while 4.2b and 4.3b depict length input of SOL respectively. Figures 4.2c and 4.3c depict the force output of FHL. Figure 4.2d and Figure 4.3d represent length input of the distal muscle FHL respectively. Additionally, Figure 4.2a, 4.3a, 4.2c and 4.3c contain blue broken lines on force responses indicating state 2 when the recipient muscle was stretched along with the donor muscle in each case. Both figure 4.2 and 4.3 represent raw data obtained in a single trial consisted of 45 to 60 muscle stretches. Bidirectional force feedback between FHL and SOL is observed in decerebrate cats during XER ((Bonasera and Nichols 1994). Figure 4.2a also demonstrates strong isometric inhibition of SOL by

FHL even when it is acting as a donor and not being stretched (isometric response of donor) in state 1.

Figure 4.4 further elaborate the comparative amount and direction of inhibition between SOL and FHL. Each stretch is broken down into three time points here namely; mechanical, dynamic and static time point. Each black circle represents individual stretch of recipient muscle in state one at mechanical (a, d), dynamic (b, e) and (c, f) static time point. Each colored circle (red for SOL and blue for FHL) represents an individual stretch in state 2 at the three time points. The difference in heights of the black and colored circles depicts change in force response of recipient muscle from state 1 to state 2.

To evaluate the strength and sign of feedback during a trial with XER, individual force responses at specific time points were obtained from the baseline subtracted force data and background force was obtained from the original force trace from raw data (Figure 4.2, Figure 4.3). Figure 4.5 and Figure 4.6 depicts the typical analysis, whereby force responses for a specific time point in this case (a) mechanical (b) dynamic and (c) static time point are plotted as a function of background force for each recipient muscle. Each data point/circle in figure 4.5 and 4.6 represents a response of the recipient muscle obtained when the muscle was either stretched alone in state 1 (black circles) or response of the recipient muscle when it was stretched with another muscle in state 2 (blue circles for FHL and red circles for SOL). Polynomial fits and 95% confidence intervals were fit to each population of data at each time point for each muscle as shown in figure 4.5 (a, b, c) and 4.6 (a, b, c). The wide separation of two populations of data (state 1 and 2) in figure 4.5 clearly demonstrates very strong inhibition of SOL by FHL. Figure 4.6 on the

other hand shows a very narrow separation of the two populations of data suggesting a weak inhibition of FHL by SOL.

Figure 4.7 represents the amount of inhibition calculated in (a) Newton (N) and (b) % inhibition at static time point (4.5c and 4.6c) for SOL and FHL force response respectively. Each circle represent inhibition calculated for the given time point by subtracting actual stretches in state two from state 1 (shown in Figure 4.5c, Figure 4.6c). Polynomial fits were applied to each population of data at static time point for each muscle as shown in figure 4.7a and 4.7b. The inhibition between SOL and FHL was highly force dependent and increased from dynamic time point to static time point across limbs and cats. Therefore even after SCI muscle response properties were preserved and there were increases in force responses of each recipient muscle from dynamic to static time point.

Figure 4.8a and 4.8b shows statistical analysis of the (same two trials) trials from SOL and FHL respectively in the same animal. The P value for SOL inhibition by FHL is << 0.01 in Figure 4.8a that is highly statistically significant in contrast to P value of > 0.01 for FHL inhibition by SOL in Figure 4.8b. Also, % inhibition, mean change, range and SD are all higher for SOL in comparison to FHL. The same calculations were performed for mechanical and dynamic time point too not shown here. We observed increases in inhibition from dynamic to static time point in each case. SOL is a major antigravity muscle in hindlimb hence its strong inhibition by FHL is an evidence of rearrangement of intermuscular force feedback after SCI that made the animal incapable to response to change in state or any perturbation and probably poor stability too.

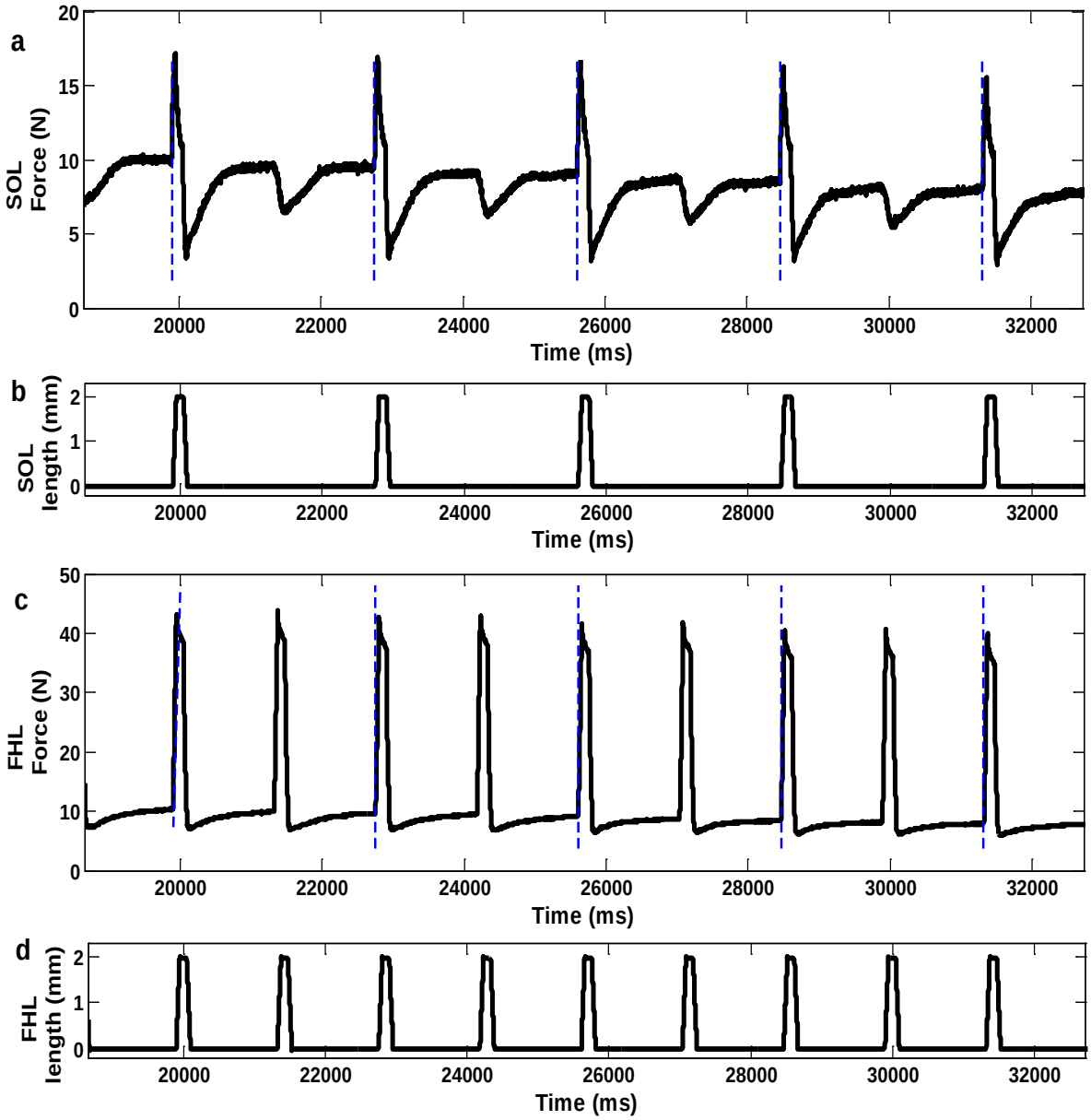

Figure 4.2 Representative trial depicting force feedback interactions between SOL and FHL in a cat following chronic LSH. (a) Donor muscle (SOL) stretch-evoked force response during XER. (b) Donor muscle (SOL) length input to two-state stretch (c) Recipient muscle (FHL) stretch-evoked force response during XER. Dashed blue lines on stretches indicate state 2. (d) Recipient muscle length input for two-state stretch. There is clearly little inhibition from SOL onto FHL in state 2 (c). XER is done by stimulating tibial nerve in the hindlimb on the side without LSH at 2T evokes an increase in the background force of the recipient and donor muscles on the right hindlimb (injured side in this example), SOL and FHL respectively (a, c). The same conventions as Figure 3.7 apply.

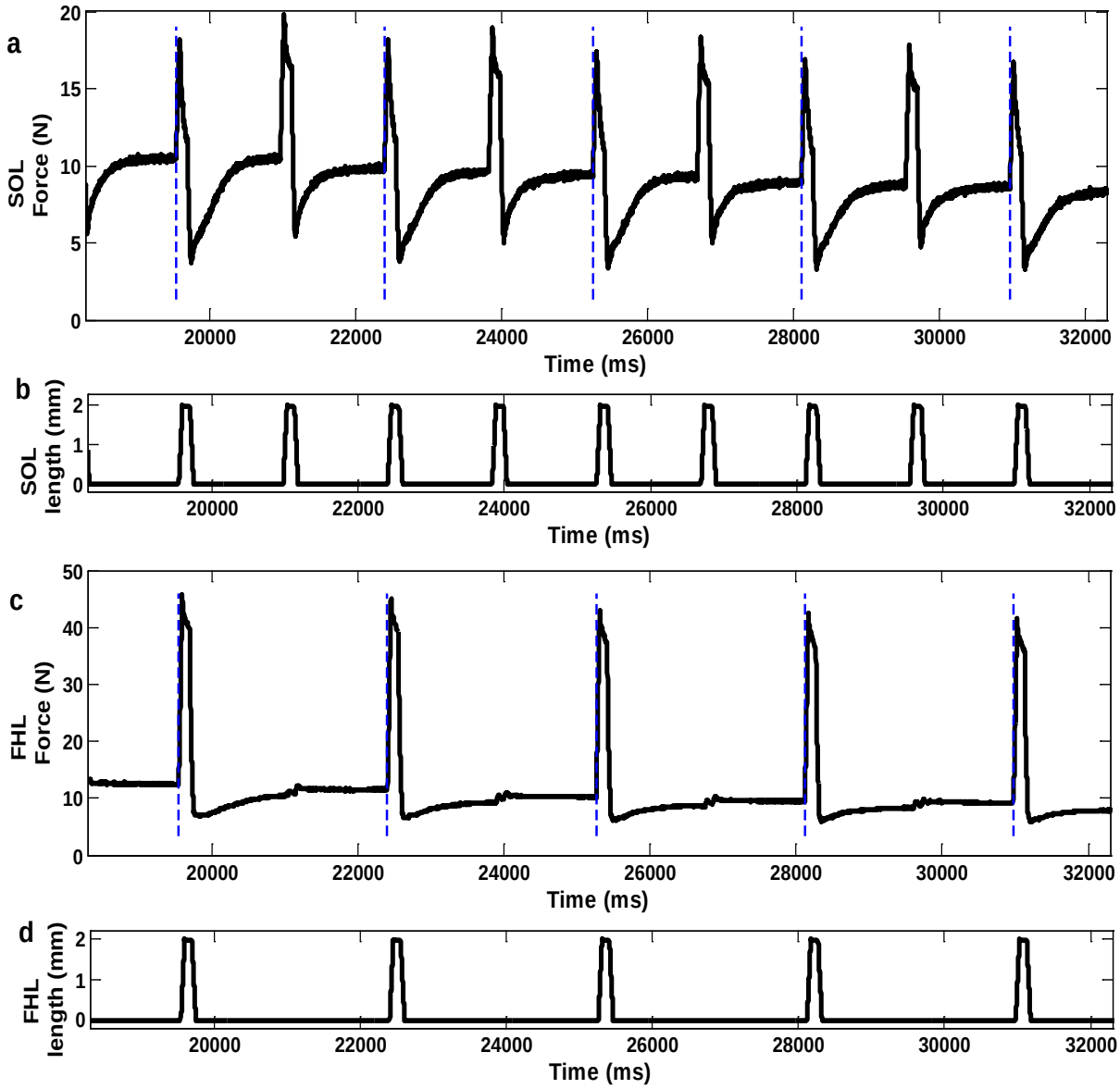

Figure 4.3 (a) Recipient muscle SOL (b) donor muscle FHL stretch-evoked force response during XER in a cat 4 weeks following chronic LSH. Dashed blue lines on stretches indicate state 2. (b) Recipient muscle (SOL) length input to two-state stretch (d) Donor muscle length input for two-state stretch. There is significant inhibition from FHL onto SOL in state 2. XER is done by stimulating tibial nerve in the hindlimb on the side without LSH in this example at 2T that causes an increase in the background force of the recipient and donor muscles on the hindlimb of injured side, SOL and FHL respectively (a, c). The same conventions as Figure 3.5 apply.

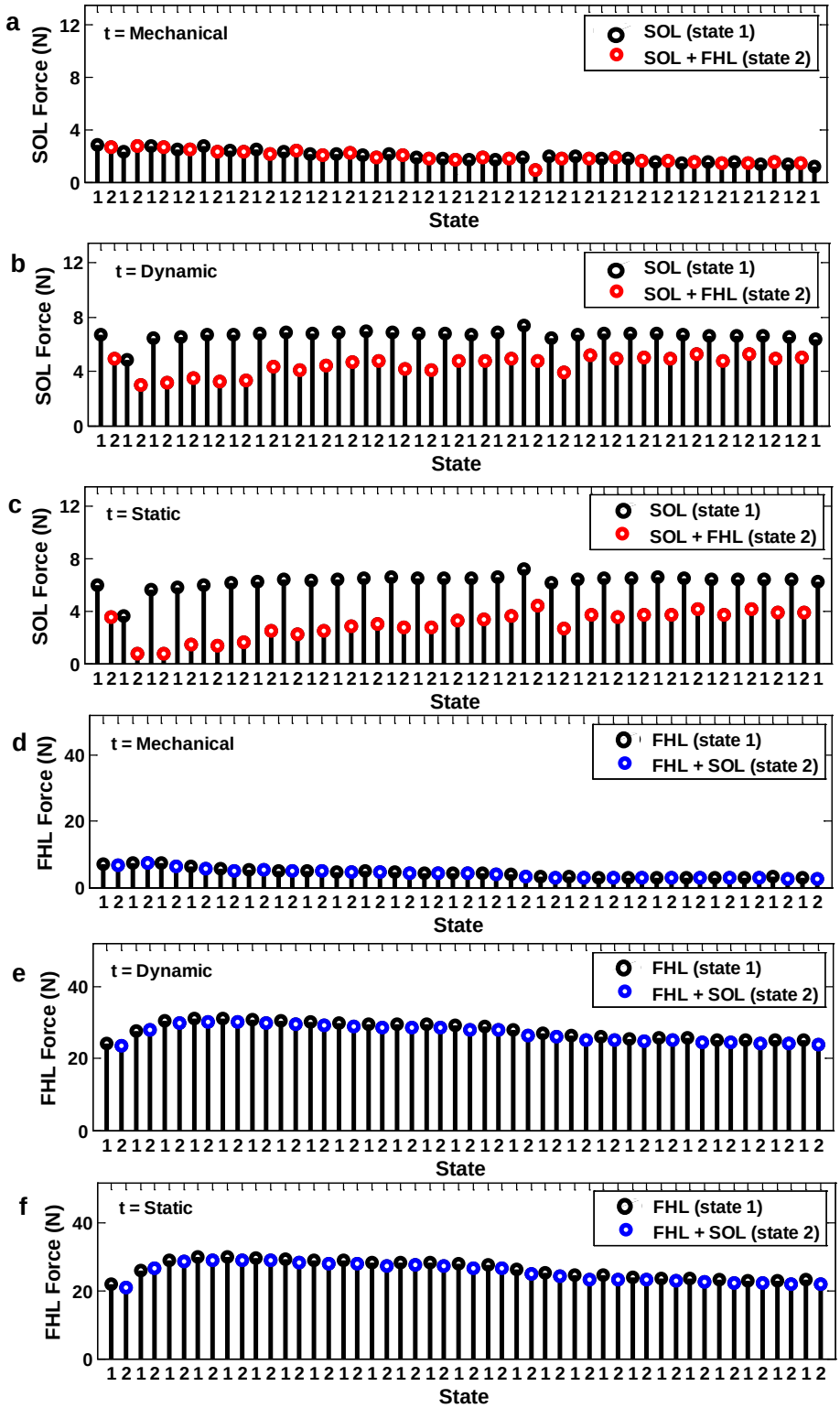

Figure 4.4 (a, b, c) Inhibition of SOL by FHL (d, e, f) Inhibition of FHL by SOL at mechanical, dynamic and static time point respectively. Each circle represents individual stretch response of recipient muscle in state 1 (black) and state 2 (red for SOL and blue for FHL). The difference of heights of the colored circles and black circles depict relative inhibition in state 2 and 1.

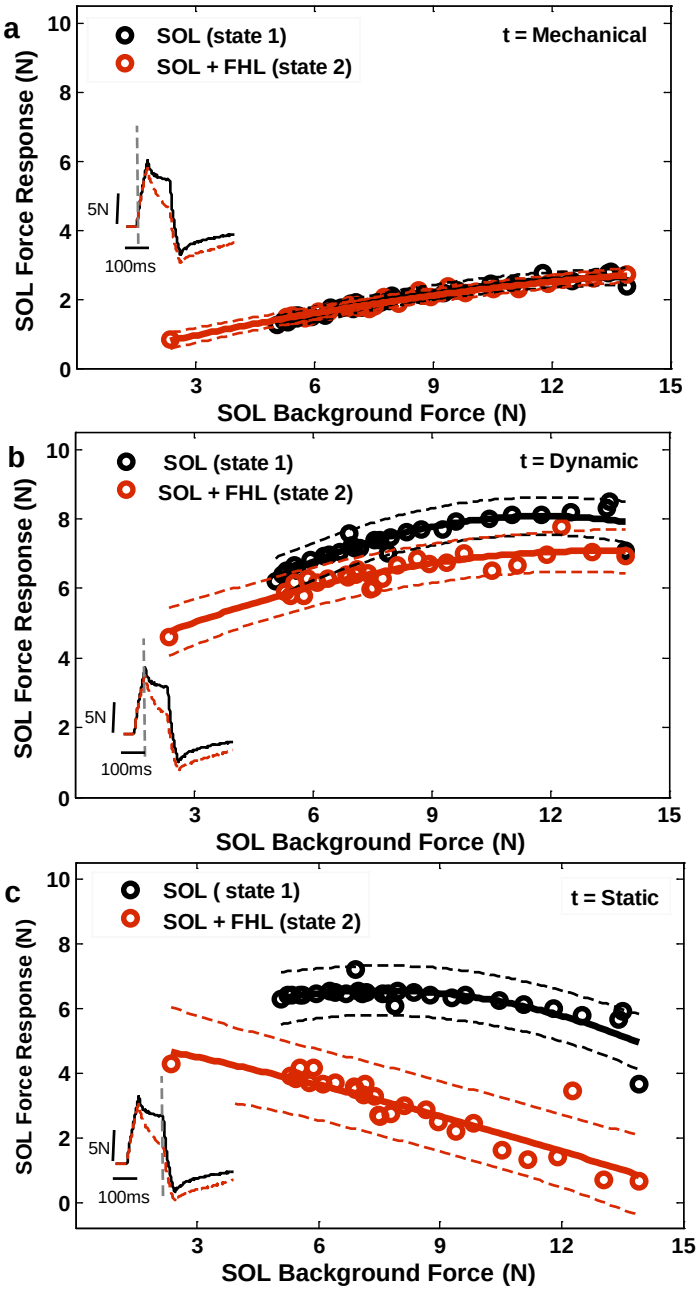

Figure 4.5 Inhibition from FHL (donor) onto SOL (recipient) during XER in a cat 4 weeks following chronic LSH at the (a) mechanical (b) dynamic (c) static time point. Force responses are shown in circles (black state 1 and red state 2). Polynomial and 95% confidence intervals are fit to each population of data. Inhibition of SOL by FHL increases from dynamic to static time point. The maximum inhibition is shown by clear separation of confidence intervals at P≤0.001 at static time point. The inserts in (a), (b) and (c) shows two traces matched at mean background force of the recipient muscle in state 1 (black line) and state 2 (red line) superimposed to illustrate the magnitude of inhibition from FHL onto SOL during XER, and the vertical line indicates the sample time.

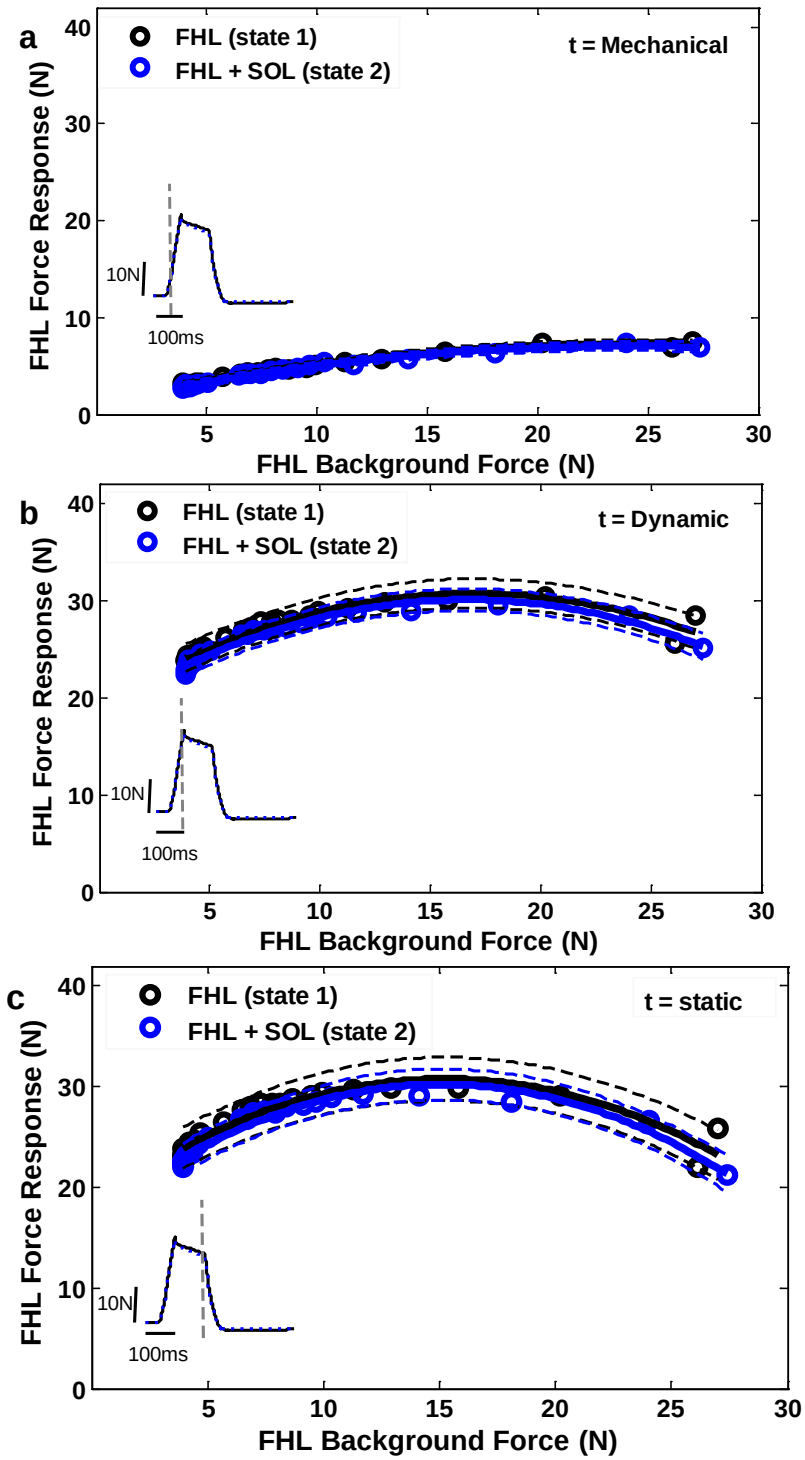

Figure 4.6 Inhibition from SOL (donor) onto FHL (recipient) during XER in a cat 4 weeks following chronic LSH for (a) mechanical (b) dynamic (c) static time point. Force responses are shown in circles (black state 1 and blue state 2). The same conventions as Figure 4.5 apply. The overlapping of confidence intervals depict weak inhibition of FHL by SOL at P>0.01.

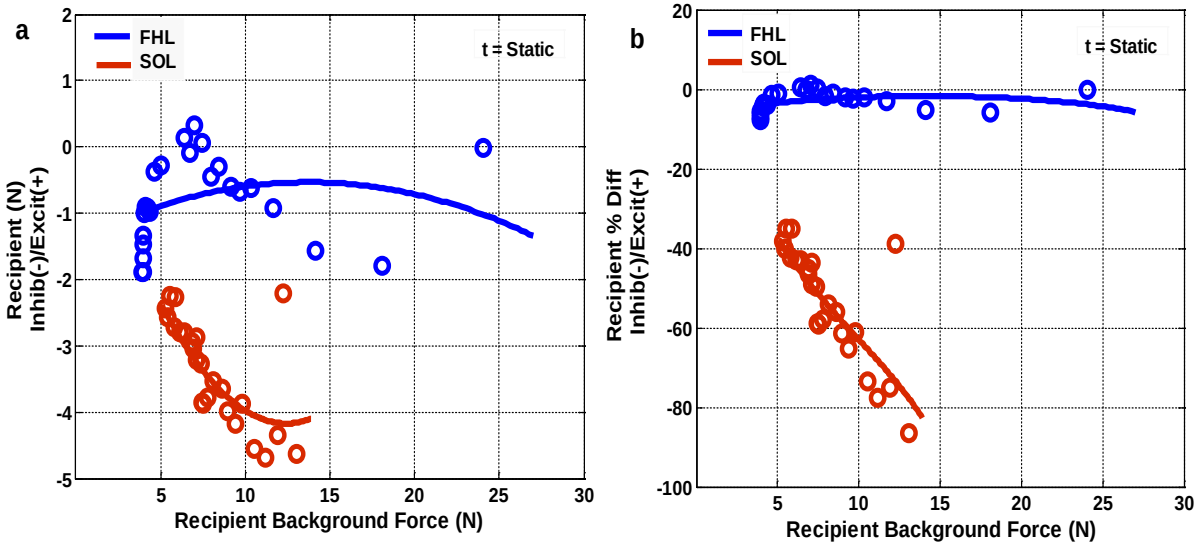

Figure 4.7 (a) Shows comparative amount of inhibition of SOL (red) and FHL (blue) in Newton at static time point. Each circle represents the difference of state 1 and state 2 force responses/stretches of each muscle at matched background force and time. (b) Amount of inhibition is converted to percent change for both SOL (red) and FHL (blue). There is strong inhibition of SOL and week inhibition of FHL. Polynomials are fit to each population of data.

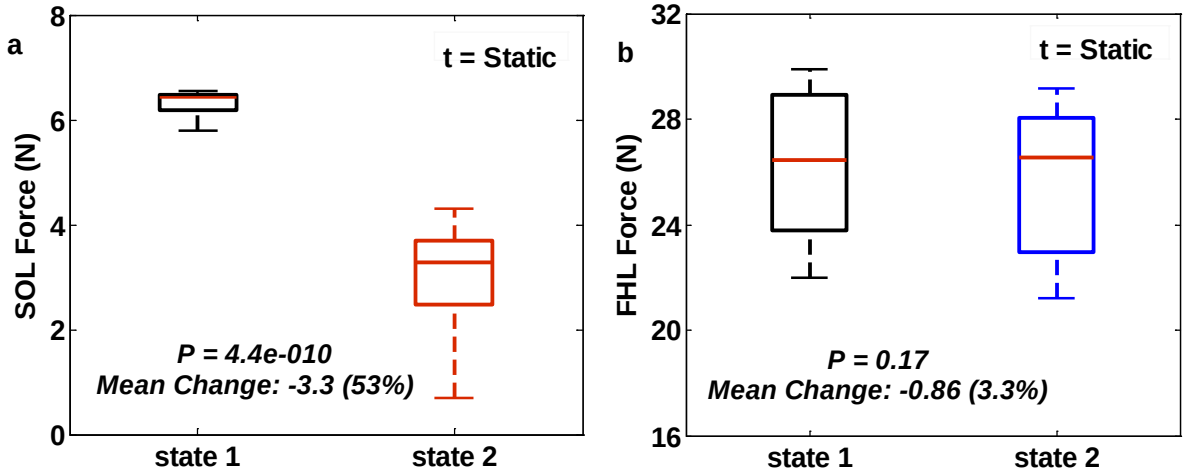

Figure 4.8 Box plots representing statistical analysis of the representative trials at static time point for (a) SOL (b) FHL in a cat following chronic LSH. State one is shown in black and state 2 in red (SOL), Blue (FHL). The median is shown in red color across stretches in a trial at a given time point. The P value, mean change and percent change are calculated for to demonstrate the amount of inhibition across state and time point. The comparison clearly shows stronger inhibition of SOL by FHL in chronic LSH.

4.3.2 Inhibitory feedback between SOL and FHL reorganizes across limbs in cats following chronic LSH

Previous studies have mapped the organization of feedback in the intercollicular decerebrate cat under conditions of XER (Bonasera and Nichols 1994; Nichols 1999). In our experiments there was partial lesion involving one half of spinal cord therefore; one might expect to see different force feedback in two limbs of the cat. However, as described in chapter 3 the same kind of inhibitory pattern was observed across limbs in each cat for force feedback interactions between GA and FHL. We therefore, compared the data for two lhind limbs in each animal to determine the force feedback across limbs for interaction between SOL and FHL. We hypothesize that if the same pattern of intermuscular force feedback inhibition exists across limb between SOL and FHL like GA and FHL it will prove that the reorganization of force feedback is similar in two limbs for all hindlimb ankle extensors and is not affected by the muscle type (slow/fast twitch or multiarticular/single joint muscle).

Figure 4.9 depicts the comparative summary of force feedback between SOL and FHL across the two limbs of an animal with chronic LSH. The pattern of inhibition was similar in both legs (distal to proximal). The amount of inhibition was calculated as % inhibition for both SOL and FHL response respectively as described earlier for Figure 4.7. Each circle represent inhibition calculated for the given time point by subtracting actual stretches in state two from state 1 and normalizing the difference by converting it to % change in each limb for the static time point. A quadratic polynomial was fit to each population of data at the static time point for each muscle. These same calculations were performed for dynamic time point too not shown here. The results were similar for both

limbs at each time point with the exception of more inhibition at static than at the dynamic time point for each limb for SOL and FHL. The amount of inhibition was always greater on the injured side limb in comparison to the uninjured side limb. We also observed very little inhibition of FHL by SOL bilaterally.

Table 4.1 and 4.2 summarize the intermuscular interactions in two limbs of each animal used in our study. The results clearly indicated that the change occurred bilaterally irrespective of the side of hemisection and time post chronic LSH.

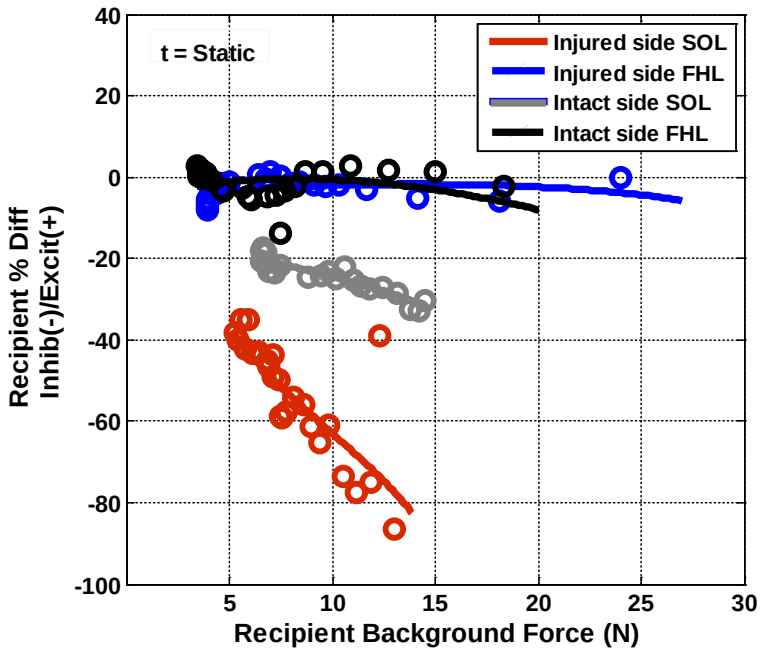

Figure 4.9 Comparison of force feedback between two limbs of the same cat with chronic partial SCI (LSH). Amount of inhibition shown in terms of percent change for both SOL and FHL. Strong inhibition of SOL (red) and week inhibition of FHL (blue) observed bilaterally. Each circle represents difference of recipient force response in state one and two at static time point at a given background force. Polynomial was fit to each population of data for static time point for each limb and muscle.

4.3.3 Patterns of inhibition between SOL and FHL is similar across cats irrespective of time post chronic SCI

We compared data across animals to determine the possibility of existence of a pattern of inhibition across animal characteristic of SCI. We observed the same pattern between SOL and FHL across cats in chronic LSH. We observed strong inhibition of SOL by FHL in 100% of animals. Figure 4.10 and Figure 4.11 summarize the pattern of intermuscular interactions between SOL and FHL across limbs and animals. We selected trials with comparable background forces. It is obvious from the figure that inhibition from FHL onto SOL is strong in all three animals irrespective of the time post LSH (4 weeks to 20 weeks).

The statistical results of the analyses across limbs and cats over different time points post LSH are summarized in Table 4.1 and Table 4.2. Both tables include measurements for both hindlimbs in each animal. The tables contain the range of inhibition, range of background force of recipient muscle, mean inhibition, SD and P values in each limb observed across each of the three animals. Therefore we propose that this altered heterogenic inhibition between ankle extensors appears in chronic LSH animals after injury and possibly stay there up to at least 20 week post LSH. It does not change with improvement in locomotor activity of the animal and is not limited to a single muscle instead it is widespread among ankle extensors. Figure 4.11 represent the suggested model for intermuscular inhibition between FHL and SOL following chronic LSH.

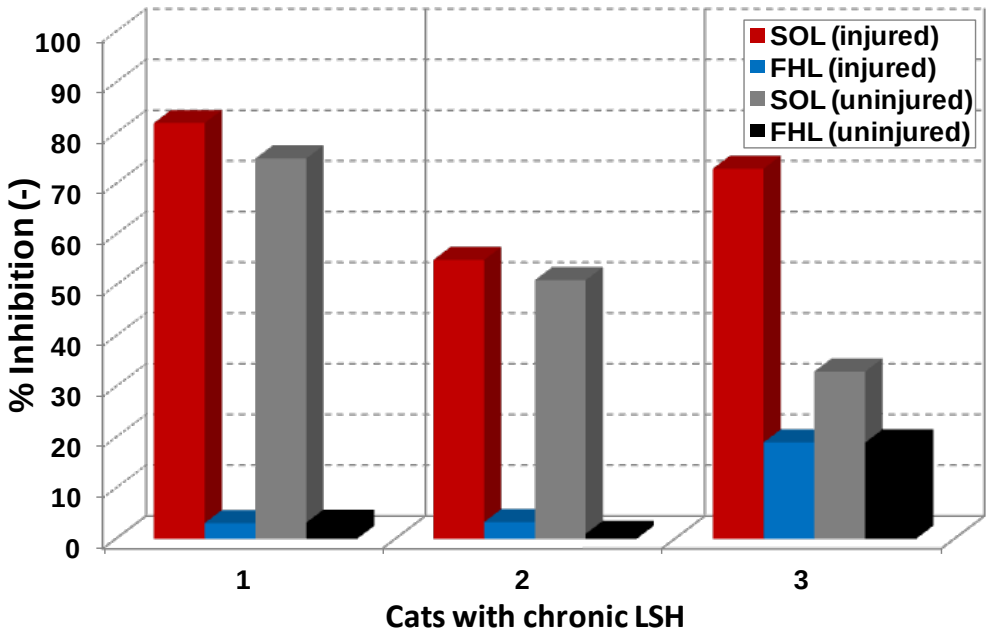

Figure 4.10 Comparative analysis of force feedback interaction between SOL and FHL across animals post chronic LSH. (1= 4weeks, 2= 4weeks, 3= 20weeks)

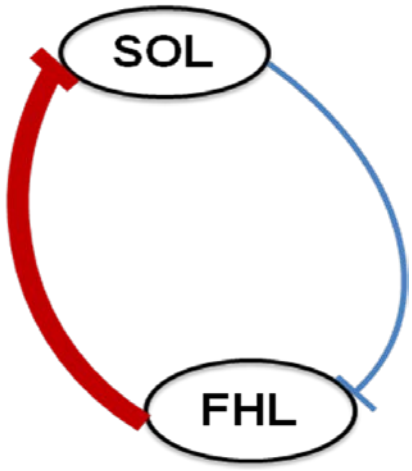

Figure 4.11 Summary diagram/Proposed model of the inhibition between ankle knee extensors FHL and SOL following chronic LSH in the intercollicular decerebrate cat. Inhibition between SOL and FHL has a greater strength in distal to proximal direction (red) in comparison to proximal to distal direction (blue). The net effect of the modulation was to produce a distal to proximal directionality/pattern of inhibition.

Table 4.1 Magnitudes of inhibition with XER between SOL (recipient) and FHL (Donor) muscles with range of maximum background force of recipient muscle in percentage change, range, SD and P values for each limb in three cats with chronic LSH at, 4, 4 and 20 weeks post LSH. Inhibition is statistically significant if P≤0.01 on both injured and uninjured side limb in each cat. The data shown includes 4 to 6 observations in each limb in every cat each trial consisted of 45-60 stretches each.

RECIPIENT (SOL)	DONOR (FHL)							
	Cats/Weeks post LSH	Recipient Muscle Max Backgrou-nd force Range	Injured side limb			Uninjured side limb		
			%Δ (-) Range	% Δ (-) Mean ± SD	P value	% Δ (-) Range	%Δ (-) Mean ± SD	P value
	Cat1 = 2W		___	___	___	___	___	___
	Cat2 = 4W		___	___	___	___	___	___
	Cat3 = 4W	9 ~ 17	57 ~ 82	72.7 ± 13.7	< 0.001	44 ~ 75	60.7 ± 15.6	< 0.001
	Cat4 = 4W	15 ~ 18	42 ~ 55	49.7 ± 6.8	< 0.001	23 ~ 51	36.7 ± 14	< 0.001
	Cat5 = 8W		___	___	___	___	___	___
	Cat6 = 20W	6 ~ 12	55 ~ 73	62.3 ± 9.5	< 0.001	28 ~ 33	35.3 ± 11	< 0.001

Table 4.2 Magnitudes of inhibition with XER between SOL (donor) and FHL (recipient) muscles. Same conventions as Table 4.1 apply. Inhibition is statistically significant if P<0.01 on both injured and uninjured side limb in each cat. The data shown includes 4 to 6 observations in each limb in every cat each trial consisted of 45-60 stretches each.

RECIPIENT (FHL)	DONOR (SOL)							
	Cats/ Weeks post LSH	Recipient Muscle Max Backgrou-nd force Range	Injured side limb			Uninjured side limb		
			%Δ (-) Range	% Δ (-) Mean ± SD	P value	% Δ (-) Range	%Δ (-) Mean ± SD	P value
	Cat1 = 2W		___	___	___	___	___	___
	Cat2 = 4W		___	___	___	___	___	___
	Cat3 = 4W	20 ~ 35	2.6 ~ 3.1	2.9 ± 0.4	≤ 0.1	0.6 ~ 3.2	2.1 ± 1.3	≤ 0.6
	Cat4 = 4W	24 ~ 30	1.8 ~ 3.3	2.4 ±	≤ 0.4	0.4 ~ 1	0.6 ±	≤ 0.6
	Cat5 = 8W		___	___	___	___	___	___
	Cat6 = 20W	16 ~ 20	11 ~ 19	15 ± 5.7	≤ 0.01	17 ~ 19	18 ± 1.4	≤ 0.01

4.3.4 FHL strongly inhibits PLT, while PLT very weakly inhibits FHL following chronic SCI

PLT and FHL both are mainly classified as ankle extensors, however due to their insertions into the Flexor digitorum brevis muscle (FDB) and Flexoe digitorum longus muscle (FDL) respectively they also exhibit toe flexion function. PLT muscle also act as abductor around ankle like GA and SOL while FHL is a strong adductor. Therefore it is important for these two muscles to have proper force feedback state dependent interactions during motor activity in order to maintain balance around ankle.

According to previous studies in our laboratory PLT muscle exchanges predominately force-dependent inhibition with the FHL during quiet stance (Bonasera and Nichols 1994) and locomotion (Ross and Nichols 2009). While stronger inhibition from FHL onto PLT was found during locomotion in some animals (4/11), little to no inhibition was found from PLT onto FHL during either locomotion or XER in the premammillary decerebrate preparation (Ross and Nichols 2009).

The strength and distribution/pattern of inhibition between PLT and FHL muscles during SCI was examined in five out of total six experiments. All of the animals used in these experiments were able to walk within a week following SCI and exhibited poor balance control/weight support irrespective of the time post SCI. Out of the five experiments evaluating the force feedback between PLT and FHL during XER, 5/5 (100%) demonstrated statistically very strong inhibition from FHL on to PLT (distal to proximal pattern/directionality of inhibition).

The raw data in Figure 4.12 and 4.13 depict a representative example of patterns of force feedback between PLT and FHL following LSH. Figure 4.12 represents strong inhibition of PLT by FHL and Figure 4.12 shows weak inhibition of FHL by PLT. Each muscle was stretched to 2mm length as shown in Figure 4.11 b, 4.11d, 4.12b and 4.12d. This pattern was seen in all five animals post chronic LSH at 2 week to 20 week post SCI. Figure 4.12a also shows strong inhibition of PLT by FHL even when PLT was not stretched (isometric). Our results showed strong inhibition of PLT by FHL in non-locomoting 5/5 (100%) animals in contrast to the inhibition of PLT by FHL in locomoting animals 4/11(36%) reported earlier (Ross and Nichols 2009) and a bidirectional inhibition trend in decerebrate animals during quiet stance (chapter 2) also reported earlier (Bonasera and Nichols 1994, Nichols 1999).

Figure 4.14 represents the same trials shown in Figure 4.12 and Figure 4.13. Here, each stretch is divided into three time points (a, d) mechanical (b, e) dynamic and (c,f) static. The difference of heights of the colored circles (state 2) and black circles (state 1) depict inhibition from state one to state two.

Figure 4.15 and Figure 4.16 represent the same data shown in Figure 4.12 and Figure 4.13. We have presented here the force response of the recipient muscle PLT and FHL at (a) mechanical (b) dynamic and (c) static time point for each muscle combination to observe the inhibition developing between the two muscles. We observed stronger inhibition of PLT by FHL for the static time point in comparison to that for the dynamic time point in 100% of animals with four to six observations per combination per animal. The strong inhibition of PLT by FHL was observed both with and without XER in all

animals with chronic LSH during quiet stance. Each data point in figure 4.15 and 4.16 represent a response of the recipient muscle obtained when the muscle was either stretched alone in state 1 (black circles) or response of the recipient muscle when it was stretched with another muscle in state 2 (blue circles for FHL and red circles for PLT). Polynomial fits and 95% confidence intervals were fit to each population of data at static time point for each muscle. The wide separation of confidence intervals for the two populations of data (state 1 and state 2) in Figure 4.15 clearly demonstrates very strong inhibition of PLT by FHL. Figure 4.16 on the other hand shows a very narrow separation of the two populations of data suggesting a weak inhibition of FHL by PLT.

Figure 4.17 documents the amount of inhibition between PLT and FHL. The calculations were made by subtracting the force response of recipient muscle in state two from its force response in state one at static time point. Same calculations were done for dynamic and mechanical time point too not shown here. The inhibition was expressed in relative terms by converting the inhibition into percent change in Figure 4.17b.

Further detailed statistical analysis shown in Figure 4.18a and 4.18b for PLT and FHL to calculate P value, mean inhibition in a trial at a given time point, standard deviation, range of inhibition across 45-60 stretches and percent change. Summarized statistical analysis demonstrates strong inhibition of PLT by FHL with p value $<< 0.01$ and percent inhibition of 65% in the representative trial. However the range of inhibition across cats as shown in table 4.3 and table 4.4 shows much higher percentage of inhibition in other trials.

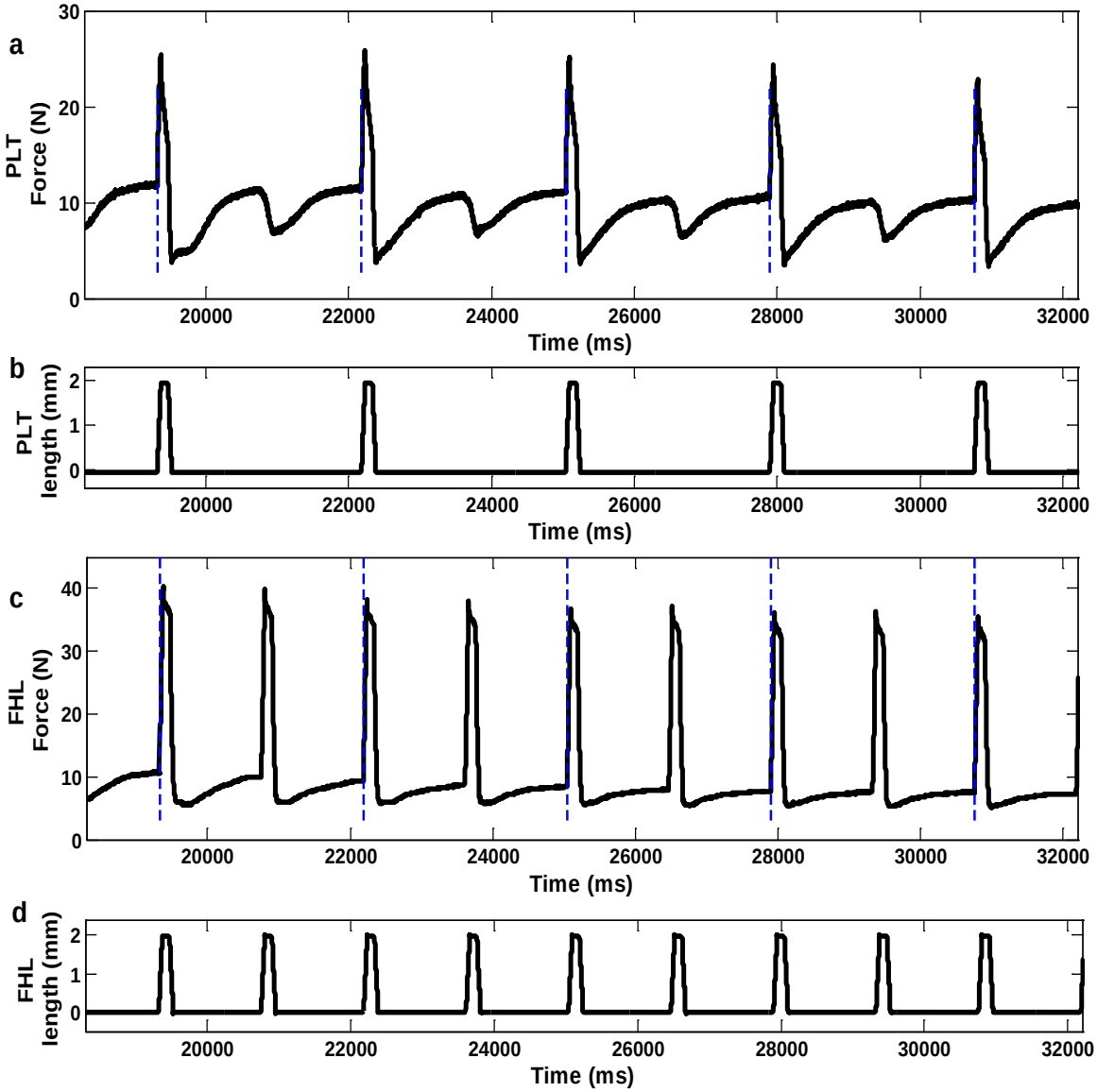

Figure 4.12 Raw data from a trial in a cat following chronic LSH using XER. (a) Donor muscle (PLT) stretch-evoked force response during XER. (b) PLT length input to two-state stretch (c) Recipient muscle (FHL) stretch-evoked force response during XER. (d) Recipient muscle length input for two-state stretch. Dashed blue lines on stretches indicate state 2. XER is done by stimulating tibial nerve in the hindlimb on the side without LSH at 2T evokes an increase in the background force of the recipient and donor muscles on the injured side hindlimb. The same conventions as Figure 3.7 apply.

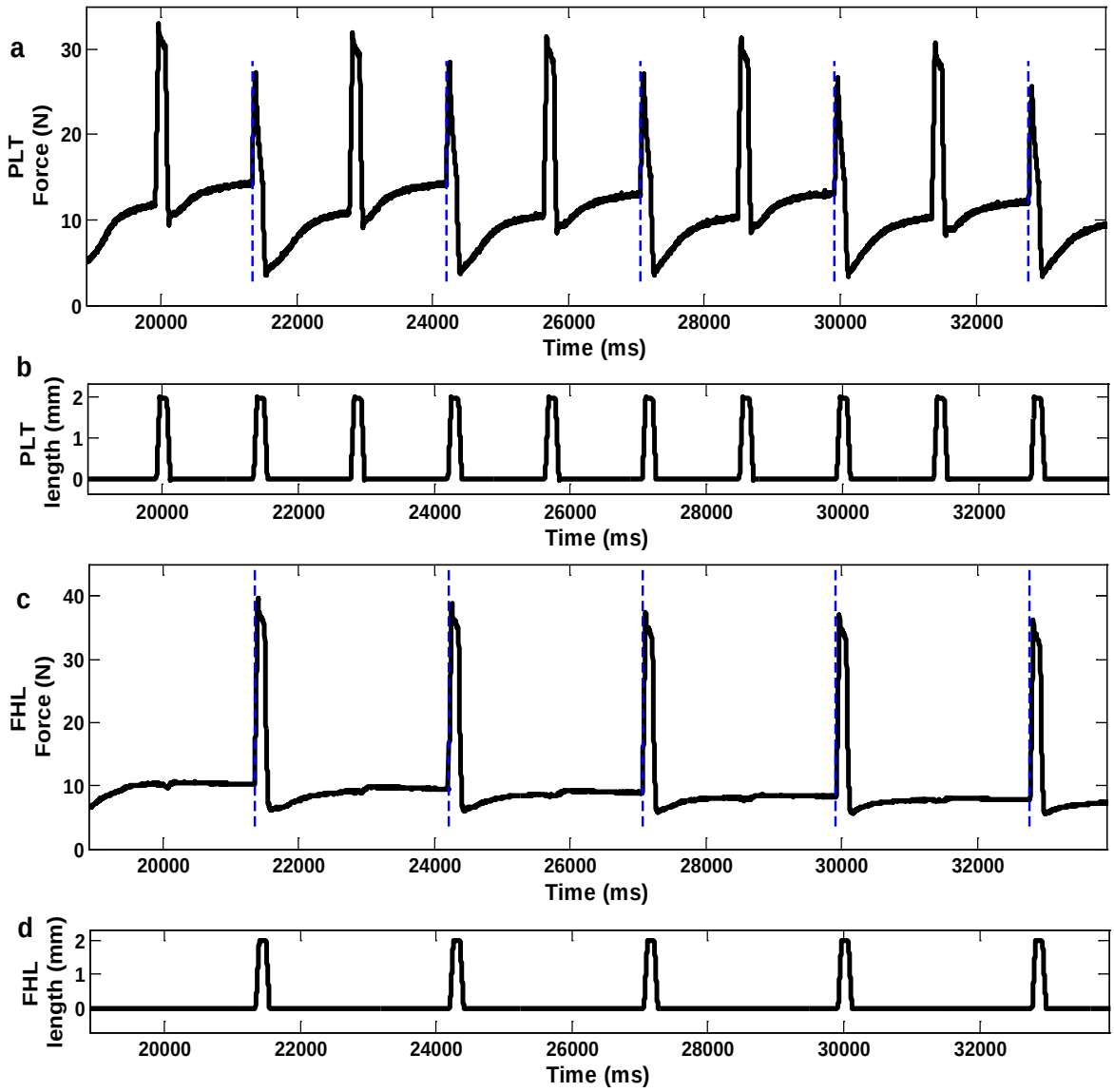

Figure 4.13 Raw data from a trial in chronic LSH using XER. (a) Recipient muscle (PLT) stretch-evoked force response during XER. (b) PLT length input to two-state stretch (c) Donor muscle (FHL) stretch-evoked force response. (d) Recipient muscle length input for two-state stretch. Dashed blue lines on stretches indicate state 2. The same conventions as Figure 3.7 apply.

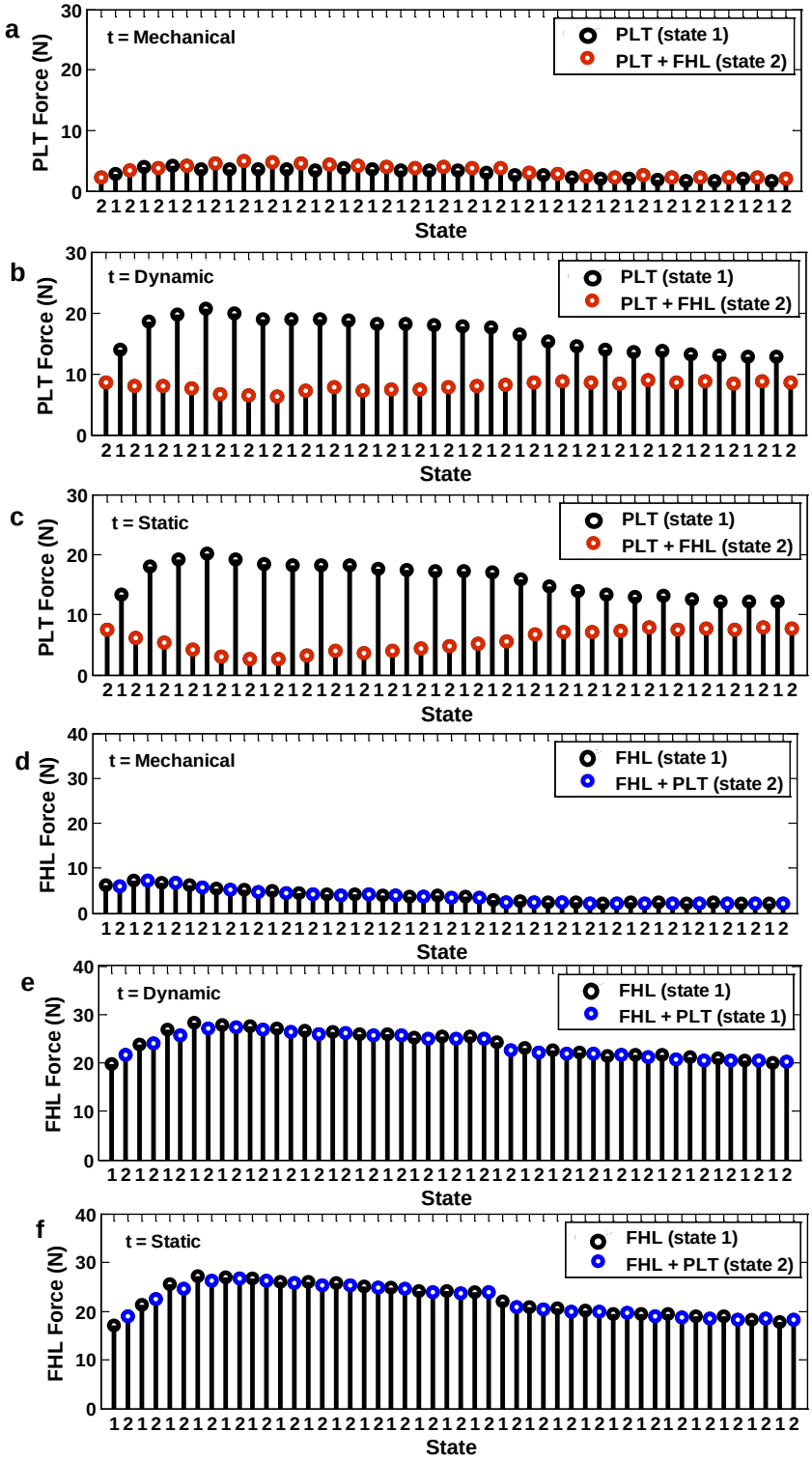

Figure 4.14 (a, b, c) Inhibition of SOL by FHL (d, e, f) Inhibition of FHL by SOL at mechanical, dynamic and static time point respectively. Each circle represents individual stretch response of recipient muscle in state 1 (black) and state 2 (red for SOL and blue for FHL). The difference of heights of the colored circles and black circles depict relative inhibition in state 2 and 1.

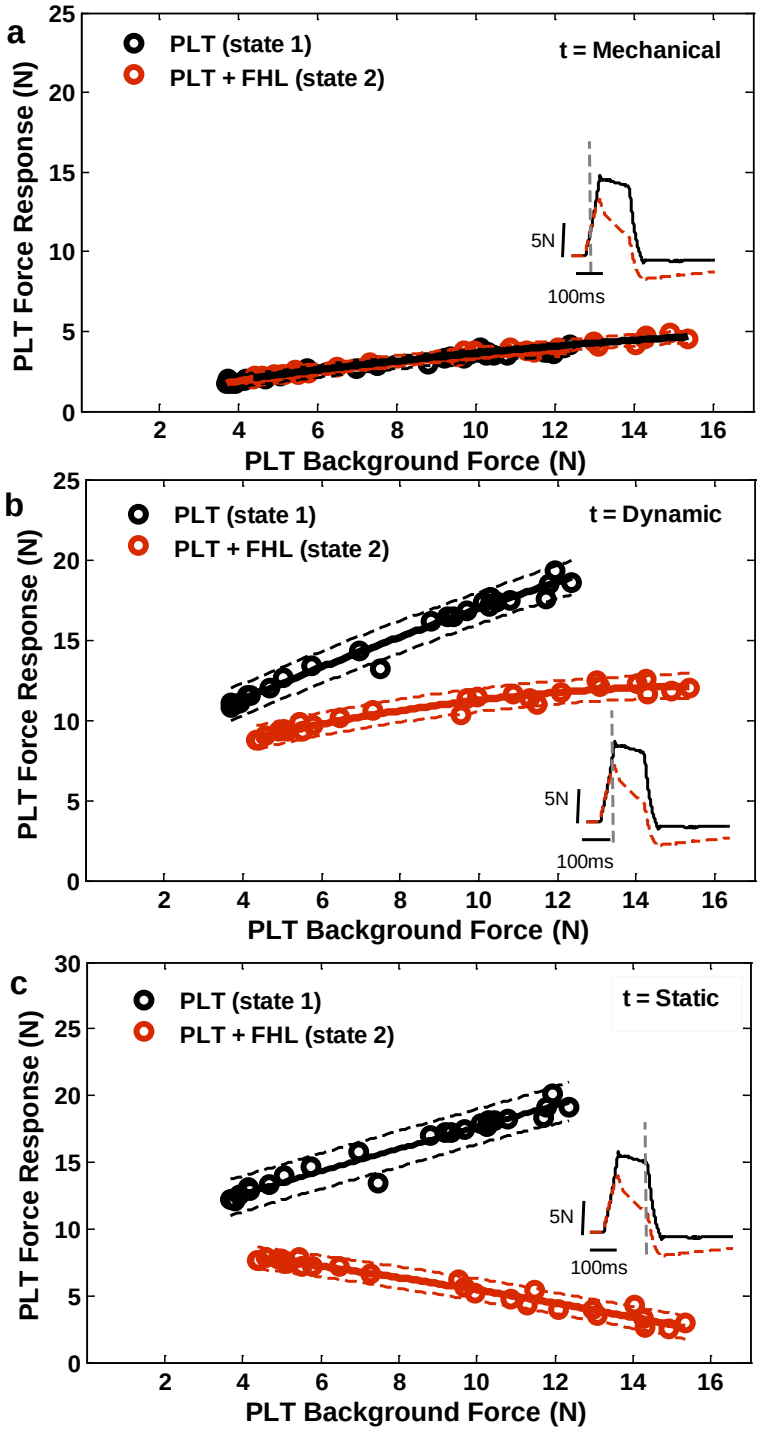

Figure 4.15 (a) Inhibition of PLT (recipient) by FHL (donor) at (a) mechanical (b) dynamic (c) static time point during XER following chronic LSH. Each circle represents individual stretch response of recipient muscle PLT (blue circles/state 2 and black circles/state 1). Same conventions as Figure 4.5 apply. The overlapping of confidence intervals here depicts very weak inhibition of FHL by PLT.

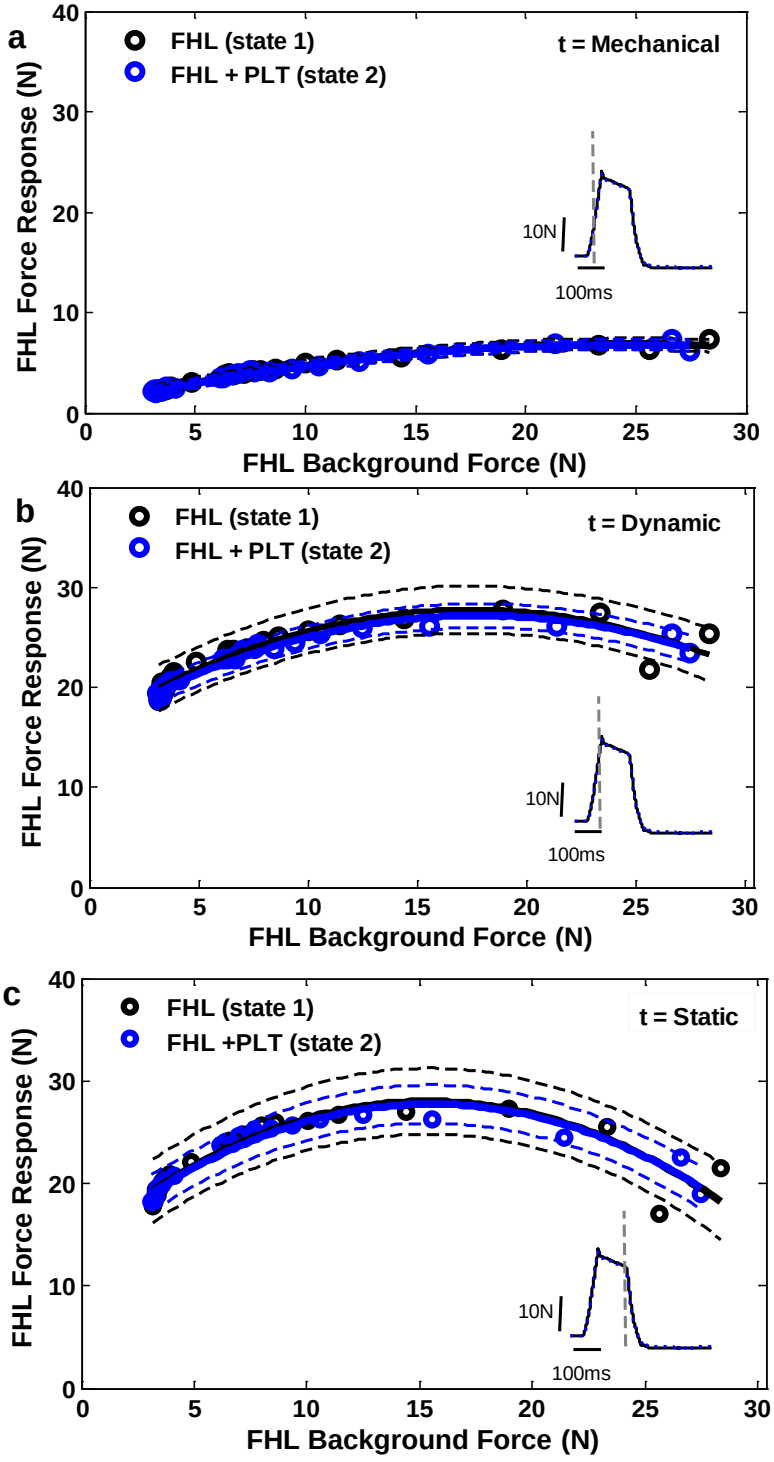

Figure 4.16 (a) Inhibition from PLT (donor) onto FHL (recipient) during XER in (a) mechanical (b) dynamic (c) static time point. Force responses are shown in black circles for state 1 and blue circles for state 2 for recipient muscle (FHL). The same conventions as Figure 4.15 apply. The overlap of confidence intervals depicts weak inhibition of FHL by PLT following chronic LSH.

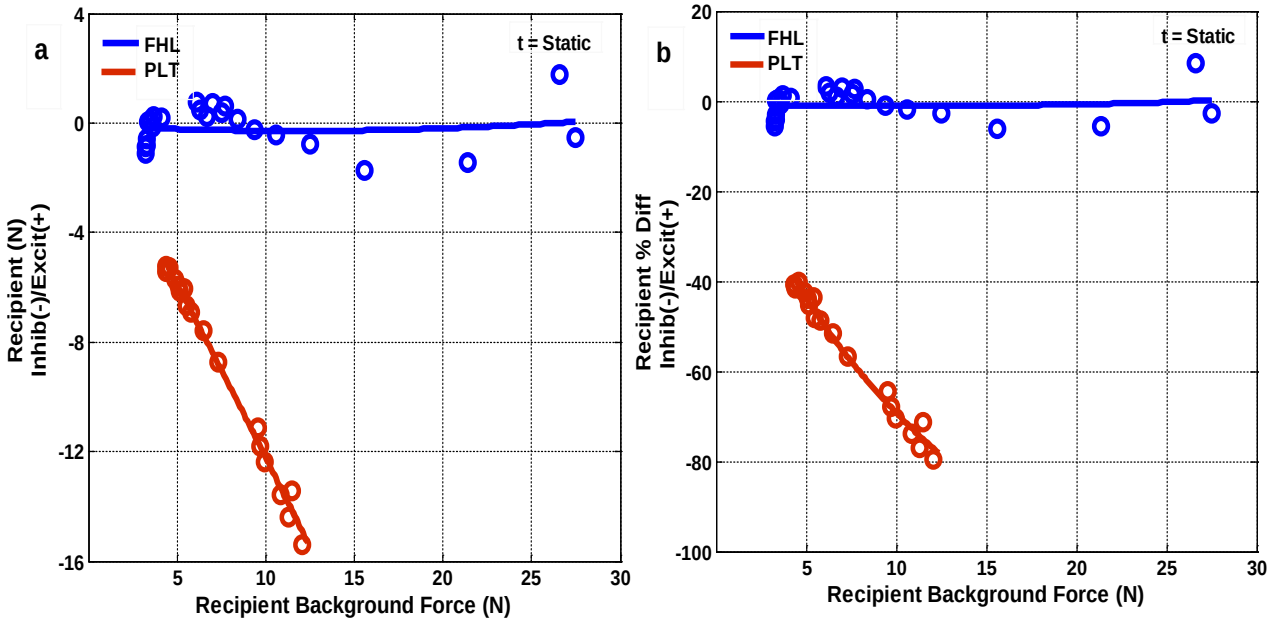

Figure 4.17 (a) Shows comparative analysis of heterogenic inhibition between PLT (red) and FHL (blue) in Newton. Each circle represents the difference of state 1 and state 2 force response of each muscle as shown in figure 4.15 and Figure 4.16. (b) Amount of inhibition normalized to percent change for both PLT and FHL. The same conventions as Figure 4.7 apply.

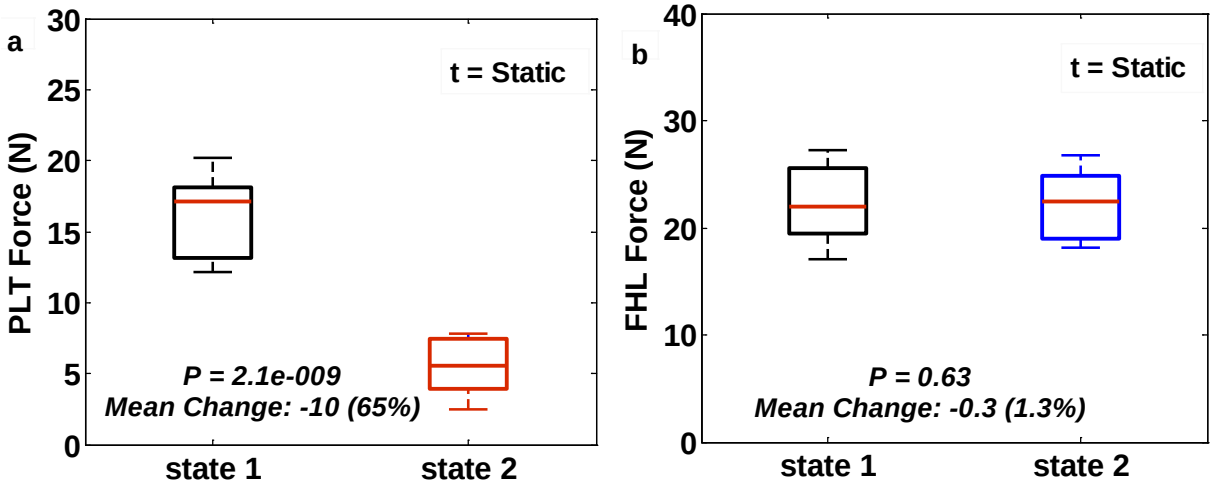

Figure 4.18 Statistical analysis, summaries for (a) PLT and (b) FHL. Horizontal axis represent state 1 (autogenic) and state 2 (autogenic + Heterogenic) of recipient muscle at static time point, while vertical axis shows force response in Newton for recipient muscle. The same conventions as Figure 4.8 apply. There is statistically significant strong inhibition of PLT by FHL following chronic LSH.

4.3.5 Altered pattern of inhibitory force feedback between PLT and FHL is bilateral following chronic LSH irrespective of the side of lesion

We collected data from all cats using both hindlimbs to compare the results in two limbs and demonstrate the effect of partial spinal cord injury on neuromuscular interactions on both the injured side of spinal cord and the uninjured side of spinal cord limb in all five cats. As observed in case of interactions between GA, SOL and FHL, we observed same pattern of intermuscular force feedback interactions in both limbs of each cat with strong inhibition of PLT and very weak inhibition of FHL.

Figure 4.19 depicts the comparison of hetrogenic inhibition between PLT and FHL in two limbs in a cat with chronic LSH at static time point. The same analysis was performed at dynamic time point too not shown here. We observed increase in inhibition from dynamic to static time point in each cat.

The results comparing the two limbs in all five animals are summarized in table 4.3 and 4.4 for PLT and FHL as recipient muscle respectively. The inhibition was always comparatively greater on the injured side limb in than on the uninjured side limb however, it was always highly statistically significant in both limbs in each animal with P value $<< 0.01$.

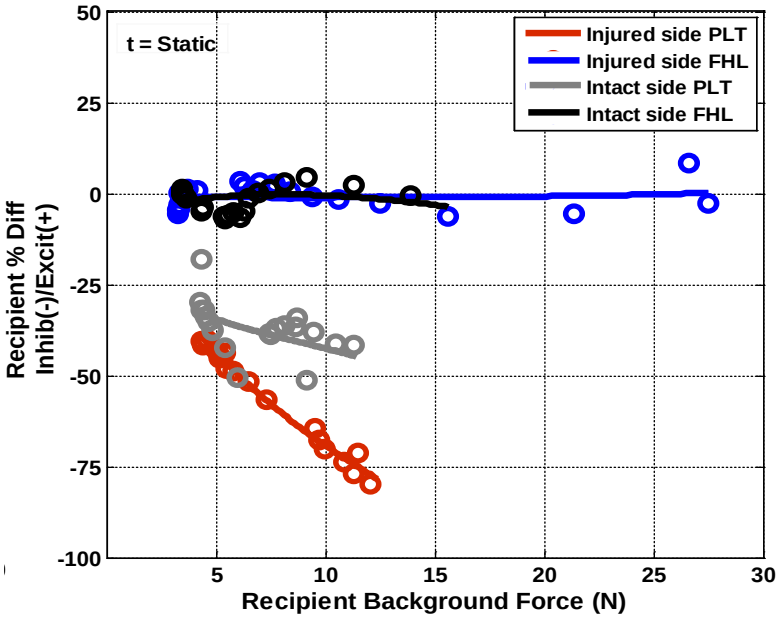

Figure 4.19 Comparison of force feedback between two hindlimbs of the same cat with chronic partial SCI (LSH). Amount of inhibition shown in terms of percent change for both PLT and FHL. Strong inhibition of PLT and week inhibition of FHL observed bilaterally. The same conventions as Figure 4.7 apply.

4.3.6 Inhibition between PLT and FHL is similar across cats following chronic LSH irrespective of the time post SCI

We observed a well defined uniform pattern of inhibition between PLT and FHL across cats. The results are summarized in Figure 4.20 and the pattern/directionality of inhibitory force feedback between PLT and FHL is demonstrated in Figure 4.21. The detailed statistical analysis is summarized in table 4.3 and table 4.4 to further validate the statistically strong inhibition of PLT by FHL across cats at different time points post SCI. We expected to see some change over time as the animal capability to walk improved but that was not demonstrated by any animal thus proving that the change in spinal cord is same across animals and not affected by the time following LSH.

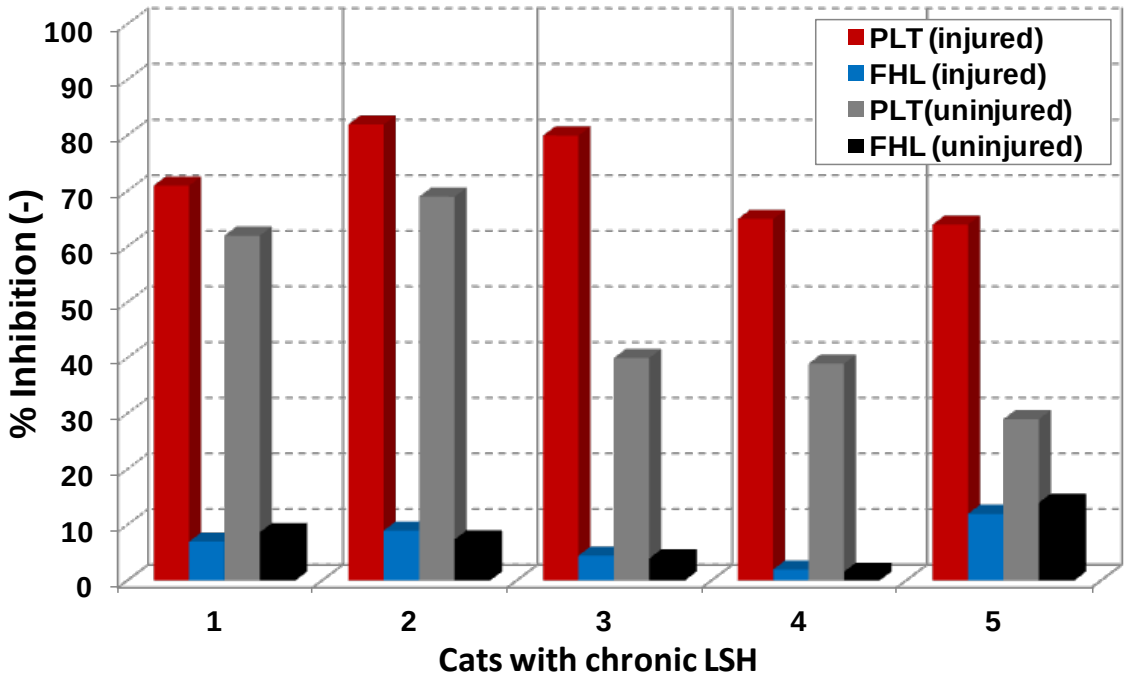

Figure 4.20 : Comparative analysis of force feedback interaction between PLT and FHL across animals post chronic LSH (1= 2weeks, 2= 4weeks, 3= 4weeks, 4= 4 weeks, 5= 20weeks).

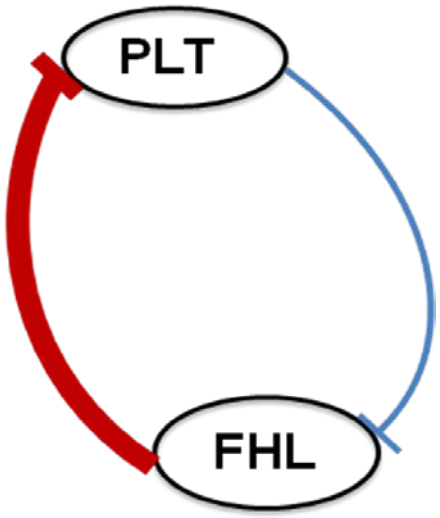

Figure 4.21 Summary diagram/Proposed model of the inhibition between ankle knee extensors FHL and PLT during chronic LSH in the intercollicular decerebrate cat. Inhibition between PLT and FHL has a greater strength in distal to proximal direction (red) in comparison to proximal to distal direction (blue). The net effect of the modulation was to produce a distal to proximal pattern of inhibition.

Table 4.3 Magnitudes of heterogenic inhibition with XER between PLT (recipient) and FHL (Donor) muscles in percentage change, range, SD and P values for each limb in cats with chronic LSH between 2 and 20 weeks post LSH. Inhibition is statistically significant if P< 0.01 on both injured and uninjured side limb in each cat. The data shown includes 4 to 6 observations in each limb in every cat each trial consisted of 45-60 stretches each.

RECIPIENT (PLT)	DONOR (FHL)							
	Cats/Weeks post LSH	Recipient Muscle Max Backgrou-nd force Range	Injured side limb			Uninjured side limb		
			%Δ (-) Range	% Δ (-) Mean ± SD	P Value	% Δ (-) Range	%Δ (-) Mean ± SD	P value
	Cat1 = 2W	5 ~ 20	68 ~ 71	69.5 ± 2	< 0.001	60 ~ 62	61 ± 1.4	< 0.001
	Cat2 = 4W	6 ~ 12	80 ~ 82	81 ± 1.4	< 0.001	68 ~ 69	68.5 ± 0.7	< 0.001
	Cat3 = 4W	5 ~ 10	57 ~ 80	68.5 ± 16.2	< 0.001	31 ~ 40	35.5 ± 6.4	< 0.001
	Cat4 = 4W	15 ~ 20	60 ~ 65	62.5 ± 3.5	< 0.001	36 ~ 39	37.5 ± 2	< 0.001
	Cat5 = 8W	___	___	___	___	___	___	___
	Cat6 = 20W	5 ~ 15	54 ~ 64	59 ± 7	< 0.001	20 ~ 29	24.5 ± 6.3	< 0.01

Table 4.4 Magnitudes of heterogenic inhibition with XER between FHL (recipient) and PLT (Donor) muscles in percentage change, range, SD and P values for each limb in cats with following chronic LSH between 2 and 20 weeks post LSH. The data shown includes 4 to 6 observations in each limb in every cat each trial consisted of 45-60 stretches each.

RECIPIENT (FHL)	Donor (PLT)							
	Cats/Weeks post LSH	Recipient Muscle Max Backgrou-nd force Range	Injured side limb			Uninjured side limb		
			%Δ (-) Range	% Δ (-) Mean ± SD	P value	% Δ (-) Range	%Δ (-) Mean ± SD	P value
	Cat1 = 2W	5 ~ 30	1.6 ~ 7	3.6 ± 2.9	≤ 0.8	8 ~ 8.7	8.4 ± 0.5	≤ 0.5
	Cat2 = 4W	25 ~ 30	8.5 ~ 9	8.8 ± 0.4	≤ 0.8	7 ~ 7.4	7.2 ± 0.3	≤ 0.3
	Cat3 = 4W	25 ~ 30	2.1 ~ 4.5	3.1 ± 1.3	≤ 0.2	0.5 ~ 4	2.2 ± 2.5	≤ 0.2
	Cat4 = 4W	25 ~ 35	1.3 ~ 2	1.7 ± 0.5	≤ 0.6	1 ~ 1.6	1.3 ± 0.4	≤ 0.3
	Cat5 = 8W	___	___	___	___	___	___	___
	Cat6 = 20W	5 ~ 15	11 ~ 12	11.5 ± 0.7	≤ 0.03	4.4 ~ 14	9.2 ± 6.8	≤ 0.9

4.3.7 Clasp knife inhibition

No evidence of clasp knife inhibition was expressed among SOL, PLT and FHL in cats following chronic LSH in contrast to its presence documented earlier in complete spinal transaction (Nichole and Cope 2001). The hallmark of clasp knife inhibition after complete transaction of spinal cord has been described as a profound autogenic and heterogenic inhibition that occurs with the latency of more than 80 ms (Nichols and Cope 2001). The heterogenic inhibition in state 1 and 2 was observed even at very low background forces of the recipient muscle.

Figure 4.22 depicts a representative example of the absence of any autogenic inhibition both between SOL and FHL (4.22a) as well as between PLT and FHL (4.22b) following LSH. There is no autogenic inhibition in state one depicted by the absence of force drop in state 1 during the muscle stretch (black line). The latency of reflex response is comparable to decerebrate cats (Bonasera and Nichols 1994) with intact spinal cord described earlier in chapter 2, Figure 2.10 (28 ± 4 ms). This latency is much smaller than the clasp knife inhibition reflex latency of more than 80 ms (Nichols and Cope 2001). The sum of autogenic and heterogenic inhibition in state 2 was not strong enough to drop the force response of the recipient muscle to almost zero (Nichols and Cope 2001). We also did not find any evidence of the clasp knife inhibition in acute LSH. The absence of clasp knife inhibition was observed in 6/6 cats with chronic LSH (100%) and 3/3 (100%) cats with acute LSH in both hindlimbs. The large isometric responses (without stretch) observed in the donor muscle in state 1(Figure 4.12 for PLT and 4.2 for SOL) are short latency, but they are prolonged. They indicate the strong inhibition of PLT and SOL

respectively by FHL even when they are acting as donor muscles and not been stretched in state 1.

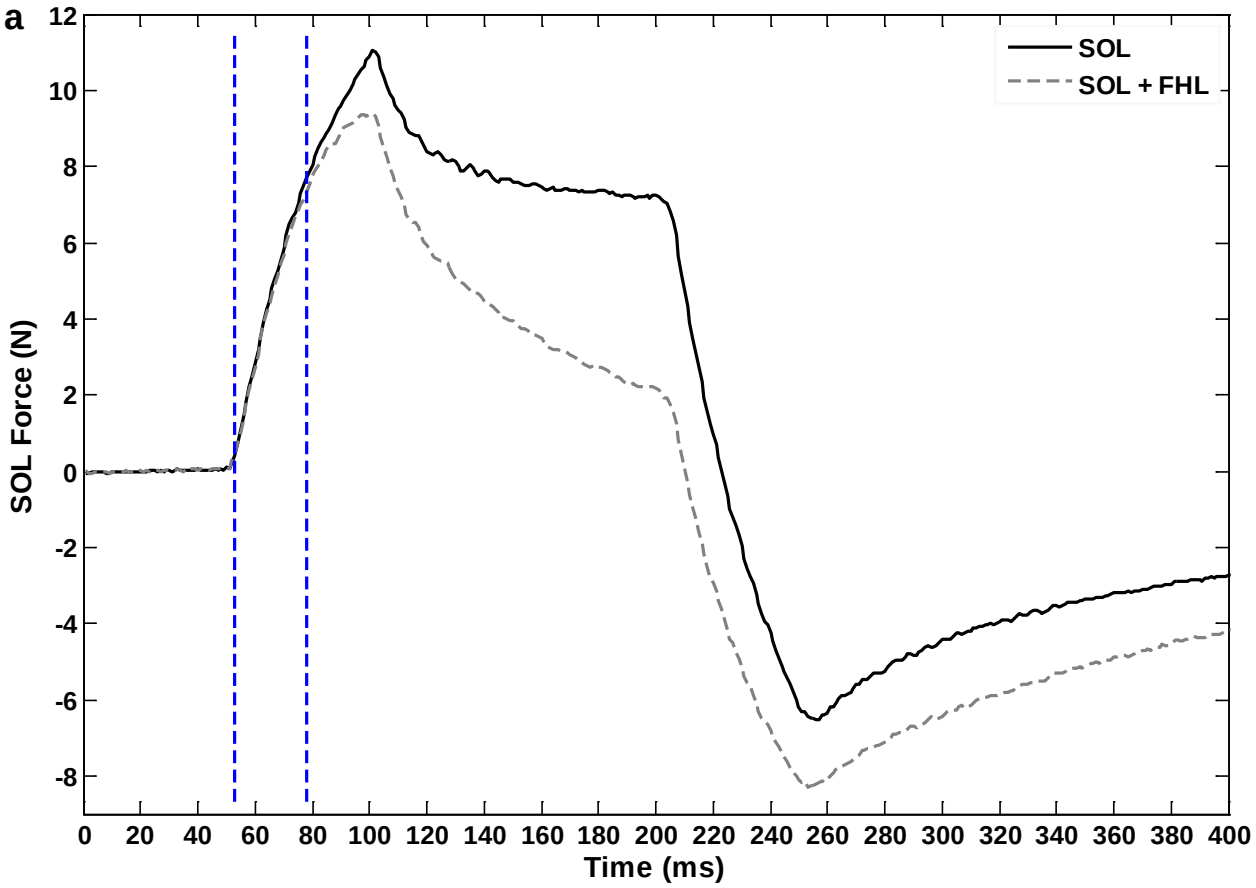

Figure 4.22 (continued)

Figure 4.22 (continued)

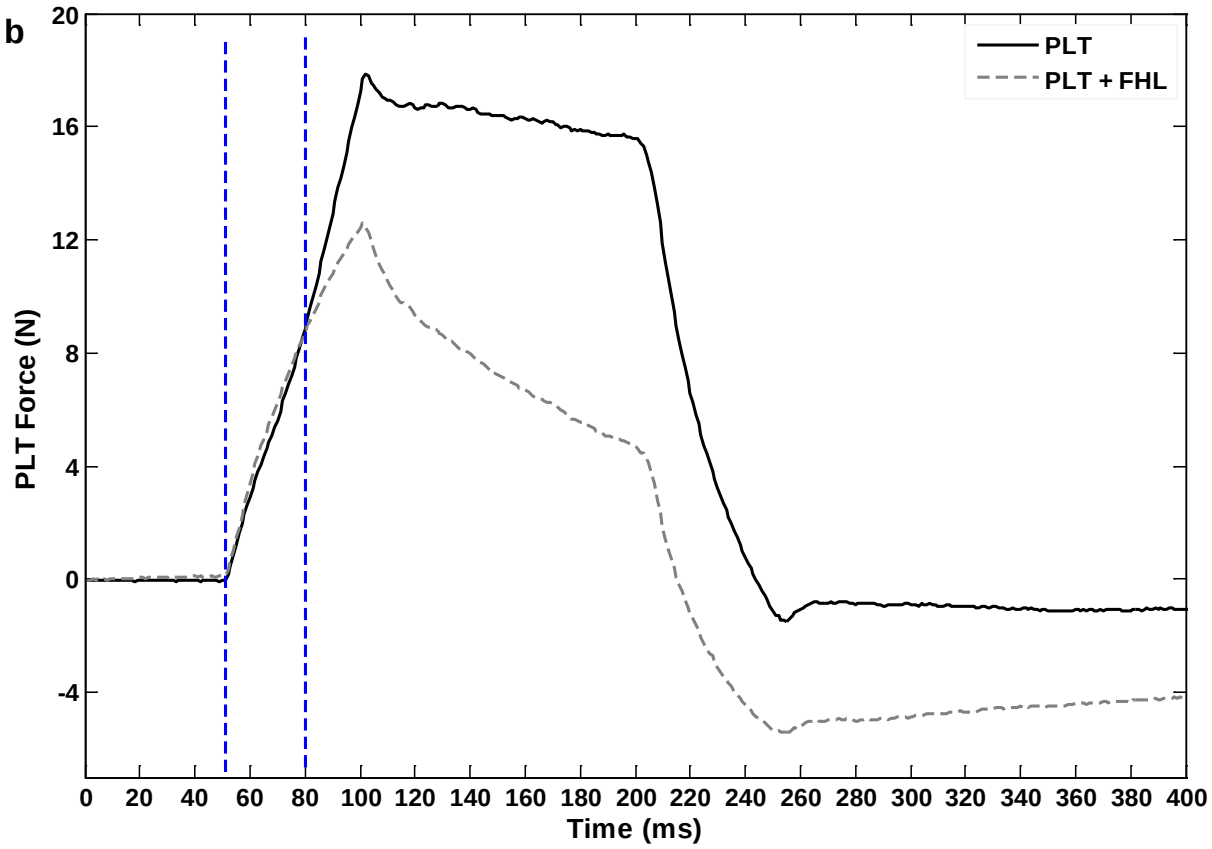

Figure 4.22 Reflex latency for the (a) FHL/SOL and (b) FHL/PLT interactions were calculated at 28 ± 4 ms. Distance between the two blue dashed lines indicates latency of reflex. There was no autogenic inhibition in state 1 (black line).

DISCUSSION

In this study, we have attempted to address the implications of chronic partial spinal cord injury on the organization of force feedback among ankle extensors, namely SOL, PLT and FHL in decerebrate cats with chronic LSH. Our most recent data from decerebrate animals (chapter 2) has shown bidirectional weak inhibition between SOL and FHL. In addition we observed stronger inhibition from FHL onto PLT in decerebrate cats with intact spinal cord. Our study presented in this chapter has shown that the force feedback linking PLT, SOL and FHL remained inhibitory following SCI with a uniform pattern and consistent results across animals. The pattern of inhibition was always a strong inhibition from FHL muscle onto SOL and PLT muscles. In essence the largest magnitude of force-dependent inhibition emanated from FHL onto either SOL or PLT. Weak inhibitory interactions were found in the opposing direction from PLT and SOL onto FHL with or without XER. Our data showed no evidence of clasp knife inhibition among FHL, SOL and PLT at both high and low background forces of muscles. There was no evidence of autogenic inhibition among FHL, PLT and SOL, but we cannot exclude it entirely. Also the force of recipient muscle never fell below zero in state two in any trial, indicating absence of clasp knife inhibition.

Postural control is a fundamental requirement during quiet standing as well as for a variety of other critical motor tasks. The animals used in this study regained locomotion within one week of SCI. They were able to maintain weight support and posture during walking, however as described earlier none of them had complete recovery of posture control and showed poor postural response to any perturbation. We propose that the altered pattern of neuromuscular interactions following chronic LSH could be due to the spared pathways from

supraspinal structures that are most probably involved in reorganizing the spinal CPG during recovery after the partial spinal lesion. In addition peripheral sensory inputs are probably also critical in ensuring that the spinal CPG functions more effectively post SCI. Reflex changes seen bilaterally in a partial lesion in our study using lateral spinal hemisection is probably due to the attempt of spinal circuitry to compensate for the loss of inputs on the damaged side. If reflex actions from group Ib afferents are to change depending on condition and motor task, the involved interneurons in CPG must be amenable to modulating influences. In fact, Ib interneurons receive a variety of convergent inputs from sensory afferents and descending tracts (Hultborn 2000; Hultborn 2006; Jami 1992; Jankowska 1992; Schomburg 1990). Therefore, loss of some of these inputs on Ib interneurons might result in altered intermuscular interactions resulting in poor inter-joint coordination and imperfect posture control

Activity-dependent plasticity occurs in the spinal cord throughout life. Driven by input from the periphery and the brain, this plasticity plays an important role in the acquisition and maintenance of motor skills and in the effects of spinal cord injury. The early development of adult spinal cord reflex patterns is driven by descending activity; disorders that disrupt descending activity later in life gradually change spinal cord reflexes. One possible explanation of the results in our study could be the fact that after SCI in adults, the infantile pattern may reappear due to the loss of descending inputs.

A proximo-distal gradient theory in muscle function is suggested by studies of limb muscle architecture and *in vivo* muscle performance during steady and incline running (Roberts et al. 1997; Biewener 1998b; Gillis and Biewener 2002; Daley and Biewener 2003,

Daley et al. 2007). The Proximal muscles at the hip and knee joints are believed to exhibit load-insensitive mechanical performance, whereas function of distal muscles at the ankle and tarsometatarso-phalangeal (TMP) joints is highly load dependent due to intrinsic mechanical effects and rapid, higher gain proprioceptive feedback (Daley et al 2007). This idea of proximal to distal gradient can be applied at ankle joint by dividing ankle extensors into proximal and distal group. The ankle extensor muscles acting at TMP can be classified as distal ankle extensors. As the angle at TMP at the start of ground contact is not altered in response to the perturbation suggesting that the activation of TMP extensors like FHL is highly load dependent (Daley et al. 2007). As the most distal muscle FHL is likely to be the first muscles to sense a change in the interaction between the limb and ground. Consequently it might respond rapidly to proprioceptive feedback in comparison to other ankle extensors. As observed in decerebrate locomoting cats the proximo-distal gradient of inhibition exists between GA and FHL (Ross and Nichols 2009). This gradient is however lost following SCI in our data suggesting that the loss of posture control could be linked to the loss of proximo-distal gradient at ankle joint.

We propose that a state dependent pattern/directionality of inhibition/gradient of force feedback is important to maintain limb compliance at joints while allowing proximal muscles to produce force necessary for locomotion and balance/posture control. Inhibitory force feedback is an important system for regulating limb dynamics for independent mobility and balance control. The alteration of its distribution after spinal cord injury limits recovery of function. In chronic spinal cats stretching FHL muscle strongly inhibited GA, PLT and SOL which reduced the reflex contribution of these, major force producing muscle in hindlimb. Therefore our results demonstrate that altered FHL, SOL and PLT intermuscular pathways

could be one of the factors that have important implications for the control of movement and posture after SCI. The altered patterns of force feedback could be due to the interruption of pathways responsible for the strength and distribution of force feedback in the spinal cord. The altered pattern could represent the unmasking of a pattern intrinsic to the spinal cord, or could be a unique pattern exhibited in the damaged spinal cord.

Adult spinal cats used in our study were able to generate weight supporting extensor activities despite of lacking appropriately timed postural responses to stance perturbations. Therefore we propose that the two functions of weight support and balance maintenance appeared to be controlled by different mechanisms and by different regions of the CNS.

It is interesting to note here that SOL, a major antigravity muscle that stays tonically contracted during quiet stance is strongly inhibited by FHL in chronic LSH. In addition PLT and SOL are ankle abductors and FHL is an ankle adductor. We propose that the redistribution of intermuscular feedback between SOL, PLT and FHL in SCI results in loss of stability at ankle due to poor maintenance of ankle torque that might affect proper foot placement required for posture control.

CHAPTER 5

DISCUSSION

Our results suggest that the ability to maintain balance/posture and resist small perturbations to balance control requires integration in the neuromuscular system that is lost following SCI. In this section, I discuss the results of our study in comparison to control data and the importance of our results for balance and weight support control from a neural, functional and biomechanical perspective. The main focus of this study has been on mapping the distribution of heterogenic force feedback among ankle extensors, including GA, PLT, SOL and FHL during mid-stance in chronic SCI (LSH). The main target of this study was to understand the mechanisms underlying the neuromuscular organization for balance and weight support. Stretch-evoked force responses were compared between control (decerebrate), chronic SCI and acute SCI both with and without XER to ascertain whether force feedback was reorganized during different spinal states.

In chapter two, we observed different patterns of inhibitory force feedback inhibition among ankle extensors in decerebrate non-locomoting cats. The most variable force feedback interactions were seen between GA and FHL. The results in chapter 2 suggest existence of a neuromuscular control system for maintenance of limb stiffness in animals with intact spinal cord.

In chapter three, we observed only one pattern of inhibitory force feedback for GA and FHL across cats following LSH (acute and chronic). The results in chapter three

reflect lack of modulation of force feedback interactions by the animals due to damaged spinal cord. Our data did not demonstrate any clasp knife inhibition between GA and FHL following both chronic and acute LSH. The latency of reflex was found consistent with previous observations (28 ± 4 ms) in decerebrate non-locomoting cats with intact spinal cord (Bonasera and Nichols 1994). The absence of clasp knife inhibition (CKI) clearly indicates that the mechanism might not be present clinically in all patients with spinal cord injury.

In chapter four, we extended our study to SOL and PLT muscles. In this chapter we observed strong inhibition of SOL and PLT by FHL in cats following LSH (acute and chronic). The main observation in chapter 4 was the generalized inhibition of ankle extensors by FHL muscle, suggesting a consistent pattern characteristic of SCI. There was no evidence of clasp knife inhibition in chapter 4 suggesting, LSH could not produce CKI, a hallmark of SCI in complete spinal cord transaction (Nichols and Cope 2001) and dorsal spinal hemisection (Cleland and Rymer 1990).

We found that the heterogenic feedback between hindlimb extensors, particularly that emanating from distal muscles specifically FHL, onto proximal muscles GA, SOL and PLT remained inhibitory following LSH, irrespective of the terminal study time following SCI. However, this inhibitory intermuscular force feedback turns into a very strong inhibition in chronic LSH in both hind limbs in comparison to control animals irrespective of the side of partial spinal injury. Inhibition from proximal muscles GA, SOL and PLT onto distal muscle FHL was much weaker and mostly statistically insignificant at P value > 0.01. We did, indeed, find evidence for a consistent pattern of

intermuscular force feedback interactions in SCI that is not observed in control decerebrate animals. Our results reflect imbalanced input on spinal circuits by the descending as well as ascending pathways. Figure 5.1 represents the summary of intermuscular force feedback interactions between ankle extensors (GA, SOL, PLT, FHL) following chronic LSH. Cats with acute LSH also exhibited strong inhibition of GA by FHL consistent with our results from chronic LSH animals.

Quantitative analysis of the data in control animals in our study has provided us with three different kinds of force feedback patterns between FHL and a proximal ankle extensor muscle GA (Figure 2.11). We found proximal to distal, distal to proximal and bi-directional intermuscular inhibitory force feedback between these muscles (GA and FHL) in control animals. The interaction between SOL, PLT and FHL stayed consistent across limbs and cats in control cats. We observed a bidirectional pattern of inhibition between SOL and FHL. The inhibitory force feedback between FHL and PLT was weak and distal to proximal in direction. Therefore, there is no characteristic pattern of intermuscular force feedback interaction between ankle extensors in control decerebrate animals. These results indicate capability of spinal cord to modulate intermuscular force feedback according to the state of animal.

Decerebrate non-locomoting cats exhibit a consistent definitive pattern of intermuscular force feedback between ankle extensor muscles as shown in figure 5.2. During locomotion there is strong inhibition of FHL by GA, balanced bidirectional weak inhibition between FHL and SOL and a strong inhibition of PLT by FHL across animals.

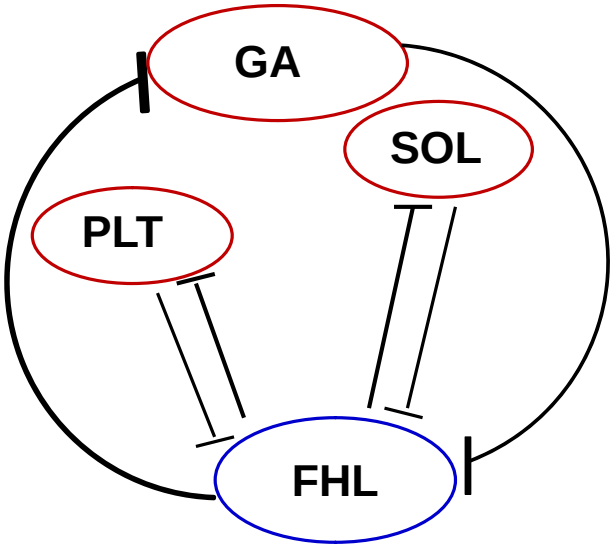

Force Feedback SCI/ LSH model

Figure 5.1 Summary diagram/Proposed model of Force feedback between ankle extensors FHL, GA, SOL and PLT following chronic LSH in the intercollicular decerebrate/non-locomoting cat. The net effect of the modulation of force feedback was to produce a consistent distal to proximal pattern/directionality of inhibition characteristic of only SCI.

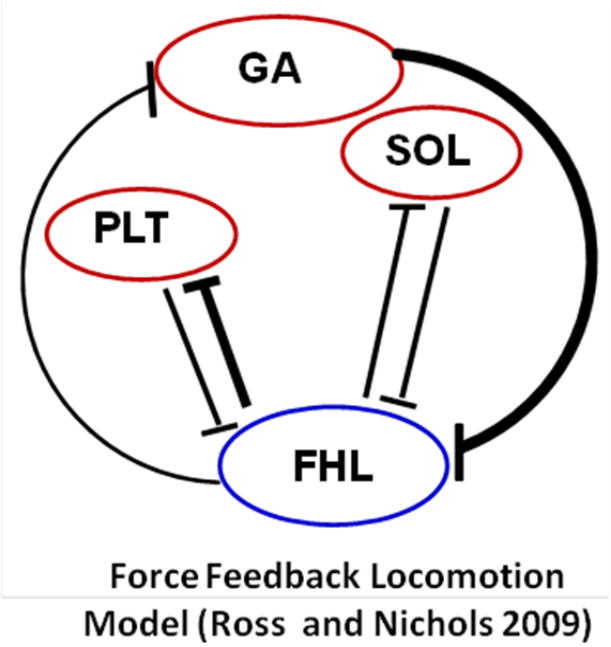

Figure 5.2 Summary diagram/model of Force feedback between ankle extensors FHL, GA, SOL and PLT in the locomoting decerebrate cat.

Cats with SCI can be trained to stand independently (De Leon et al. 1998) and withstand small perturbations to balance (Macpherson and Fung 1999); however, their intermuscular interactions are much different than cats with intact spinal cord and they fail to regain full control of balance and weight support. According to our current data we can say with confidence that the intermuscular interactions used for postural control are not accessible via spinal circuits alone, at least when these circuits do not receive normal supraspinal input. However, basic locomotion patterns may be produced by spinal CPGs (McCrea and Rybak 2008; Rossignol et al 2006), which are modulated by sensory feedback pathways within the spinal cord (Forssberg et al. 1980; Rossignol et al. 2008), even in the absence of descending input in SCI. We propose that balance control requires multisensory integration and interlimb coordination that is not evident in spinalized animals (Macpherson and Fung 1999) or animals lacking connectivity to the brain stem (Deliagina et al. 2008; Lyalka et al. 2009) and likely requires brain stem processing (Stapley and Drew 2009).

One possible explanation for altered yet consistent intermuscular inhibitory force feedback between ankle extensors in LSH could be the loss of input from one or more supraspinal pathway. There is also loss of sensory input from sensory organs (visual, proprioception, skin). In decerebrate animals with intact decending pathways from midbrain, cerebellum, reticular formation and vestibulospinal tract it is possible for the animal to adjust task dependent intermuscular interaction at spinal level (Nichols et al. 2014). Since, heterogenic inhibition is thought to play an important role in coordinating and stabilizing the limb during movement, it would make sense; from a design standpoint that one would want to maintain that stability quickly as the body posture is challenged

by environmental perturbations during quiet standing. We propose that the heterogenic intermuscular force feedback interactions are task dependent and are different from one animal to the other because the intact animal is capable to correct its posture by adapting different intermuscular interactions driven by proprioreseptor feedback and other sensory input to spinal circuitary (visual, sensory, memory). There is a strong evidence of a consistent intermuscular heterogenic force feedback inhibition pattern in locomoting animals from previous studies conducted in our laboratory (Ross and Nichols 2009) demonstrating proximal to distal pattern of inhibition between FHL and GA, strong distal to proximal pattern/directionality of inhibition between FHL and PLT (not as strong inhibition as seen in our data from SCI). This is probably due to the supraspinal signals generated in conjunction with the commands for locomotion. These results suggest that the limb stiffness is regulated by a proprioceptive network in the spinal cord and the site of the regulation is the musculature of the distal limb specifically FHL in our study, which are directly responsible for the mechanical interaction of the body with the environment. The patterns of activity of the hind limb muscles and their regulation through proprioceptive feed back are appropriately regulated according to their specific functions in these motor tasks.

Now the question arises that why the chronic LSH cats are unable to maintain balance during perturbation/posture control challenging situations while they exhibit better control of posture during locomotion? On the basis of our results presented in this study we can give three plausible explanations. Firstly, the generation of appropriate muscle activation patterns in the hind limbs certainly requires complex hierarchical neural framework integration, where each higher unit is responsible for increasingly

complex integration of sensory and environmental information. We propose that the sensory feedback required for appropriate muscle activation patterns needed to maintain balance during locomotion after SCI is located within the lowest level of this neural hierarchy, the spinal cord and therefore preserved or regained following SCI. However, complex posture and weight support needs input from higher centers (Lyalka et al. 2005; Nichols et al. 2002). Lyalka and coworkers note that spinal cord hemi-sectioned animals show a significant recovery of postural responses when supra-spinal support is present. We know that brainstem regions such as the ventral and dorsal tegmental fields can adjust postural tone through excitatory or inhibitory influences on the spinal cord (Mori 1987; Mori et al. 1989).

Secondly, the cortex has the capacity to dynamically control posture by integration of information about global parameters, limb position, and environmental conditions (Dietz et al. 1984). This is possible because of the pyramidal tract excited by contralateral limb movements (Beloozerova et al. 2005; Beloozerova et al. 2003a). Since, in lateral spinal hemisection only half of the spinal cord is damaged it is possible that the contralateral cortex (from intact side) still influence the balance control on ipsilateral/ LSH side via uncrossed pyramidal fibers that are making connections on the injured side through the interneurons in chronic LSH. These left over neuronal connections can help correct the balance during a learned behavior like walking.

The corticospinal system that is unilaterally damaged in LSH has stronger influence over distal than that over proximal muscles (Brouwer and Ashby 1990; Lemon and Griffiths 2005; McKiernan et al. 1998; Palmer and Ashby 1992; Turton and Lemon

1999). This could explain distal joints and muscle control loss after stroke and upper motor neurons insult patients (Turton and Lemon 1999; Colebatch and Gandevia 1989). Reticular formation and brain stem affects proximal muscles more potently than distal muscles (Davidson and Buford 2006; Riddle et al. 2009; De Domenico and McCloskey 1987; Tan et al. 1994; Hall and Mc-Closkey 1983; Refshauge et al. 1995) and are comparatively less damaged in LSH. The reorganization of heterogenic intermuscular force feedback following SCI could be attributed to this differential control of proximal and distal muscles in hind limb.

In addition reticulospinal tracts are a major alternative to the corticospinal tract, some fibers of the medullary reticulospinal tract cross the midline and exits at all spinal levels. It contains circuitry for many complex actions, such as orienting, stretching, and maintaining a complex posture. Commands that initiate locomotor circuits in the spinal cord are also thought to be transmitted through the medullary reticulospinal tract. Thus, we propose that this tract could be responsible for some balance control related to locomotion in chronic LSH cats. The loss of balance control for complicated tasks other than walking could be due to loss of influence from cortex. Our data supports our hypothesis that the control of balance requires inputs from higher brain centers. Therefore after SCI the animal loses its ability to maintain full balance control.

Any quick adjustment of posture requires vestibulospinal tract. This tract is damaged in LSH. Vestibulospinal tracts mediate postural adjustments and head movements. This tract detects small movements of the body by the vestibular sensory neurons, and sends motor commands to counteract these movements to appropriate

muscle groups throughout the body. The lateral vestibulospinal tract excites antigravity muscles in order to exert control over postural changes necessary to compensate for tilts and movements of the body. The medial vestibulospinal tract effect spinal circuits bilaterally, it innervates neck muscles in order to stabilize head position as one moves around the world. It is also important for the coordination of head and eye movements. Loss of vestibular feedback causes subjects to generate hypermetric responses (Macpherson and Inglis 1993), indicating that vestibular influences the scale of muscle responses. This tract's input on spinal circuitary may be responsible for rearrangement of spinal networks involved in somatosensory integration. We therefore suggest that one of the possible reasons for comparatively better balance control during locomotion in chronic LSH is the partly intact medial vestibulospinal tracton the injured side of spinal cord. The poor response of animal to sudden perturbation or change of terrain could be due to the damaged lateral vestibulospinal tract on injured side in LSH. The altered patterns of force feedback are observed bilaterally in our study using cats with LSH. We suggest that this could be due to the interneurons connecting the two halves of the spinal cord. Following LSH the descending information from lateral vestibulospinal tract on the uninjured side of the spinal cord reaches the injured half through the interneurons, however the information is altered or incomplete due to damaged spinal cord. However the inhibitory muscular interactions though altered in pattern and amount remain inhibitory following SCI that could be due to alteration of input on spinal circuitry by the left over medial vestibulospinal tract.

To address this question we collected data from an animal with dorsal spinal hemisection (DSH). Our data from this experiment using acute DSH showed no distal to

proximal pattern of intermuscular inhibition between FHL and GA that we have observed in our LSH animals. However, this single observation does not statistically prove the association of altered intermuscular interactions observed in our data in SCI with damaged vestibulospinal tract and may need more investigation in future studies.

Following unilateral SCI (hemisection), compensation by remaining descending inputs could be involved in reshaping the CPG to compensate for the loss of damaged pathways. To deal with partial loss of brain inputs and to produce locomotor behavior after hemisection, the spinal cord could have been imprinted by new descending commands and therefore "memorized" a new mode of functioning (Chen et al. 2002; Chen and Wolpaw 2002). It has been argued that isolated spinal circuits with intact musculoskeletal systems are responsible for quiet sophisticated motor tasks (Edgerton et al. 2001; Stein and Daniels-McQueen 2004; Timoszyk et al. 2002) and sensorimotor transformations (Bosco and Poppele 2001; Poppele and Bosco 2003). In contrast, the poor postural responses of spinalized cats (Fung and Macpherson 1999; Macpherson and Fung 1999a; Pratt et al. 1994) have been interpreted to indicate that spinal pathways are not adequate for appropriate muscle activation. Increases in inhibitory neurotransmitters, and re-organization of spinal synapses (Edgerton et al. 2001); all likely influence spinal cord functionality. More recent studies suggest that spinal circuits can support postural control as long as supraspinal influences remain intact (Deliagina et al. 2008; Deliagina et al. 2006; Lyalka et al. 2005; Musienko et al. 2008). A reduction in supraspinal drive may reduce activation of some neurons while facilitating activation of others (Ettema 1997; Venugopal et al. 2011).

Following incomplete SCIs in rodents, substantial increases in collateral sprouting of the corticospinal tract have been reported during the first 2 months post-injury (Bareyre et al., 2004; Li et al., 1994). Direct anatomical evidence of interneuronal sprouting in the cat (Fenrich and Rose 2009) has also been reported. We propose that this collateral imperfect growth could lead to altered intermuscular pathways following SCI. We hypothesize that a central circuit, located within the spinal cord, makes up the foundation from which most postural corrections are made following SCI. This foundational circuit utilizes feedback from muscle, Golgi tendon organ and remaining decending pathways to generate appropriate intermuscular activation patterns to maintain balance. Therefore, intermuscular force feedback pathways changes following SCI. These altered pathways are different from intact animals and are not perfect enough to meet the challenges of balance control in a challenged environment. We further propose that CPG is also modulated by other sources of feedback such as cutaneous, vestibular, visual, and joint along with feedback from other limbs and supra-spinal sources. Therefore its output is a complex mechanism. Since some of these inputs are lost in LSH while others still exist we can say that an imbalance of the neural input to spinal circuits could be responsible for altered force feedback responses and poor balance control.

The ascending pathways on the other hand are damaged extensively on the damaged side in LSH. Therefore, we propose that information from muscle receptors reach the spinal cord but cannot reach cortex and other higher centers and therefore, neuromuscular interactions are strongly effected as shown in our study. However, further experimental data is required to support the role of ascending pathways in posture control.

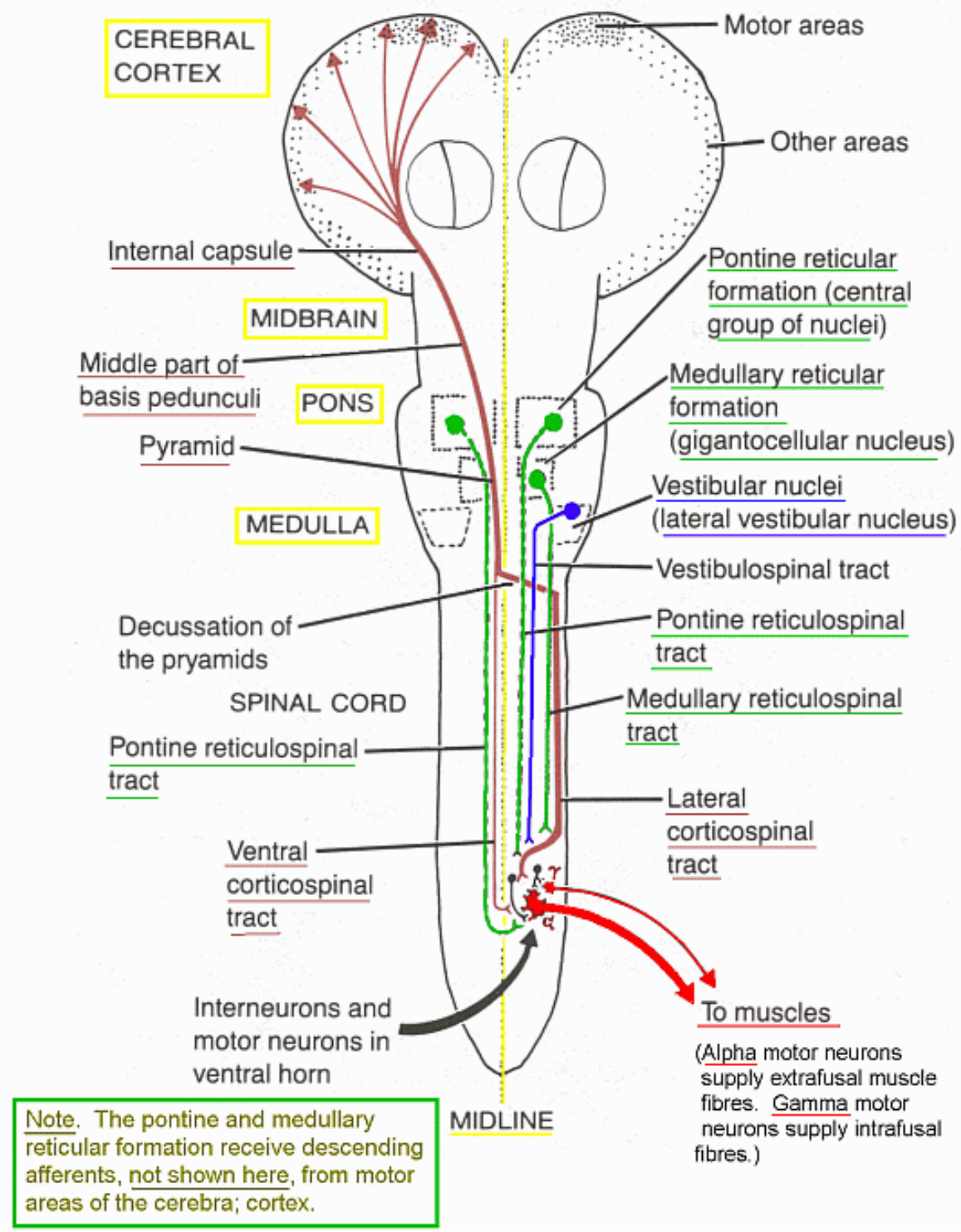

Figure 5.2 Diagrammatic representation of descending spinal pathways.

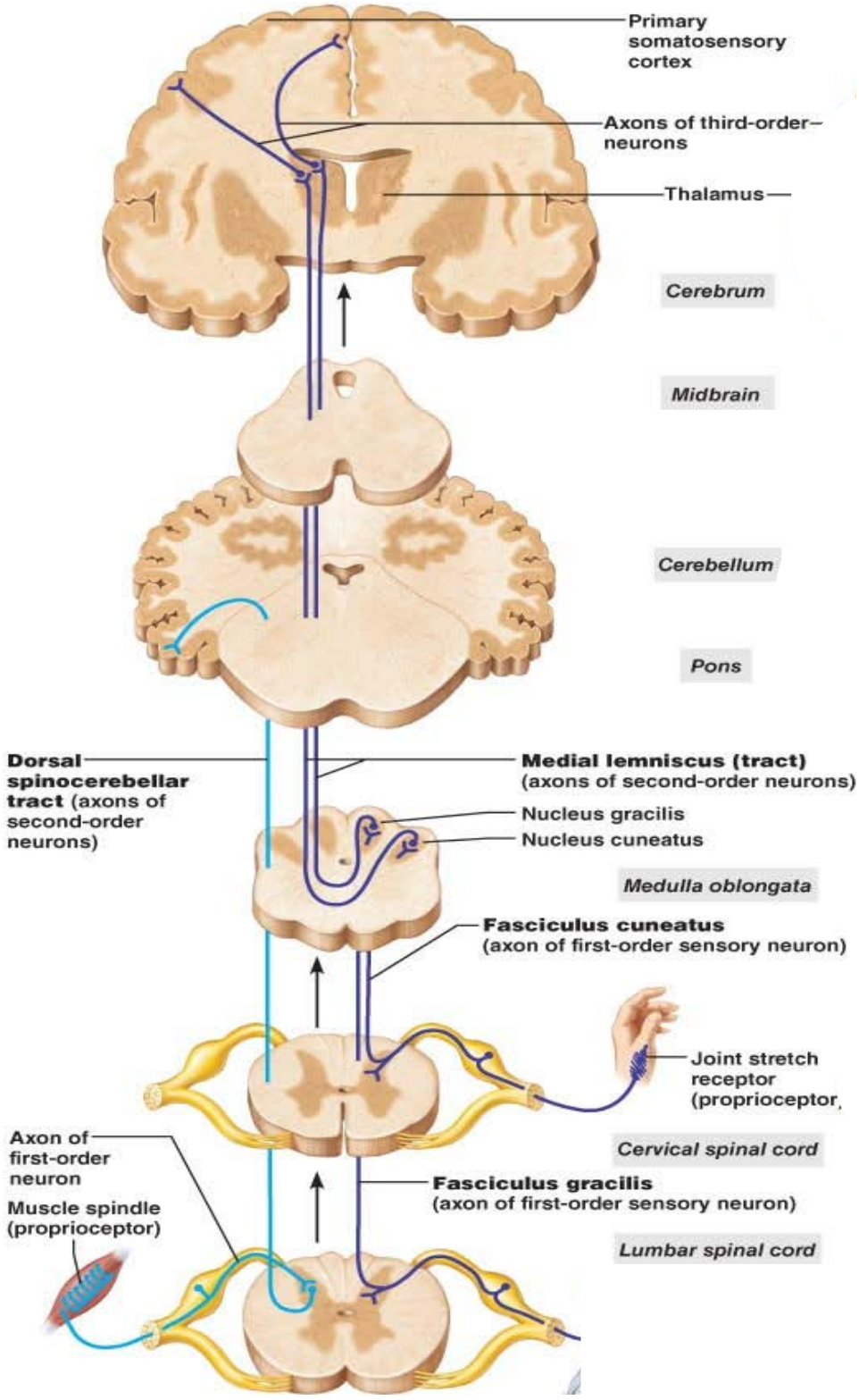

Figure 5.3 Ascending pathways in spinal cord (The central nervous system classes.midlandstech.edu)

The influence of length (i.e. Ia, II) and force (i.e. Ib) feedback acting on the same muscle, its synergists and antagonists has been extensively studied ((Eccles et al. 1957; Bonasera and Nichols 1994; Wilmink and Nichols 2003). Importantly, the effects of group Ia, Ib, and II afferents on the muscle of origin, synergists, and antagonists are thought to regulate stiffness of individual joints in response to unexpected perturbations (Honeycutt et al. 2009) and on an ongoing basis during walking in cats and humans (Mazzaro et al. 2005, Mazzaro et al. 2006). Group Ib and group II afferents are widely distributed to other muscles in the limbs (Nichols 1999; Bras et al. 1990). Inhibitory force feedback, by virtue of its distribution, has been proposed as a neuromechanical link promoting interjoint coordination (Nichols 1999). Therefore, greater relative inhibitory force feedback from some proximal muscles to distal muscles could facilitate compliance of distal joints when impacting the ground (especially during locomotion), whereas greater relative inhibition from distal to some of the proximal muscles could be beneficial in specific motor tasks like landing after a jump. Therefore, we suggest that the motor deficits such as instability at knee and ankle resulting in poor balance control as observed in our study in cats with LSH could be the result of a widespread inhibition of all the major extensors of ankle by FHL which is the most distal extensor of ankle. The pattern of distal to proximal inhibition is one of the patterns observed in non-locomoting cats as described in chapter 2. However, we must remember that widespread distal to proximal inhibition pattern is never observed in decerebrate cats with intact spinal cord.

Over the years, the spinal reflex effects exerted by group Ib afferents from Golgi tendon organs have turned out to be much more complex than originally thought. These effects are state dependent, that is, dependent on the context and task of motor acts. This

task dependence is reflected in different group Ib reflex effects during quiescent states on the one hand versus upright stance and the locomotor stance phase on the other hand. Ib interneurons affect α- motoneurons, γ Motoneurons, Ib interneurons (mutual inhibition), Group II interneurons, ventral spinocerebellar tract (VSCT), dorsal spinocerebellar tract, Primary sensory afferents probably exerting presynaptic inhibition as GABAergic, neurons (Jami 1992, Jankowska 1992, Schomburg 1990).

The reorganization of force feedback is seen bilaterally in LSH, we propose that spinal circuits responsible for inter limb co-ordination remain functional after LSH and could contribute to compensatory changes in both hind limbs. We also, propose that in chronic LSH cats due to altered intermuscular force feedback activity at ankle the animals are not able to maintain proper posture. Additionally, our data suggests that there is a well defined and consistent pattern of distal to proximal intermuscular force feedback inhibition following LSH at ankle joint. However, we need more data from muscles acting at hip and knee joints to prove the idea of gradient of force feedback between proximal and distal joint muscles. We propose that this altered pattern of force feedback between ankle extensors is characteristic of SCI. Therefore, if there is any reorganization of neuromuscular interaction at spinal level in these animals following SCI that stays consistent across animals. Since, we performed decerebration before collecting terminal data in LSH cats that we did in all control animals without SCI too with different outcome. We propose that the changes in intermuscular inhibitory pathways at the ankle are probably due to the effect of loss of connections with these structures or formation of new connections that are not seen in intact animals.

Our data shows strong inhibition of GA, SOL and PLT by FHL in LSH. In addition PLT that is inhibited very strongly by FHL in chronic LSH exhibits the same kind of force feedback interaction in locomoting animals (Ross and Nichols 2009) with intact spinal cord. The difference is however the fact that in LSH, FHL is not inhibited by any of the ankle extensor in contrast to locomoting animals where it is inhibited by GA and SOL. Therefore, it is important to look at our results from biomechanical and anatomical point of view. FHL act as an extensor, planterflexor and adductor at ankle and toe flexor at foot joints and contributes to claw protrusion (Goslow et al. 1972; Lawrence et al. 1993; Lawrence and Nichols 1999). The origin of FHL is on the upper portion of the fibula and inserts into the flexor digitorum longus (FDL).

PLT is an ankle extensor, plantarflexor and abductor of ankle. PLT originates on the lateral side of the patella with a large, broad tendon that wraps around the tendons of GA and SOL, lays atop the calcaneus and inserts onto the tendon of flexor digitorum brevis (Crouch 1969). Both the FHL and PLT act indirectly on toes through their insertion into FDL and FDB respectively. However, due to difference of their action at ankle they can effect foot placement and clearance. Proper foot placement is an important part of balance control. Accordingly, if there is stronger adduction/inversion by FHL at ankle coupled by weaker abduction/eversion and extension by SOL, GA and PLT in SCI then the net result is ankle spraining and poor foot clearance. Since all the major force producing antigravity muscles are strongly inhibited after SCI loss of weight support and balance control is a major outcome. Poor obstacle clearance has already been reported in chronic LSH cats by Dena Howland laboratory (Adele et.al 2011). Also, GA and PLT are both multi-joint muscles and their strong inhibition naturally disturb interjoint co-

ordination following LSH. SOL on the other hand is a uniarticular muscle acting at ankle so its strong inhibition by FHL in our study suggests that the redistribution of inhibitory force feedback at ankle is not limited to multiarticular muscles. Also, SOL is a major antigravity muscle that stays active throughout the stance therefore; its inhibition could result in loss of posture control under the influence of gravity.

Cats with SCI can be trained to stand independently (De Leon et al. 1998) and withstand small perturbations to balance (Macpherson and Fung 1999); however, their intermuscular interactions are much different than cats with intact spinal cord and they fail to regain full control of balance and weight support. According to our current data we can say with confidence that the intermuscular interactions used for postural control are not accessible via spinal circuits alone, at least when these circuits do not receive normal supraspinal input. However, basic locomotion patterns may be produced by spinal CPGs (McCrea and Rybak 2008; Rossignol et al 2006), which are modulated by sensory feedback pathways within the spinal cord (Forssberg et al. 1980; Rossignol et al. 2008), even in the absence of descending input in SCI. We propose that balance control requires multisensory integration and interlimb coordination that is not evident in spinalized animals (Macpherson and Fung 1999) or animals lacking connectivity to the brain stem (Deliagina et al. 2008; Lyalka et al. 2009) and likely requires brain stem processing (Stapley and Drew 2009).

The clasp-knife reflex, which consists of brief excitation followed by powerful, long-lasting inhibition in homonymous and synergistic muscles, has been extensively investigated in reduced animal preparations (Burke et al. 1972; Cleland and Rymer 1990;

Rymer et al. 1979; Sherrington 1909), chronically spinalized animals (Nichols and Cope 1989; Sherrington 1909), and spastic human patients (Burke et al. 1971; Rademaker 1947). It is distributed within and between antigravity muscles in complete transaction of spinal cord (Nichols and Cope 2001) and DSH ((Burke et al., 1972). Our data did not show any evidence of clasp knife inhibition in chronic LSH cats. We observed absence of autogenic inhibition in state 1, lack of prolongation of reflex latency and absence of profound inhibition of PLT, SOL, GA and FHL in state 2. We propose that as shown by Cleland and Rymer (Cleland and Rymer 1990) dorsal half of spinal cord might be responsible for clasp knife inhibition. In our study partial spinal injury (LSH) preserved half of the spinal cord (uninjured half with intact dorsal spinal cord) and therefore we were not able to witness this phenomenon.

Methodological considerations

We strongly believe that our method of recording reflexes using different animals for control, acute LSH and chronic LSH data is the best approach to study changes incurred after injury. First it minimizes the variance in a group because same environment was provided to each group of animals. Also, chronic LSH, pre and post surgical care was provided by the same person (Dena Hawland) to avoid variability in surgical procedure across animals. We believe that this approach helped us reduce the number of experimental animals used. We didn't use the same animal to collect control and post LSH data because our experiments requires decerebration to avoid any effect of brain and other special senses on intermuscualr interactions/reflex pathways.

Reflexes can be highly variable from one cat (Loeb 1993) or human (Zehr et al. 1997) to another, which probably extends to most species, including rats and mice. Our data shows asymmetrical pattern (distal to proximal) of the amount of inhibitory force feedback between proximal and distal muscles following chronic LSH. We propose that it could be because of asymmetric descending influences from structures rostral to the partial spinal lesion. With the present approach, changes in reflex pathways after a partial spinal lesion cannot be attributed to specific structures, and more work is required to elucidate the relative contribution of different structures in the observed changes.

REFERENCES:

Alexander RM. Elastic energy stores in running vertebrates. *Am zool* 24: 85–94, 1984.

Alexander RM. Tendon elasticity and muscle function. *Comp biochem physiol a mol integr physiol* 133: 1001–1011, 2002.

Alexander RM, Bennet-Clark HC. Storage of elastic strain energy in muscle and other tissues. *Nature* 265: 114–117, 1977.

Amatachaya S, Thaweewannakij T, Adirekudomrat J, and Siritaratiwat W. Factors related to obstacle crossing in independent ambulatory patients with spinal cord injury. *J. Spinal Cord Med* 33: 144–149, 2010.

Baldwin KM, Roy RR, Sacks RD, Blanko C and Edgerton VR. Relative independence of metabolic enzymes and neuromuscular activity. *J appl Physiol* 56:1602–1607, 1984.

Barbeau H, Fung J, Leroux A, Ladouceur M. A review of the adaptability and recovery of locomotion after spinal cord injury. *Progr Brain Res* 137: 9-25, 2002.

Barbeau H, Rossigol S. Recovery of locomotion after chronic spinalization in the adult cat. *Brain Research* 412: 84-85, 1987.

Bareyre FM, Kerschensteiner M, Raineteau O, Mettenleiter TC, Weinmann O, and Schwab ME. The injured spinal cord spontaneously forms a new intraspinal circuit in adult rats. *Nat. Neurosci* 7: 269–277, 2004.

Behrman AL, Nair PM, Bowden MG, Dauser RC, Herget BR, Martin JB, Phadke CP, Reier PJ, Senesac CR, Thompson FJ, Howland DR. Locomotor training restores walking in a nonambulatory child with chronic, severe, incomplete cervical spinal cord injury. *Physical Therapy* 88(5):580-590, 2008.

Beloozerova IN, Sirota MG, Orlovsky GN, and Deliagina TG. Activity of pyramidal tract neurons in the cat during postural corrections. *J Neurophysiol* 93: 1831-1844, 2005.

Beloozerova IN, Sirota MG, Swadlow HA, Orlovsky GN, Popova LB, and Deliagina TG. Activity of different classes of neurons of the motor cortex during postural corrections. *J Neurosci* 23: 7844-7853, 2003a.

Bernhard M, Andre Gries, Paul Kremer, Bernd W. Bottiger. Spinal cord injury (SCI)—Prehospital management. *Resuscitation* 66: 127-139, 2005.

Biewener, AA. Muscle-tendon stresses and elastic energy storage during locomotion in the horse. *Comp. Biochem. Physiol.* 120B: 73-87, 1998b.

Biewener AA and Roberts TJ. Muscle and tendon contributions to force, work, and elastic energy savings: a comparative perspective. *Exer Sport Sci Rev* 28: 99-107, 2000.

Bonasera SJ, Nichols TR. Mechanical actions of reflexes linking long toe flexors and extensors of the knee and ankle in the cat. *J Neurophysiol* 71: 1096–1110, 1994.

Bonasera SJ, and Nichols TR. Mechanical actions of heterogenic reflexes among ankle stabilizers and their interactions with plantarflexors of the cat hindlimb. *J Neurophysiol* 75: 2050-2070, 1996.

Bosco G, Poppele RE. Proprioception from a spinocerebellar perspective. *Physiol Rev* 81: 539–568, 2001.

Bras H, Jankowska E, Noga B, Skoog B. Comparison of Effects of Various Types of NA and 5-HT Agonists on Transmission from Group II Muscle Afferents in the Cat. *Eur J Neurosci* 2: 1029-1039, 1990.

Brouwer B, Ashby P. Corticospinal projections to upper and lower limb spinal motoneurons in man. *Electroencephalogr Clin Neurophysiol* 76: 509–519, 1990.

Brown IE, Loeb GE. A reductionist approach to creating and using neuromusculoskeletal models. *Chapter in: Biomechanics and Neural Control of Movement, edited by Winters JM, Crago PE. Springer, New York,* 148–163, 1997.

Burke RE, Fedina L, Lundberg A. Spatial synaptic distribution of recurrent and group Ia inhibitory systems in cat spinalmotoneurons, *J Physiol (Lond)* 214: 305–326, 1971.

Burke D, Knowles L, Andrews C, Ashby P. Spasticity, decerebrate rigidity and the clasp-knife phenomenon: an experimental study in the cat. *Brain* 95: 31–48, 1972.

Burke RE, Levine DN, Tsairis P, Zajac FE. Physiological types and istochemical profiles in motor units of the cat gastrocnemius. *J Physiol* 234: 723-748, 1973.

Burke, RE, Levine, DN, Salcman M, and Tsairis P. Motor units in cat soleus muscle: Physiological, histochemical and morphological characteristics. *J Physiol (Lond),* 238: 503–514, 1974.

Burke DA, Linden RD, Zhang YP, Maiste AC, Shields CB. Incidence rates and populations at risk for spinal cord injury: a regional study. *Spinal Cord* 39(5): 274–278, 2001.

Carter MC, And Smith, J. L. Simultaneous control of two rhythmical behaviors. II. Hindlimb walking with the paw-shake response in the spinal cat. *J Neurophysiol* 56: 184–195, 1986.

Chen XY, Carp JS, Chen L, Wolpaw JR. Corticospinal tract transaction prevents operantly conditioned H-reflex increase in rats. *Exp Brain Res* 144: 88–94, 2002.

Chen XY, Wolpaw JR. Probable corticospinal tract control of spinal cord plasticity in the rat. *J Neurophysiol* 87: 645–652, 2002.

Chin NK, Cope M and Pang M. Number and distribution of spindle capsules in seven hindlimb muscles of the cat. *Symposium on Muscle Receptors.* D. Barker. Hong Kong, Hong Kong University Press: 241-248, 1962.

Cleland CL and Rymer WZ. Neural mechanisms underlying the clasp-knife reflex in the cat: I. Characteristics of the reflex. *J Neurophysiol* 64: 1303-l318, 1990.

Crowe A, Matthews PB. The effects of stimulation of static and dynamic fusimotor fibres on response to stretching of primary endings of muscle spindles. *J Physiol* 174: 109–131, 1964.

Colebatch JG, Gandevia SC. The distribution of muscular weakness in upper motor neuron lesions affecting the arm. *Brain* 112: 749–763, 1989.

Cook C, McDonagh MJN. Measurement of muscle and tendon stiffness in man. *Eur J Appl Physiol Occup Physiol* 72: 380–382, 1996.

Cote MP, Gossard JP. Step training-dependent plasticity in spinal cutaneous pathways. *The Journal of neuroscience* 24: 11317-11327, 2004.

Cote MP, Menard A, Gossard JP. Spinal cats on the treadmill: changes in load pathways. *The Journal of neuroscience* 23: 2789-2796, 2003.

Crouch JE. *Text-Atlas of Cat Anatomy*. Philadelphia: Lea & Febiger, 1969.

Davidson A, Buford J. Bilateral actions of the reticulospinal tract on arm and shoulder muscles in the monkey: stimulus triggered averaging. *Exp Brain Res* 173: 25–39, 2006.

Daley MA, Felix, Biewener. Running stability is enhanced by a proximo-distal gradient in joint neuromechanical control *J Exp. Biol* 210: 383-394, 2007.

De Leon RD, Hodgson JA, Roy RR, Edgerton VR. Full weight-bearing hindlimb standing following stand training in the adult spinal cat. *J Neurophysiol* 80: 83-91, 1998.

Deliagina TG, Orlovsky GN, Zelenin PV, and Beloozerova IN. Neural bases of postural control. *Physiology (Bethesda)* 21: 216-225, 2006.

Deliagina TG, Beloozerova IN, Zelenin PV, Orlovsky GN. Spinal and supraspinal postural networks. *Brain Res Rev* 57: 212–221, 2008.

De Vries JIP, Visser GHA, Prechtl HFR. Fetal motility in the first half of pregnancy. In: Prechtl HFR, editor. Continuity of Neural Functions from Prenatal to Postnatal Life, *Clinics in Developmental Medicine.* Vol. 94. Oxford: *Spastics International Medical Publications* 46–64, 1984.

De Domenico G and Mccloskey DI. Accuracy of voluntary movements at the thumb and elbow joints. *Experimental Brain Research* 65: 471-478, 1987.

Dietz V, Quintern J, and Berger W. Cerebral evoked potentials associated with the compensatory reactions following stance and gait perturbation. *Neurosci Lett* 50: 181-186, 1984.

Dietz V and Duysens J. Significance of load receptor input during locomotion: *a review. Gait Posture* 11: 102–110, 2000.

Dimitrijevic MR, Gerasimenko Y, Pinter MM. Evidence for a spinal central pattern generator in humans. *Ann NY Acad Sci* 860: 377–392, 1998.

Ditunno JF, Little JW, Tessler A, Burns AS. Spinal shock revisited: a four-phase model. *Spinal Cord* 42(7) 383-395, 2004.

Doperalski AE, Tester NJ, Jefferson SC and Howland DR. Altered obstacle negotiation after low thoracic Hemisection in the cat. *Journal of Neurotrauma* 28:1983–1993, 2011.

Duysens, J, Pearson. KG. Inhibition of flexor burst generation by loading ankle extensor muscles in walking cats. *Brain Res* 187: 321-332, 1980.

Duysens, J., F. Clarac and H. Cruse."Load-regulating mechanisms in gait and posture: comparative aspects." *Physiol Rev* 80(1): 83-133, 2000.

Eccles JC, Eccles RM, Lundberg A. Synaptic actions on motoneurons caused by impulses in the Golgi tendon organ afferents. *J Physiol* 138: 227–252, 1957**.**

Eccles JC, Eccles RM, Lundberg A. The convergence of monosynaptic excitatory afferents on to many different species of alpha motoneurons. *J Physiol* 137: 22–50, 1957.

Eccles RM and Lundberg A. Integrative pattern of Ia synaptic actions on motoneurones of hip and knee muscles. *J Physiol* 144: 271-298, 1958.

Eccles RM and Lundberg A. Supraspinal control of interneurons mediating spinal reflexes. *J Physiol* 147: 565-584, 1959.

Edgerton VR, Leon RD, Harkema SJ, Hodgson JA, London N, Reinkensmeyer DJ,Roy RR, Talmadge RJ, Tillakaratne NJ, Timoszyk W, and Tobin A. Retraining the injured spinal cord. *J Physiol* 533: 15-22, 2001.

Edin BB, Vallbo AB. *Dynamic*-response of human muscle-spindle afferents to stretch. *J Neurophysiol* 63: 1297–1306, 1990.

Eldred E, Bridgman CF, Swett JE and Eldred B. Quantitative comparisons of muscle receptors of the cat's medial gastrocnemius, soleus, and extensor digitorum brevis muscles. *Symposium on Muscl Receptors.* D. Barker. Hong Kong, Hong Kong University Press: 207-213, 1962.

Ettema GJ. Gastrocnemius muscle length in relation to knee and ankle joint angles: verification of a geometric model and some applications. *Anat Rec* 247: 1–8, 1997.

Fenrich KK, Rose PK. Spinal interneuron axons spontaneously regenerate after spinal cord injury in the adult feline. *J. Neurosci.* 29: 12145-12158, 2009.

French DD, Campbell RR, Sabharwal S, Nelson AL, Palacios PA, Gavin-Dreschnack D. Health care costs for patients with chronic spinal cord injury in the Veterans Health Administration. *Journal of Spinal Cord Medicine* 30(5): 477–81, 2007.

Fox EJ, Tester NJ, Phadke CP, Nair PM, Senesac CR, Howland DR, Behrman AL. Ongoing Walking Recovery 2 Years After Locomotor Training in a Child With Severe Incomplete Spinal Cord Injury. *Physical Therapy* 90(5): 793-802, 2010.

Fulk GD; Schmitz TJ; Behrman AL. "Traumatic Spinal Cord Injury: Clinical Syndromes". In S.B. O'Sullivan; T.J. Schmitz. *Physical Rehabilitation* (5th ed.). Philadelphia, Pennsylvania: F.A. Davis. 937–997, 2007.

Forssberg H, Grillner S, Halbertsma J, Rossignol S. The locomotion of the low spinal cat. II. Interlimb coordination. *Acta Physiol Scand* 108: 283–295, 1980.

Frigon A, Rossignol S. Functional plasticity following spinal cord lesions. *Prog Brain Res* 157: 231–260, 2006.

Fung J, Macpherson J. Attributes of quiet stance in the chronic spinal cat. *J Neurophysiol* 82: 3056–3065, 1999.

Gillis GB and Biewener AA. Effects of surface grade on proximal hindlimb muscle strain and activation during rat locomotion. *J. Appl.Physiol.* 93: 1731-1743, 2002.

Gandevia SCAnd Kilbreath SL. Accuracy of weight estimation for weights lifted by proximal and distal muscles of the human upper limb. *J Physiol* 423: 299-310, 2001.

Goslow, GE, EK Stauffer, WC Nemeth and DG Stuart. Digit flexor muscles in the cat: Their action and motor units. *J Morph* 137(3): 335-352**,** 1972.

Gottschall JS, and Nichols TR. Head pitch affects muscle activity in the decerebrate cat hindlimb during walking. *Exp Brain Res* 182: 131-135, 2007.

Grillner S. Locomotion in vertebrates: central mechanisms and reflex integration. *Physiol Rev* 55:247–304, 1975.

Grey MJ, Ladouceur M, Andersen JB, Nielsen JB, Sinkjaer T. Group II muscle afferents probably contribute to the medium latency soleus stretch reflex during walking in humans. *J Physiol* 534: 925-933, 2001.

Hall LA & Mccloskey DI. Detections of movements imposed on finger, elbow and shoulder joints. *Journal of Physiology* 335: 519-533, 1983.

Hamilton AF, Jones KE, Wolpert DM. The scaling of motor noise with muscle strength and motor unit number in humans. *Exp Brain Res* 157: 417–430, 2004.

Hof A . In vivo measurement of the series elasticity release curve of human triceps surae muscle. *J Biomech* 31: 793–800, 1998.

Herzog W, Leonard TR, Renaud JM, Wallace J, Chaki G and Bornemisza S. Force–length properties and functional demands of cat gastrocnemius, soleus and plantaris muscles. *J Biomech.* 25: 1329–1335, 1992.

Hoffer JA, Andreassen S. Regulation of soleus muscle stiffness in premammillary cats: intrinsic and reflex components. *J Physiol* 45: 267-285, 1981.

Hogan N . The mechanics of multi-joint posture and movement control. *Biol Cybern* 52: 315–331, 1985.

Honeycutt CF, Gottschall JS, Nichols TR. Electromyographic responses from the hindlimb muscles of the decerebrate cat to horizontal support surface perturbations. *J Neurophysiol* 101: 2751-2761, 2009.

Honeycutt CF, Nichols TR. The decerebrate cat generates the essential features of the force constraint strategy. *J Neurophysiol* 103: 3266-3273, 2010.

Horak FB, Macpherson JM. Postural orientation and equilibrium. In: Shepard J, Rowell L, editors. Handbook of Physiology: Section 12, Exercise: Regulation and Integration of Multiple Systems. Oxford University Press; New York: pp. 255–292, 1996.

Houk JC. Regulation of stiffness by skeletomotor reflexes. *Annu Rev Physiol* 41: 99–114, 1979.

Hultborn H. State-dependent modulation of sensory feedback. *J Physiol* (Lond) 533: 5–13, 2000.

Hultborn H. Spinal reflexes, mechanisms and concepts: from Eccles to Lundberg and beyond. *Pro. Neurobiol* 78: 215–232, 2006.

Ichiyama RM, Broman J, Roy RR, Zhong H, Edgerton VR, and Havton LA. Locomotor training maintains normal inhibitory influence on both alpha- and gamma-motoneurons after neonatal spinal cord transection. *The Journal of neuroscience* 31: 26-33, 2011.

Jami L. Golgi tendon organs in mammalian skeletal muscle: functional properties and central actions. *Physiol Rev* 72: 623–666, 1992.

Jankowska E, Edgley SA. Functional subdivision of feline spinal interneurons in reflex pathways from group Ib and II muscle afferents; an update. *Eur J Neurosci* 32881-32893, 2010.

Jankowska E. Interneuronal relay in spinal pathways from proprioceptors. *Prog Neurobiol* 38: 335-378 1992.

Jefferson SC, Tester NJ, Howland DR. Chondroitinase ABC Promotes Recovery of Adaptive Limb Movements and Enhances Axonal Growth Caudal to a Spinal Hemisection. *J Neurosci* 31(15):5710-20, 2011.

Joris HJ, Van Muyen AJ, van Ingen Schenau GJ and Kemper HC. Force, velocity and energy flow during the overarm throw in female handball players. *Journal of Biomechanics* 18: 409-414, 1985.

Kandel E, Schwartz J, Jessel T. *Principles of Neural Science*. New York: McGraw-Hill, 2000.

Kistemaker DA, Rozendaal LA. In vivo dynamics of the musculoskeletal system cannot be adequately described using a stiffness-damping-inertia model. *PLoS One* 6: e19568, 2011.

Knikou M, Angeli CA, Ferreira CK, Harkema SJ. Flexion reflex modulation during stepping in human spinal cord injury. *Exp Brain Res* 196: 341-51, 2009.

Kirkwood PA and Sears TA. Monosynaptic excitation of motorneurons from muscle spindle secondary endings of intercostals and triceps surae muscles in the cat. *J Neurophysiol* 245: 64–66, 1975.

Kurata K, Tanji J. Premotor cortex neurons in macaques: activity before distal and proximal forelimb movements. *J Neurosci* 6: 403–411, 1986.

Lawrence JH III and Nichols TR. A three-dimensional biomechanical analysis of the cat ankle joint complex: I. Active and passive postural mechanisms. *Journal of Applied Biomechanics.* 15: 95-105, 1999.

Lawrence JH III, Nichols TR and English AW. Cat hindlimb muscles exert substantial torques outside the sagittal plane. *J Neurophysiol* 69: 282-285, 1993.

Lidell EGT and Sherrington C. Reflexes in response to stretch (myotatic reflexes). *Proc Roy Soc* XCVI: 212-242, 1924.

Lloyd DPC. Facilitation and inhibition of spinal motoneurones. *J Neurophysiol* 9: 421-438, 1946a.

Lloyd DPC. Integrative pattern of excitation and inhibition in two-neuron reflex arcs. *J Neurophysiol* 9: 439-444, 1946b.

Lemon RN, Griffiths J. Comparing the function of the corticospinal system in different species: organizational differences for motor specialization? *Muscle Nerve* 32: 261–279, 2005.

Loeb GE. The distal hindlimb musculature of the cat: interanimal variability of locomotor activity and cutaneous reflexes. *Exp Brain Res* 96: 125–140, 1993.

Li WWY, Yew DTW, Chuah MI, Leung PC,Tsang DSC. Axonal sprouting in the hemisected adult rat spinal cord. *Neuroscience* 61: 133–139, 1994.

Lyalka VF, Musienko PE, Orlovsky GN, Grillner S, Deliagina TG. Effect of intrathecal administration of serotoninergic and noradrenergic drugs on postural performance in rabbits with spinal cord lesions. *J Neurophysiol* 100: 723–732, 2008.

Lyalka VF, Orlovsky GN, Deliagina TG. Impairment of postural control in rabbits with extensive spinal lesions. *J Neurophysiol* 101: 1932–1940, 2009.

Lyalka VF, Zelenin PV, Karayannidou A, Orlovsky GN, Grillner S, and Deliagina TG. Impairment and recovery of postural control in rabbits with spinal cord lesions. *J Neurophysiol* 94: 3677-3690, 2005.

Lyle MA, Bunderson NE, Tuthill C, Niazi IF, Nichols TR. Variable gradient of intermuscular inhibition as preliminary evidence for spinal mediated modulation of task dependent limb behavior. *Soc Neurosci Abstr* 827.19/KK26, 2014.

Lyle MA, Niazi IF, Howland DR, Nichols TR. Supraspinal regulation of force feedback networks in the spinal cord. *KSCHIRT Symp* 2015.

Macpherson JM, and Inglis JT. Stance and balance following bilateral labyrinthectomy. *Prog Brain Res* 97: 219-228, 1993.

Macpherson JM, Deliagina TG, Orlovsky GN. Control of body orientation and equilibrium in vertebrates. In: *Neurons, Networks, and Motor Behaviour*, edited by Stein PSG, Grillner S, Selverston AI, and Stuart DG. Cambridge, MA: MIT Press, p. 257-267, 1997.

Macpherson JM, Fung J. Weight support and balance during perturbed stance in the chronic spinal cat. *J Neurophysiol* 82: 3066–3081, 1999.

Marchand-Pauvert V, Nicolas G, Marque P, Iglesias C, Pierrot-Deseilligny E. Increase in group II excitation from ankle muscles to thigh motoneurones during human standing. *J Physiol (Lond)* 566: 257-271, 2005.

Massion L, Dufosse M. Coordination between posture and movement: why and how? *News Physiol Sci* 3: 88-93, 1988.

Mazzaro N, Grey MJ, Sinkjaer T. Contribution of afferent feedback to the soleus muscle activity during human locomotion. *J Neurophysiol*. 93: 167–177, 2005.

Mazzaro N, Grey MJ, Feix do Nascimento O, Sinkjaer T. Afferent mediated modulation of the soleus muscle activity during the stance phase of human walking. *Exp Brain Res* 173: 713–723, 2006.

Mccrea da, Rybak ia. Organization of mammalian locomotor rhythm and pattern generation. *Brain Res Rev* 57: 134–146, 2008.

McGraw-Hill Irwin. Boston Applied linear statistical models. 5th ed. Kutner MH, editor. 2005.

McKinley W, Santos K, Meade M, Brooke K. Incidence and outcomes of spinal cord injury clinical syndromes. *J Spinal Cord Med.* 30: 215–224, 2007.

McKiernan BJ, Marcario JK, Karrer JH, Cheney PD. Corticomotoneuronal postspike effects in shoulder, elbow, wrist, digit, and intrinsic hand muscles during a reach and prehension task. *J Neurophysiol* 80: 1961–1980, 1998.

Michael-Titus, Adina T Nervous System: *Systems of the Body Series. Churchill Livingstone.* ISBN 9780443071799, 2007.

Mori S. Integration of posture and locomotion in acute decerebrate cats and in awake, freely moving cats. *Prog Neurobiol* 28: 161-195, 1987.

Mori S, Sakamoto T, Ohta Y, Takakusaki K, and Matsuyama K. Site-specific postural and locomotor changes evoked in awake, freely moving intact cats by stimulating the brainstem. *Brain Res* 505: 66-74, 1989.

Musienko P, Courtine G, Tibbs JE, Kilimnik V, Savochin A, Garfinkel A. Somatosensory control of balance during locomotion in decerebrated cat. *J Neurophysiol.* 107: 2072-2082, 2012.

Musienko PE, Zelenin PV, Lyalka VF, Orlovsky GN, and Deliagina TG. Postural performance in decerebrated rabbit. *Behav Brain Res* 190: 124-134, 2008.

Musienko PE, Zelenin PV, Orlovsky GN, Deliagina TG. Facilitation of postural limb reflexes with epidural stimulation in spinal rabbits. *Journal of neurophysiology* 103: 1080-1092, 2010.

Musselman, KE, Yang JF. Walking tasks encountered by urban-dwelling adults and persons with incomplete spinal cord injury. *J Rehabil Med* 39: 567–574, 2007.

Musselman K, Brunton K, Lam T, Yang J. Spinal cord injury functional ambulation profile: a new measure of walking ability. *Neurorehabil and Neural Repair* 25: 285–293, 2011.

NSCISC (National Spinal Cord Injury Statistical Center). Spinal Cord Injury (SCI) Facts and figures. 2014.

Niazi IF, Nichols TR, and Howland DR. Altered muscular activation patterns and force feedback after spinal cord injury**.** *FASEB J* 26:904.9, 2012.

Niazi IF, Nichols TR, Rising A, Little L, Mondello S, Howland DR. Reorganization of heterogenic inhibitory force feedback between hindlimb extensors after both acute and chronic time points post spinal cord injury. *Soc Neurosci Abstr* 885.16/HH7, 2012.

Niazi IF, Nichols TR, and Howland DR. Reorganization of inhibitory force feedback to and from hind limb toe flexors after chronic spinal cord injury in the cat. *Soc Neurosci Abstr* 827.20/KK27, 2014.

Nichols TR. A technique for measuring the mechanical actions of (intermuscular) reflexes in the decerebrate cat. *J Neurosci Methods* 21: 265–273, 1987.

Nichols TR. The organization of heterogenic reflexes among muscles crossing the ankle joint in the decerebrate cat. *J Physiol* 410: 463-477, 1989.

Nichols TR. A biomechanical perspective on spinal mechanisms of coordinated muscular action: an architecture principle. *Acta Anatomica* 151: 1-13 1994

Nichols TR. Receptor mechanisms underlying reflexes among the triceps surae muscles of the cat. *J Neurophysiol* 81: 467–478, 1999.

Nichole TR, Cope TC. Motor Neurobiology of the spinal cord. 305-326, 2001.

Nichols TR, Houk JC. Improvement in linearity and regulation of stiffness that results from actions of stretch reflex. *J Neurophysiol* 39: 119–142, 1976.

Nichols TR, Ross KT. The implications of force feedback for the lambda model. *Adv Exp Med Biol* 79: 629-663, 2009.

Nichols TR, Wilmink RJH, Burkholder TJ. The multidimensional and temporal regulation of limb mechanics by spinal circuits, in: M.L. Latash (Ed.), Progress in Motor Control, Structure–Function Relations in Voluntary Movements, Human Kinetics, vol. 2, pp. 179–193, 2002.

Nichols TR, Gottschall JS, Tuthill C. The Regulation of Limb Stiffness in the Context of Locomotor Tasks. Levin MF (ed.) Progress in motor control. Adv .in exp med & Biol Springer 826: 41-54, 2014.

Nooijen CF, Ter Hoeve N, Field-Fote EC. Gait quality is improved by locomotor training in individuals with SCI regardless of training approach. *J Neuroeng Rehabil* 6:36, 2009.

Nooijen CF, Nienke ter Hoeve and Edelle C Field-Fote. Gait quality is improved by locomotor training in individuals with SCI regardless of training approach. *J Neuroeng Rehabil* 6: 36, 2009.

Orlovsky GN, Deliagina TG, Grillner S. *Neuronal Control of Locomotion.From Mollusc to Man.* Oxford, UK: Oxford Univ. Press, 1999.

Palmer E, Ashby P. Corticospinal projections to upper limb motoneurones in humans. *J Physiol* 448: 397–412, 1992.

Pearson KG, Collins DF. Reversal of the influence of group Ib afferents from plantaris on activity in medial gastrocnemius muscle during locomotor activity. *J Neurophysiol* 70: 1009–1017, 1993.

Pearson KG. Proprioceptive regulation of locomotion. *Curr Opin Neurobiol* 5(6): 786-791, 1995.

Peiper A. Cerebral Function in Infancy and Childhood. New York: Consultants Bureau; 1961.

Poppele R, Bosco G. Sophisticated spinal contributions to motor control, *Trends Neurosci* 26: 269–276, 2003.

Pratt CA, Fung J, and Macpherson JM. Stance control in the chronic spinal cat. *J Neurophysiol* 71: 1981-1985, 1994.

Pratt CA. Evidence of positive force feedback among hindlimb extensors in the intact standing cat. *J Neurophysiol* 73: 2578-2583, 1995.

Prochazka A. Muscle spindle function during normal movement. *Int Rev Physiol* 25: 47–90, 1981.

Prochazka A. Proprioceptive feedback and movement regulation. Handbook of Physiology. Section 12: Excercise: Regulation and Integration of Multiple Systems. L. B. Rowell and J. T. Shepherd. New York, Oxford. 1996.

Prochazka A, Gorassini M. Models of ensemble firing of muscle spindle afferents recorded during normal locomotion in cats. *J Physiol* 507: 277–291, 1998b.

Prochazka A, Gorassini M. Ensemble firing of muscle afferents recorded during normal locomotion in cats. *J Physiol (Lond)* 507: 293– 304, 1998.

Rademaker, GGJ. On the lengthening and shortening reactions and their occurrence in man. *Brain* 70: 109-126, 1947.

Refshauge KM, Chan R, Taylor JL, McCloskey DI. Detection of movements imposed on human hip, knee, ankle and toe joints. *J Physiol* 488: 231–241, 1995.

Riddle CN, Edgley SA, Baker SN. Direct and indirect connections with upper limb motoneurons from the primate reticulospinal tract. *J Neurosci* 29: 4993–4999, 2009.

Roberts TJ, Marsh RL, Weyand PG and Taylor CR. Muscular force in running turkeys: the economy of minimizing work. *Science* 275: 1113-1115, 1997.

Rossignol S, Barriere G, Frigon A, Barthelemy D, Bouyer L, Provencher J, Leblond H, Bernard G. Plasticity of locomotor sensorimotor interactions after peripheral and/or spinal lesions. *Brain Res Rev* 57: 228–240, 2008.

Rossignol S, Bouyer L, Barthelemy D, Langlet C, Leblond H. Recovery of locomotion in the cat following spinal cord lesions. *Brain Res Rev* 40: 257–266, 2002.

Rossignol S, Chau C, Brustein E, Belanger M, Barbeau H and Drew T. Locomotor capacitiesafter complete and partial lesions of the spinal cord. *Acta Neurobiol Exp* 56: 449-463, 1996.

Rossignol S, Drew T, Brustein E, Jiang W. Locomotor performance and adaptation after partial or complete spinal cord lesions in the cat. In: *Peripheral and Spinal Mechanisms in the Neural Control of Movement*, edited by Binder MD. Amsterdam: Elsevier, p. 349–365, 1999.

Rossignol S, Dubuc R. Spinal pattern generation. *Curr Opin Neurobiol* 4: 894–902, 1994.

Rossignol S, Dubuc R, Gossard JP. Dynamic sensorimotor interactions in locomotion. *Physiol Rev* 86: 89–154, 2006.

Rossignol S, Frigon A. Recovery of locomotion after spinal cord injury: some facts and mechanisms. *Annual review of neuroscience* 34: 413-440, 2011.

Ross KT, Nichols TR. Feedback Between Hindlimb Extensors in the Spontaneously Locomoting Premammillary Cat. *J Neurophysiol* 101: 184-197, 2009.

Rymer WZ, Hasan Z. Absence of force-feedback regulation in soleus of the decerebrate cat. *Brain Res* 184: 203–209, 1980.

Rymer, WZ, Houk, JC And Crago, PE. Mechanism of the claspknife reflex studied in an animal model. *Exp Brain Res* 37: 93-l 13, 1979.

Sacks RD and Roy RR. Architecture of the hind limb muscles of cats: functional significance. *J Morph* 173: 185–195, 1982.

Sherrington CS. On plastic tonus and proprioceptive reflexes. *Exp Physiol* 2: 109-l56, 1909.

Spector SA, Gardiner PF, Zernicke RF, Roy RR and Edgerton VR. Muscle architecture and Force–Velocity characteristics of cat Soleus and medial Gastrocnemius: Implications for motor control. *J Neurophysiol* 44: 951–960, 1980.

Sekhon LHS, Fehlings MG. Epidemiology, demographics, and pathophysiology of acute spinal cord injury. *Spine 26(245):S2–S12.*

Stapley PJ, Drew T. The pontomedullary reticular formation contributes to the compensatory postural responses observed following removal of the support surface in the standing cat. *J Neurophysiol* 101: 1334 –1350, 2009.

Stein PS, and Daniels-McQueen S. Variations in motor patterns during fictive rostral scratching in the turtle: knee-related deletions. *J Neurophysiol* 91: 2380-2384, 2004.

Stein RB, Misiaszek JE and Pearson KG. Functional role of muscle reflexes for force generation in the decerebrate walking cat. *J Physiol* 525: 781-791, 2000.

Schomburg ED. Spinal sensorimotor systems and their supraspinal control, *Neurosci Res.* 7: 265–340, 1990.

Schepens B, Stapley P, Drew T. Neurons in the post medullary reticular formation signal posture and movementboth as an integrated behavior and independently. *Journal of Neurophysiology* 100: 2235- 2253, 2008.

Sinkjaer T, Andersen JB, Ladouceur M, Christensen LO, Nielsen JB, Major role for sensory feedback in soleus EMG activity in the stance phase of walking in man, *J Physiol (Lond)* 523: 817–827, 2000.

Tan E, Lynn J and Amato AA. Immunosuppressive treatment in motor neuron syndromes, Attempt to distinguish a treatable disorder. *Arch Neurol* 51: 194-200, 1994.

Tator CH. Update on the pathophysiology and pathology of acute spinal cord injury. *Brain Pathol* 5: 407-413**,** 1995.

Timoszyk WK, De Leon RD, London N, Roy RR, Edgerton VR, and Reinkensmeyer DJ. The rat lumbosacral spinal cord adapts to robotic loading applied during stance. *J Neurophysiol* 88: 3108-3117, 2002.

Turton A, Lemon RN. The contribution of fast corticospinal input to the voluntary activation of proximal muscles in normal subjects and in stroke patients. *Exp Brain Res* 129: 559–572, 1999.

Tuthill C, Goolsby WN, Niazi IF, Nichols TR. Mapping task dependent changes to limb impedance: A robotic approach. *Soc Neurosci Abstr* 787.5/VV8, 2010.

Van Soest AJ, Schwab AL, Bobbert MF, van Ingen Schenau GJ. The influence of the biarticularity of the gastrocnemius muscle on vertical-jumping achievement. *J Biomech* 26: 1–8, 1993.

Valero-Cabre A, Tsironis K, Skouras E, Navarro X, Neiss WF. Peripheral and spinal motor reorganization after nerve injury and repair. *J Neurotrauma* 2004: 21: 95–108.

Venugopal S, Hamm TM, Crook SM, Jung R. Modulation of inhibitory strength and kinetics facilitates regulation of persistent inward currents and motoneuron excitability following spinal cord injury. *J Neurophysiol* 106: 2167–2179, 2011.

Walmsley B and Proske U. Comparison of stiffness of soleus and medial gastrocnemius muscles in cats. *J Neurophysiol* 46: 250–259, 1981.

West SP, Roy RR and Edgerton VR. Fiber type and fiber size of cat ankle, knee and hip extensors and flexors following low thoracic spinal cord transection at an early age. *Exp Neurol* 91: 174–182, 1986.

Wolpert DM, Ghahramani Z, Jordan MI. An internal model for sensorimotor integration. *Science* 269: 1880–1882, 1995.

Wolpert DM, Miall RC, Kawato M. Internal models in the cerebellum. *Trends Cogn Sci* 2: 338–347, 1998.

Wilmink RJH, Nichols TR. Distribution of reflexes among the quadriceps and triceps surae muscles of the cat hindlimb. *J Neurophysiol* 90: 2310–2324, 2003.

Wirth b, van hedel hj, curt a. Changes in corticospinal function and ankle motor control during recovery from incomplete spinal cord injury. *J Neurotrauma* 25: 467–478, 2008.

Young RP, Scott SH, Loeb GE. Joint-angle-dependent moment arm of feline ankle muscles. An intrinsic mechanism to stabilize posture. *Neurosci Lett* 145: 137-140, 1992.

Zehr EP, Komiyama T, Stein RB. Cutaneous reflexes during human gait: electromyographic and kinematic responses to electrical stimulation. *J Neurophysiol* 77: 3311-3325, 1997.